XRCC1 PLAYS DIVERSE ROLES IN DNA STRAND BREAK REPAIR AND HUMAN DISEASE

A Dissertation

by

BRADLEY JOHN ECKELMANN

Submitted to the Office of Graduate and Professional Studies of
Texas A&M University
in partial fulfillment of the requirements for the degree of

DOCTOR OF PHILOSOPHY

Chair of Committee,	Sankar Mitra
Committee Members,	Muralidhar Hegde
	John Ford
	David Huston
	Julian Leibowitz
Head of Department,	Carol Vargas Bautista

May 2021

Major Subject: Medical Sciences

ABSTRACT

Microhomology-mediated end joining (MMEJ), an error-prone pathway for DNA double-strand break (DSB) repair, is implicated in genomic rearrangement and oncogenic transformation; however, its contribution to repair of radiation-induced DSBs has not been characterized. We used recircularization of a linearized plasmid to recapitulate DSB repair via MMEJ or nonhomologous end-joining (NHEJ). MMEJ was significantly enhanced in irradiated cells, independent of their radiation-induced arrest in the G2/M phase. MMEJ activation was dependent on XRCC1 phosphorylation by casein kinase 2 (CK2), enhancing XRCC1's interaction with the end resection enzymes MRE11 and CtIP. Both endonuclease and exonuclease activities of MRE11 were required for MMEJ. Furthermore, the XRCC1 co-immunoprecipitate complex (IP) displayed MMEJ activity in vitro, which was significantly elevated after irradiation. Our studies thus suggest that radiation-mediated enhancement of MMEJ in cells surviving radiation therapy may contribute to their radioresistance and could be therapeutically targeted.

Homologous recombination (HR)-deficient cancers, especially those with mutations in BRCA1 or BRCA2, utilize alternative methods of DNA double-strand break (DSB) repair, in particular microhomology-mediated end joining (MMEJ), for repair of DSBs that arise in S/G2 cell cycle phases as a result of replication stress. Depletion of MMEJ factors, including XRCC1, PARP1, and POLQ, is synthetic lethal with BRCA2 deficiency. While POLQ and PARP1 have been well-studied in the context of HR-deficiency, whether XRCC1 participates in MMEJ in HR-deficient cancers is unknown. We used a variety of approaches to demonstrate XRCC1’s critical role in MMEJ in BRCA2-deficient cells, and discovered that XRCC1 forms an active repair complex with POLQ and MRE11 after replication stress that has MMEJ activity *in vitro*. Formation of this complex was suppressed by BRCA2. Moreover, XRCC1 contributed to

replication fork restart and fork degradation in BRCA2-deficient cells. Expression of XRCC1 is altered in HR-deficient cancers, along with other DNA repair factors in the same region of chromosome 19. Collectively, these studies identify new roles for XRCC1 in HR-deficient cancers and suggest chemotherapeutic strategies targeting MMEJ complex formation.

DEDICATION

To my family, who are a home no matter where I am.

ACKNOWLEDGEMENTS

I would first like to acknowledge my mentor, Dr. Sankar Mitra, and express my immense gratitude for his guidance and tutelage. He both taught me how to ask questions, and gave me the opportunity to ask my own. He fostered my sense of curiosity and challenged me with his energy. Both his criticisms and support have sharpened my scientific abilities, and my confidence going forward in my career is a testament to him. Most importantly, he was always thinking of others and how to help them. I am honored to be the last trainee of his long, respected career.

I am also very grateful for the mentorship of Dr. Muralidhar Hegde, whose scientific insights proved invaluable to my work. He always encouraged me to follow my ideas and often taught me how. I would also like to acknowledge Dr. Arijit Dutta, who took me under his wing and taught me how to become a thoughtful, technical biochemical scientist. He also was a good friend and source of support, and I am indebted to him for his guidance. The rest of the Mitra and Hegde research groups were instrumental in my work and I thank them for their various contributions, including Dr. Shiladitya Sengupta, Dr. Chunying Yang, Dr. Joy Mitra, Dr. Velmarini Vasquez, Dr. Erika Guerrero, Dr. Haibo Wang, Dr. Prakash Dharmalingam, Dr. Suganya Rangaswamy, Dr. Arvind Pandey, and Dr. Kazi Mokim Ahmed. I would also like to acknowledge the Structural Biology of DNA Repair Machines program project and their continued support for my work, in particular the group of Dr. John Tainer, especially John, Dr. Susan Tsutakawa, Dr. Zamal Ahmed, Dr. Zu Ye, and Dr. Albino Bacolla.

Thanks are also due to the other members of my graduate committee – Dr. John Ford, Dr. David Huston, and Dr. Leibowitz – for their continued advice and encouragement. Specifically, Dr. Ford for sparking my interest in radiation biology, Dr. Huston for his guidance and perspective,

and Dr. Leibowitz for his patience and wisdom. I would also like to thank Dr. Leibowitz, the director of the MD/PhD program, for his consideration of my application to the program and for taking a chance on me as a student. Thanks also to the MD/PhD program coordinators, Amanda Watkins, Michael Dewsnap, Lacie Warren, and Mary Imran, who always looked out for me.

Several other faculty played key roles in my development as a scientist. Dr. Kayla Bayless and Dr. David Zawieja were wonderful mentors during research rotations. Dr. Nancy Turner was a source of advice and guidance who encouraged my application for the NSBRI fellowship, and who considered and accepted my application. Dr. Ruth Globus, Dr. Ann-Sofie Schreurs and the rest of the Globus group at NASA Ames helped me broaden my perspective and taught me about bone and space biology.

Thanks to the Houston Methodist team for accepting me with open arms and making me feel at home. Especially to Dr. Amy Wright, who was there for me no matter what I needed, and also to Tim Boone, Trevor Burt, and Ruth Sanchez.

To those who fueled my interest in science. To Dr. Mitch Turker, at OHSU, who picked me out of a hat and changed my life, along with my coworkers there, Cristian Dan and Anna Ohlrich; and the physics department at Carleton College, which will always have a special place in my heart.

To all of my friends who have helped me through this time and continue to be there for me, I love you all.

And finally to my family. To Monique, Dad, Lindsey and David, Stephen and Megan, Julia, and Mom. Every time I think or speak or write there is a part of each of you in that. Your love makes things possible for me. I love you all very much.

CONTRIBUTORS AND FUNDING SOURCES

Contributors

This work was supervised by a dissertation committee consisting of Professors Sankar Mitra (advisor) and Muralidhar Hegde of the Houston Methodist Radiation Oncology Department, Professor John Ford of the TAMU Nuclear Engineering Department, and Professors David Huston and Julian Leibowitz of the TAMU Department of Microbial Pathogenesis and Immunology.

Data and figures from Dutta, Eckelmann et al. (Nucleic Acids Research, 2017) was completed in conjunction with Dr. Arijit Dutta and other contributing authors. All other work contained in this dissertation was performed by Brad Eckelmann, in conjunction with Albino Bacolla, Haibo Wang, Erika Guerrero, Wei Jiang, and Zu Ye.

Funding Sources

Graduate study was supported by the TAMHSC MD/PhD Program and the Houston Methodist Research Institute. Research was supported by USPHS grants R01 CA158910 and R01 GM105090 (to Sankar Mitra), P01 CA92548 (to John Tainer and Sankar Mitra), and National Space Biomedical Research Institute NCC 9-58 (to Brad Eckelmann).

NOMENCLATURE

Alt-EJ	Alternative end joining
AP	Apurinic/Apyrimidinic
APE1	Apurinic/apyrimidinic endonuclease 1
APLF	Aprataxin and PNKP like factor
APTX	Aprataxin
ATM	Ataxia telangiectasia mutated
ATR	Ataxia telangiectasia and Rad3 related
BER	Base excision repair
BIR	Break-induced replication
BLM	Bloom Syndrome protein
BRCA1	Breast cancer type 1 susceptibility protein
BRCA2	Breast cancer type 2 susceptibility protein
BrdU	Bromodeoxyuridine
BRCT	BRCA1 C Terminus
CFS	Chromosome fragile site
CGR	Complex genome rearrangement
CHK1/2	Checkpoint kinase 1/2
CK2	Casein kinase 2
CldU	Chlorodeoxyuridine
CO	Crossover
Co-IP	Co-immunoprecipitation
CNV	Copy number variation

CTD	C terminal domain
CtIP	Carboxy-terminal binding protein (CtBP)-interacting protein
dHJ	double Holliday junction
DNA-PK	DNA dependent protein kinase
DSB	Double strand break
ERCC1	Excision Repair Cross Complementing Group 1
ERCC2	Excision Repair Cross Complementing Group 2
EXO1	Exonuclease 1
FA	Fanconi Anemia
FEN1	Flap Structure-Specific Endonuclease 1
FHA	Forkhead-associated
GFP	Green fluorescent protein
GST	Glutathione S-transferase
HR	Homologous recombination
HRD	Homologous recombination deficiency
HRP	Horseradish peroxidase
HU	Hydroxyurea
IdU	Iododeoxyuridine
IP	Immunoprecipitate
IR	Ionizing radiation
LET	Linear energy transfer
LIG3	DNA ligase 3
LIG4	DNA ligase 4

LOH	Loss of heterozygosity
MH	Microhomology
MMBIR	Microhomology-mediated break-induced replication
MMEJ	Microhomology-mediated end joining
MMR	Mismatch repair
MRN	Mre11-Rad50-Nbs1
NCO	Non-crossover
NER	Nucleotide excision repair
NGS	Next-generation sequencing
NHEJ	Non-homologous end joining
NMF	Non-negative matrix factorization
NTD	N terminal domain
OGG1	8-Oxoguanine glycosylase 1
PALB2	Partner and localizer of BRCA2
PAR	Poly(ADP)-ribose
PARBM	Poly(ADP)-ribose binding motif
PARP	Poly(ADP)-ribose polymerase
PARPi	PARP inhibitor
PCNA	Proliferating cell nuclear antigen
PCR	Polymerase chain reaction
PLA	Proximity ligation assay
PNKP	Polynucleotide kinase phosphatase
POLB	DNA polymerase beta

POLD1	DNA polymerase delta catalytic subunit
POLQ	DNA polymerase theta
RBE	Relative biological effectiveness
RFC	Replication factor C
ROS	Reactive oxygen species
RPA	Replication protein A
SBS	Single base substitution
SCE	Sister chromatid exchange
seDSB	single-ended DSB
SSB	Single strand break
SSBR	Single strand break repair
TOP1	Topoisomerase 1
WGS	Whole-genome sequencing
WRN	Werner protein
XRCC1	X-ray repair cross-complementing protein 1
XRCC4	X-ray repair cross-complementing protein 4

TABLE OF CONTENTS

Page

LIST OF FIGURES

FIGURE Page

LIST OF TABLES

1. **INTRODUCTION AND SIGNIFICANCE**

1.1 **Introduction to DNA repair**

1.1.1 **Base Excision Repair**

Aerobic organisms that rely on hydrolysis and oxidation to drive a variety of cellular processes experience endogenous oxidative DNA damage (1). DNA bases can be modified or lost as a result, which can lead to mutations that can cause human disease. Processes to repair endogenous oxidative DNA damage have evolved to maintain genomic stability and survival, particularly the mechanism of base excision repair (BER) (1). Most BER enzymes are highly conserved across species, and tight associations between BER enzyme deficiencies and mutator phenotypes have been established (1). BER is responsible for repairing not only oxidations, but alkylations, deaminations, and depurinations (1).

Base lesions in DNA are detected by DNA glycosylases. Monofunctional glycosylases recognize uracil, thymine, and alkylated bases, and cleave the N-glycosyl bond between the sugar and the base, removing the damaged base (2). The now abasic site is recognized by the apurinic endonuclease APE1, which cleaves the abasic site, leaving a 3' hydroxyl group that is a substrate for extension by DNA polymerase β, which can also remove the sugar using 5' dRP lyase activity (2). DNA polymerase β then fills in the gap and the gap is sealed by XRCC1/Ligase III (2). XRCC1 stabilizes several components of the BER pathway through direct interactions, including Ligase III, mediating complex formation (3). On the other hand, oxidative DNA lesions are recognized by bifunctional glycosylases, which both excise the damaged base and use their AP lyase activity to cleave the phosphodiester bond of the DNA backbone, which leaves behind either 5' phosphate and 3' α, β unsaturated aldehyde (if β-elimination) or 5' phosphate and 3'phosphate (if β, δ-elimination) (2). Then, the end processing activities of APE1

(3’ α, β unsaturated aldehyde) or polynucleotide kinase phosphatase (PNKP) (3’ phosphate) generate polymerase-compatible 3’ hydroxyl termini (2). Gap filling and ligation is then accomplished similarly to the monofunctional enzyme pathway. These pathways of BER are collectively referred to as the single-nucleotide or short-patch BER (SN/SP-BER).

Other pathways of BER, termed long-patch BER (LP-BER), are typically engaged when the 5’ sugar fails to get removed by the 5’dRP lyase activity of DNA polymerase β. Instead, the 5’ strand is displaced extension of the 3’ strand by any of a number of different polymerases, including Polβ, the replicative polymerases Polδ/ε or Polλ (2). The displaced strand can be removed by flap endonuclease 1 (FEN1), and the nick is sealed by Ligase I. This pathway has been connected to DNA replication through replication factor C (RFC) and proliferating nuclear cell antigen (PCNA), which have been found in complex with DNA glycosylases, replicative polymerases, and the X-ray repair cross complementing 1 (XRCC1) scaffold (3). Precisely how the usage of each of these pathways is regulated is not well understood.

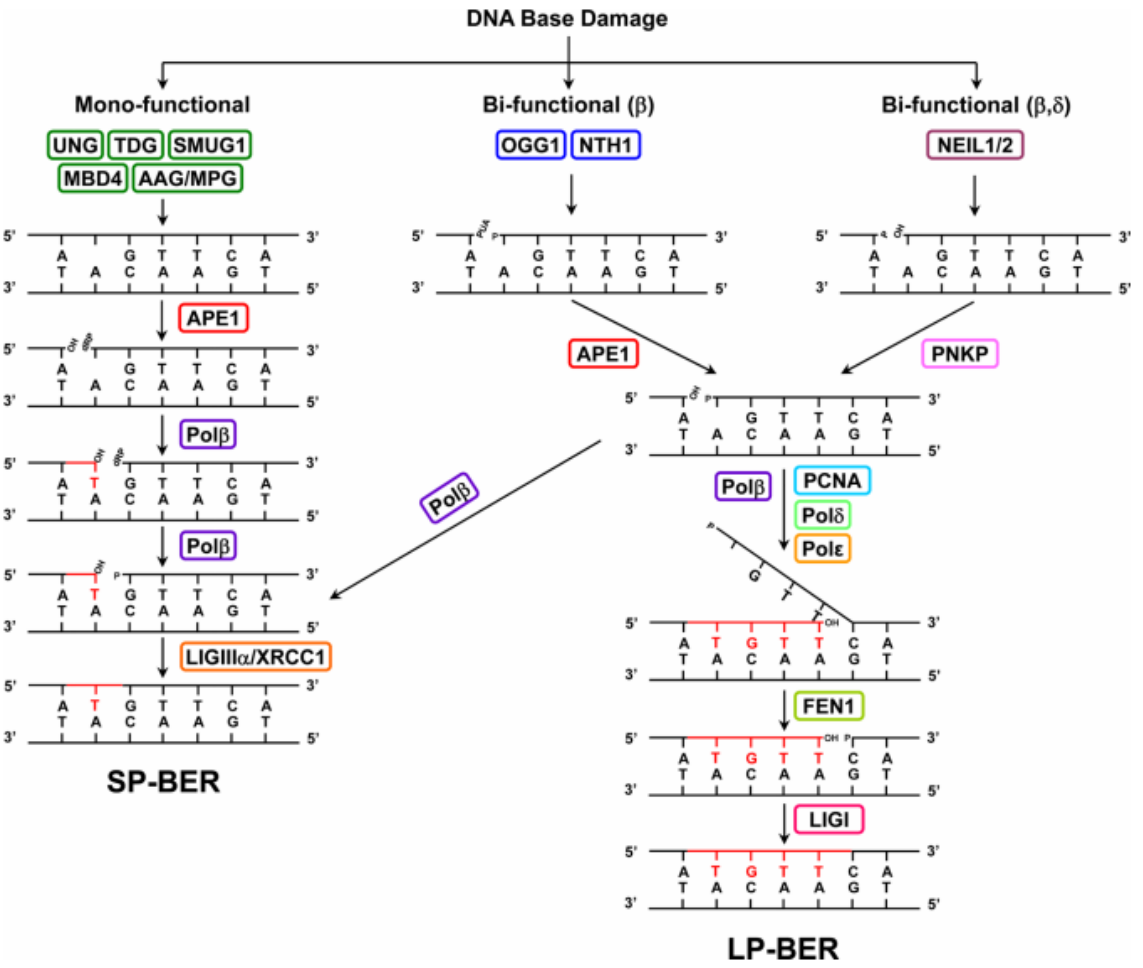

Figure 1. Summary of base excision repair pathways and components. Reprinted from (4) with permission from Bentham Science Journals.

1.1.2 **Single-strand Break Repair**

DNA single-strand breaks (SSBs) are single-nucleotide gaps in one strand of the DNA duplex. These breaks often have modified 5' and/or 3' termini, adding to the complexity of repair. SSBs are generated either directly by oxidization of the sugar backbone or indirectly during BER after strand scission (5). Additionally, transient SSBs are frequently generated during transcription and replication by DNA topoisomerase 1 (TOP1) in order to relieve topological stress induced by winding of the DNA double helix (5). These SSBs are typically

immediately religated, however, some may persist due to collision of the SSB with replication or transcription machinery, or with other DNA lesions. Persistent SSBs are dangerous to the cell, as they can lead to DNA double-strand breaks (DSBs) if they collide with replication forks, although replicating cells can typically repair these DSBs using homologous recombination (HR) (5). In post-mitotic cells, including neurons, persistence of SSBs can lead to hyperactivation of the DNA damage sensor poly (ADP-ribose) polymerase 1 (PARP1), which rapidly depletes cellular NAD+ levels and can lead to NAD+ exhaustion and cell death (5). This kind of cell death is characteristic of several pathological conditions that involve oxidative stress, especially those that occur in ischemic post-mitotic cells in the heart and brain after heart attack and stroke (5).

Detection of direct SSBs is facilitated primarily by PARP1, which catalyzes addition of poly (ADP-ribose) (pAR) chains to itself and a number of other targets (5). This addition promotes the accumulation of SSBR factors at SSBs, through interaction of pAR with pAR-binding motifs in numerous proteins, including XRCC1 (5). XRCC1 scaffolds several SSBR factors, stabilizing them and in some case stimulating their enzymatic activity (5). pAR chains are rapidly degraded by pAR glycohydrolase (PARG), which is required for efficient ligation and turnover of SSBR enzymes (5). Since most SSBs require some form of end processing to restore 5'phosphate and 3'hydroxyl groups for gap filling, several different enzymes can be recruited by XRCC1 to accomplish end cleaning. 3'phosphate, which arises at direct SSBs induced by ROS, is primarily processed by PNKP. 3'phosphoglycolate, which also arises at direct SSBs induced by ROS, is primarily processed by APE1. 5'AMP-SSBs, which result from abortive ligation attempts are processed by aprataxin (APTX). TOP1-SSBs result from abortive TOP1 activity and are processed by tyrosyl-DNA phosphodiesterase 1 (TDP1). XRCC1 interacts directly with

PNKP, APTX, and Polβ, and has been found in complex with TDP1 and APE1, highlighting its role in DNA end processing (5). After end cleaning, gap filling and ligation through either short-patch or long-patch repair pathways is completed.

The importance of SSBR in postmitotic cells is seen in neurodegenerative diseases caused by mutations in TDP1 (spinocerebellar ataxia with axonal neuropathy), APTX (ataxia and oculomotor apraxia 1) (6) and XRCC1 (ocular motor apraxia, axonal neuropathy, and progressive cerebellar ataxia) (7). Additionally, PARP hyperactivation has been directly identified as a cause of neuronal cell death and PARP inhibitors are being investigated as therapy for DNA strand break repair-defective neurological disease (7).

1.1.3 **Double-strand Break Repair**

DSBs are the most deleterious form of DNA damage. They can be introduced in a number of ways, including by endogenous ROS, repair pathway intermediates, replication-associated misrepair, and exogenous sources such as radiation and chemicals (8). DSBs also occur during immune cell development within the programmed pathways of V(D)J and class switch recombination (8). Persistent and misrepaired DSBs can result in cell death, senescence, or gross chromosomal aberrations which destabilize the genome and can drive carcinogenesis (9). Therefore, efficient mechanisms that quickly repair DSBs and preserve genome integrity are critical for cell survival and cancer avoidance. There are two major pathways of DSBR: non-homologous end joining (NHEJ), which directly ligates a broken DNA molecule; and homologous recombination (HR), which uses resection, strand invasion of a sister chromatid, and extension using the homologous template. A minor pathway, microhomology-mediated end joining (MMEJ), is also used under some circumstances to repair DSBs.

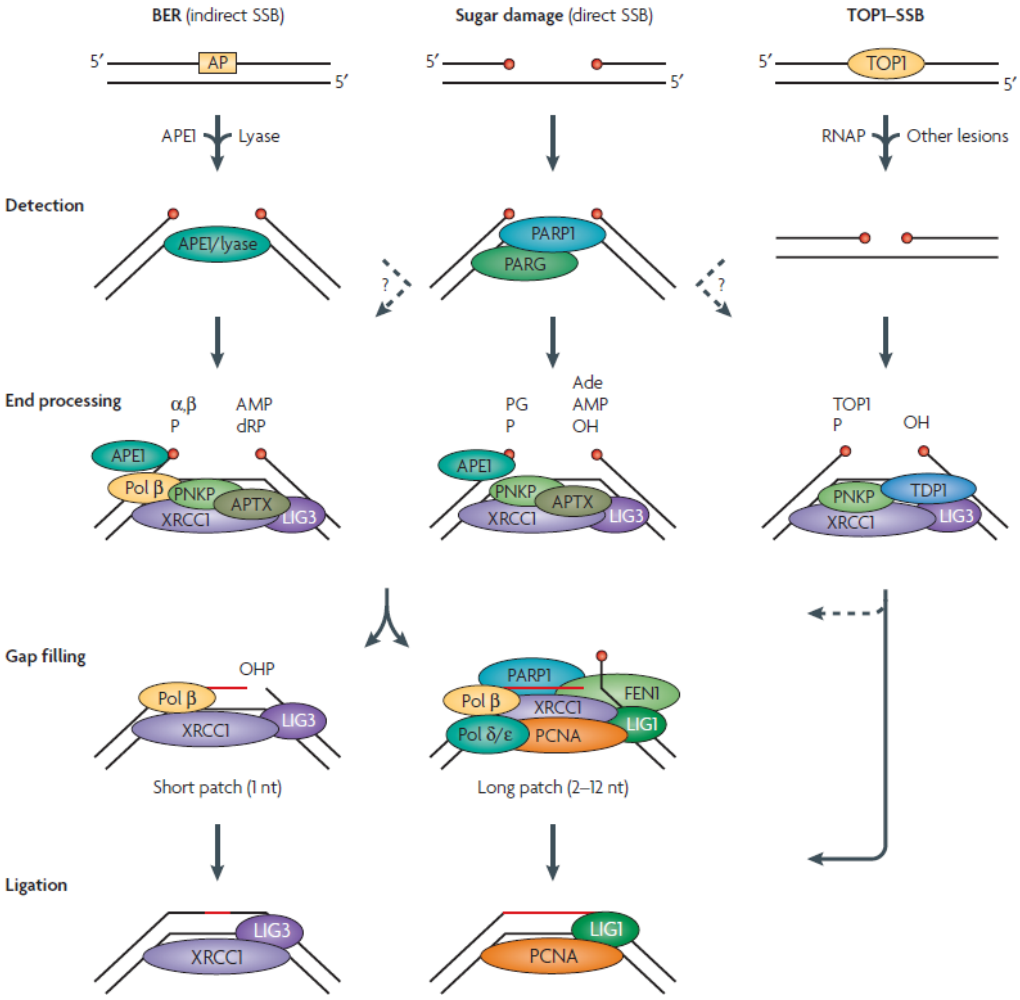

Figure 2. Pathways of single-strand break repair. Reprinted from (5) with permission from Nature Journals.

1.1.3.1 **Non-homologous end joining**

NHEJ is initiated by the recognition of broken DNA ends by the Ku70/Ku80 heterodimer, which recruits the DNA-dependent protein kinase catalytic subunit (DNA-PKcs) to form the DNA-PK holoenzyme (8). The holoenzyme both bridges the broken DNA ends, stabilizes them, and acts as an initiator of a signaling cascade. DNA-PKcs is a member of the phosphatidylinositol 3-kinase-related (PIKK) family of kinases, which includes ataxia-telangiectasia mutated (ATM) and ATM and Rad3 related (ATR) (8). These serine/threonine

kinases are all critical components of the DNA damage response, and DNA-PKcs phosphorylates a number of substrates, including itself, other NHEJ components, and downstream effectors (8). One of the characteristics of NHEJ is that is does not utilize extensive homology for repair, and end protection by Ku prevents long-range resection. However, since DNA ends are often incompatible for direct ligation, limited end resection by nucleases is a necessary component of the NHEJ machinery. Depending on the end chemistry, several different nucleases can be engaged during NHEJ. Artemis is phosphorylated by DNA-PKcs and has nuclease activity at ssDNA-dsDNA junctions, allowing it to cut at DNA overhangs to generate blunt ends (8). Artemis also has 5'-> 3' exonuclease activity on ssDNA, again removing overhangs to generate blunt ends (8). PNKP and aprataxin, similar to their roles in SSBR, can phosphorylate 5' hydroxyl groups and remove 3' phosphates (PNKP) or 5'AMP (aprataxin). Aprataxin and PNKP-like factor (APLF) and Werner (WRN) have 3'->5' exonuclease activity (8). Additionally, Ku itself has 5'dRP/AP lyase activity (8).

Gap filling by DNA polymerases may also take place during NHEJ. The family X polymerases (Pol β, Pol μ, Pol λ, and terminal deoxynucleotidyl transferase (TdT)) can participate in NHEJ, although the primary polymerases are Pol μ and Pol λ, which both have BRCA1 C Terminus (BRCT) domains that facilitate their interactions with Ku (8). TdT is not expressed in most cell types, and promotes immune diversity by adding random nucleotides to DSBs in T and B cells in V(D)J recombination (8). Pol μ can add nucleotides in both template-independent and -dependent ways, whereas Pol λ is primarily template-dependent. Template-independent activities of NHEJ polymerases are thought to be used to stabilize breaks with short overhangs by synthesizing short stretches of microhomology (MH) (8).

Ligation during NHEJ happens via the XRCC4/Ligase IV complex. XRCC4 interacts with Ligase IV and stimulates its activity via a BRCT domain. XRCC4-like factor (XLF) helps bridge DNA during this process along with XRCC4 (8).

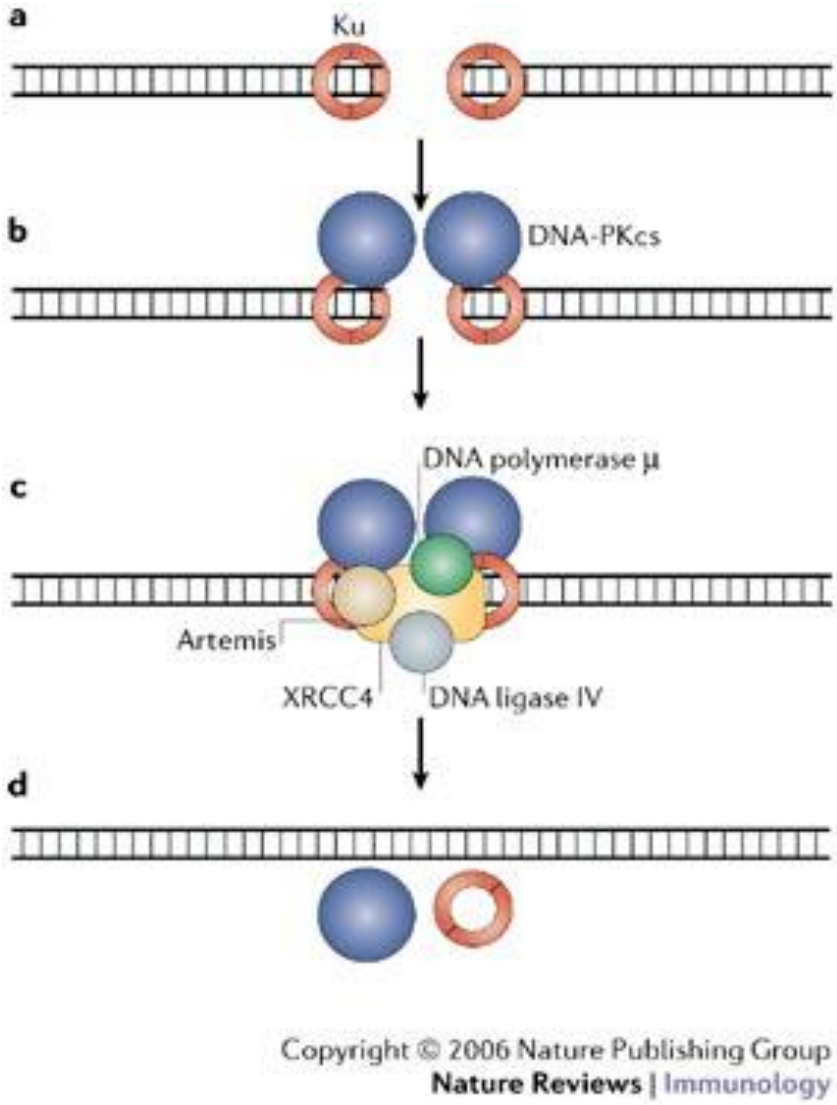

Figure 3. Non-homologous end joining. Reprinted from (10) with permission from Nature Journals.

1.1.3.2 **Homologous Recombination**

Homologous recombination is initiated by extensive resection of a DSB. Initial resection is performed by the Mre11-Rad50-Nbs1 (MRN) complex in coordination with CtIP. Mre11 nicks

the strand some distance away from the DSB with its endonuclease activity, which enables bidirectional resection (11). Mre11 resects towards the break using its 3'->5' exonuclease activity, while Exonuclease 1 (EXO1) resects away from the break using its 5'->3' exonuclease activity (11). Bloom (BLM) and DNA2 cooperate with MRN and Exo1 to promote long-range resection (12). Importantly, the choice to initiate resection is a critical point of regulation of DSBR pathway choice. End protection by Ku and 53BP1 promotes NHEJ, whereas MRN and BRCA1 promote resection and HR (13). BRCA1 plays multiple roles in HR, however, its primary role is thought to be the counteraction of 53BP1 at DNA ends, allowing for resection and subsequent HR steps (14).

Resection generates a long stretch of 3' ssDNA, which is coated by Replication Protein A (RPA) in order to protect the DNA from degradation by nucleases and formation of secondary structures (15). The Rad51 recombinase has to be loaded onto ssDNA in order for strand annealing to occur, therefore, Rad51 has to displace RPA on 3' ssDNA. This displacement is facilitated by a number of accessory proteins, including BRCA2, which interacts directly with Rad51, and the Rad51 paralogs RAD51A, RAD51B, RAD51D, XRCC2, and XRCC3 (16). The other role of BRCA1 in HR is through formation of the BRCA1-PALB2-BRCA2 complex, which is required for efficient Rad51 filament formation (17).

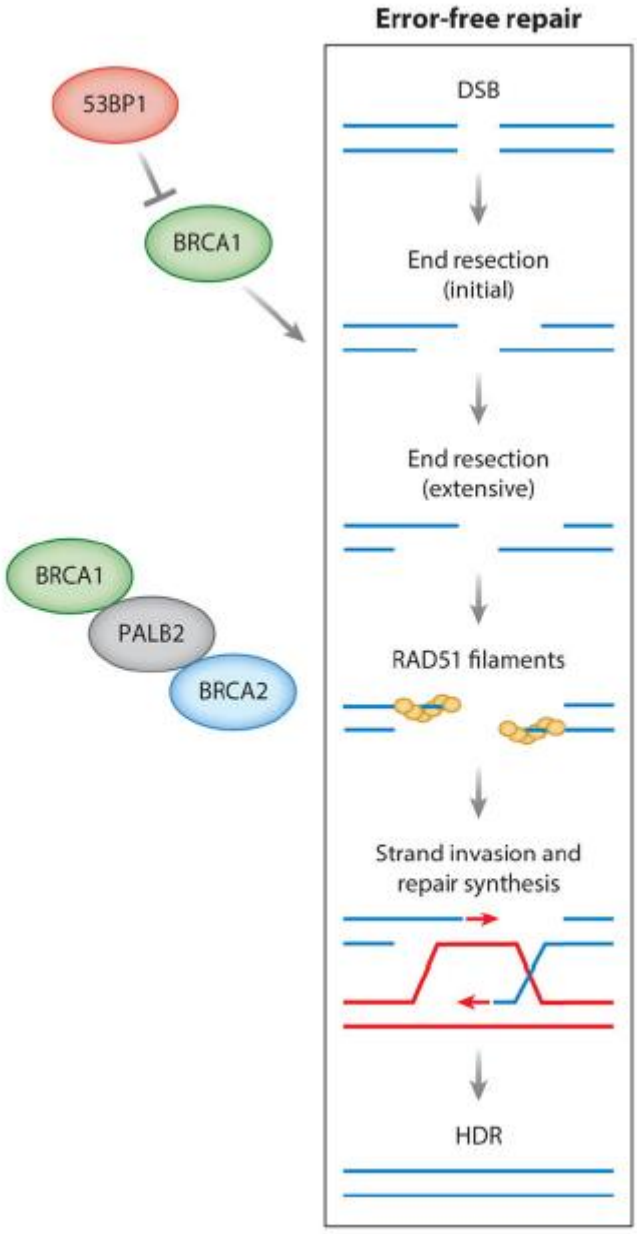

Figure 4. Homologous recombination. Reprinted from (17) with permission from Annual Review of Cancer Biology.

Rad51-coated ssDNA then invades a homologous template. Critically, this homologous template only exists as a sister chromatid during S/G2 phases of the cell cycle, restricting the timing of HR (17). The invading ssDNA acts a primer for extension using the intact duplex as a

template. Extension is performed primarily by Pol δ, but also by the translesions polymerases REV1 and Pol ζ (17). This strand invasion intermediate, called a D-loop, can be resolved in a number of ways. The newly synthesized strand can be displaced and can anneal across the original break, after which fill-in synthesis and ligation can occur, termed synthesis-dependent strand annealing (SDSA) (11). SDSA results in a non-crossover (NCO) event, and is the primary way that HR is completed in mitotic cells (11). Alternatively, double Holliday junctions (dHJs) can form if the second end is captured. dHJs can be resolved in a number of ways, but their outcome can be either NCO or crossover (CO) events (11). COs are biased towards in meiotic cells in order to ensure the correct segregation of chromosomes during meiosis 1 (11). COs in mitotic cells can lead to loss of heterozygosity (LOH) of the region distal to the CO, which can lead to loss of genetic information and potentially drive carcinogenesis (11). A distinct subpathway of HR may be engaged if a single end of a DSB engages with a homologous sequence but the other end does not, this is called break-induced replication (BIR) and will be discussed later.

1.1.3.3 **Microhomology-mediated end joining**

A backup, error-prone DSBR pathway was reported in yeast, which was able to ligate DSBs in the absence of Ku and Ligase IV and required short stretches of homology at the break site (18). NHEJ-independent pathways of DSBR have now been identified in a number of organisms, including humans (19). It is genetically distinct from NHEJ, HR, and another minor pathway, single-strand annealing (SSA) (19). We will refer to this pathway as microhomology-mediated end joining (MMEJ).

MMEJ is believed to be initiated by PARP1, which competes with Ku for DNA ends (20). PARP1 binding bridges and stabilizes DNA ends, and its subsequent activation leads to

recruitment of a number of MMEJ factors, including the MRN complex (21). Initial resection of the 5' end is carried out similarly to HR, by the MRN complex in cooperation with CtIP (22).

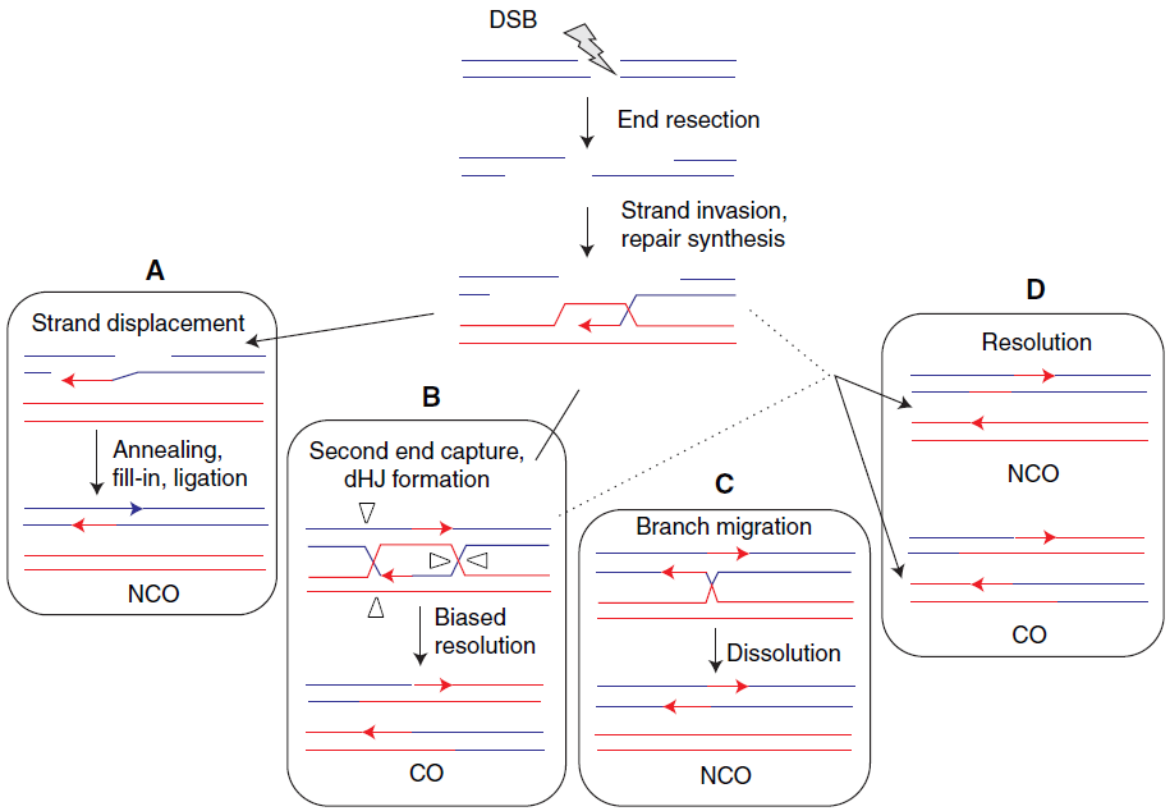

Figure 5. Outcomes of HR. Reprinted from (11) with permission from Cold Spring Harbor Perspectives.

However, long-range resection machinery, including DNA2, Exo1, and BLM, are dispensable for MMEJ (19). The 3'->5' exonuclease activity of Mre11 is sensitive to other DNA ends, and is able to pause when complementary sequences are exposed, allowing for stabilization of DNA ends via microhomology (MH) alignment (23). While both the endonuclease and exonuclease activities of Mre11 have been reported to be required for MMEJ, it is unclear how the endonuclease activity of MRN is regulated during this repair process. It is also unknown how long-range resection is prevented in situations where MMEJ is preferred.

Once MH is exposed by resection, the DNA ends anneal and are stabilized. DNA flaps are trimmed by either FEN1 or CtIP, and gap filling is carried out by Pol β, Pol λ, Pol δ, or the translesion synthesis polymerase Pol θ (POLQ) (19). Polymerase choice by MMEJ is not well-understood, although POLQ has been shown to have specific characteristics that make it compatible with MMEJ. It has a specialized helicase domain that enables displacement of RPA (which suppresses MMEJ) from ssDNA stretches, and contains RAD51-binding motifs that block HR (24-26). Additionally, POLQ can oscillate between three different modes of terminal transferase activity that are most efficient on 3' overhangs, which accounts for insertions that are frequently observed during MMEJ (27). POLQ also has a thumb subdomain in its polymerase domain that enables it to grasp the primer terminus in order to extend poorly annealed termini and bridge DNA ends (28). Importantly, while evidence has accumulated to support POLQ as a key MMEJ factor, there has been no observation of interactions between POLQ and other factors that promote MMEJ.

Significance evidence supports Ligase 3 as the primary MMEJ ligase. Ligase 3 complexes with XRCC1 in cells, which is required for its stability (29). The Lig3/XRCC1 complex physically and functionally interacts with the MRN complex in order to join duplexes with MH internal to breaks, resulting in deletion of the intervening segment between opposing MH regions (30). How these complexes interact, and whether PARP1 or the MRN complex directs Lig3/XRCC1 to MMEJ sites, is unknown. Ligase I has also been reported in several studies as acting in MMEJ (31,32). Notably, XRCC1 has also been observed to exist in complex with Lig1, although a direct interaction has not been demonstrated (3). How the choice of ligase is regulated and whether Lig1-dependent MMEJ is connected to DNA replication is unknown.

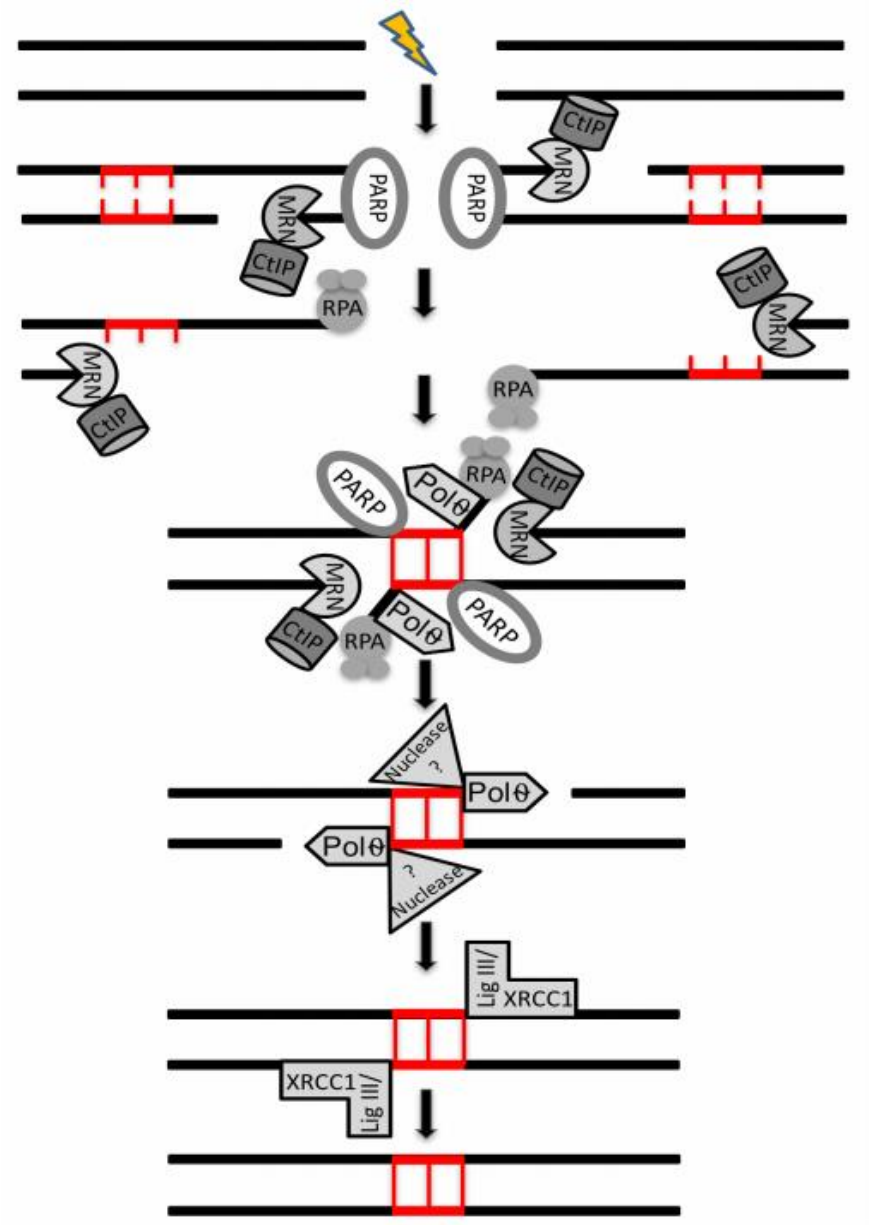

Figure 6. Microhomology-mediated end joining. Reprinted from (19) with permission from Journal of Biological Chemistry.

Crucially, the outcome of MMEJ is deletion of the intervening segment between MH, making it significantly more error-prone than NHEJ and HR (19). Insertions also commonly occur due to the template-independent activity of POLQ (33). Annealing can also take place with MH on different chromosomes, the outcome of which would be gross chromosomal

translocations. Generally, the mechanism of MMEJ is poorly understood, in particular its regulation and usage in normal cells, the roles of PARP1 and XRCC1, and its relation to genomic instability and cancer.

1.2 Replication fork repair, protection, and restart

Accurate replication of the genome is constantly challenged by DNA lesions that arise both from normal metabolic processes and exogenous agents. Additionally, DNA-protein complexes, transcription complexes, and intrinsic DNA secondary structures can act as obstacles to replication forks (34). DNA lesions can block polymerase procession and replicative helicases, replication of unrepaired DNA can result in errors, and DSBs can arise when replication forks stall and collapse (34). Coordination of DNA repair and replication ensures that DNA replication is completed with minimal errors when DNA damage is present. Both translesion synthesis and fork repriming can bypass lesions on ssDNA that are better repaired in the context of dsDNA (35). Stalled forks can be reversed, where nascent strands anneal and reverse the replisome, allowing for better access of repair machinery to the blocking lesion (35). Multiple replication origins allow for rescue of stalled forks by converging forks (35). Finally, broken and collapsed forks can be repaired by the homology-dependent pathways of fork repair that involve template switching, HR factors, break-induced replication (BIR), and microhomology-mediated BIR (MMBIR) (35). These pathways are coordinated with replication fork protection mechanisms, which prevent nascent strand degradation and promote genome stability, as well as replication restart mechanisms that ensure faithful duplication of the genome following replication fork stalling (35).

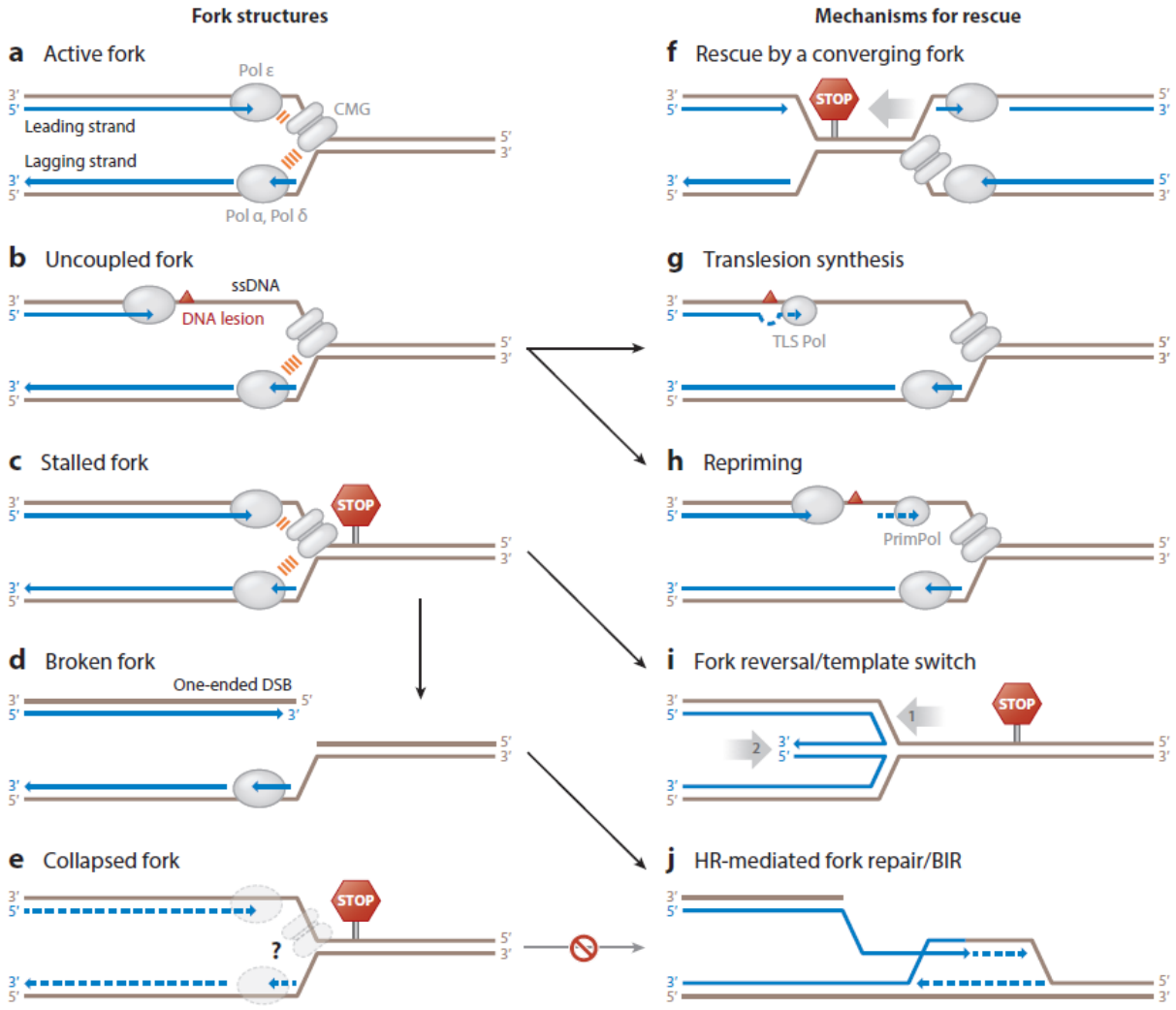

Figure 7. Replication fork-associated damage and repair. Of particular interest are stalled, broken, and collapsed forks, which are repaired by fork reversal, restart, and HR/BIR/MMBIR pathways. Reprinted from (36) with permission from Annual Review Genetics.

1.2.1 **Replication fork repair**

While a number of mechanisms operate with replication in order to ensure fidelity, we will discuss replication fork stalling, protection, and collapse, which generates single-ended DSBs (seDSBs), and mechanisms of fork restart, which repair seDSBs. DSBs can arise during DNA replication via a number of mechanisms, including A) collision of the replisome with SSBs on the leading strand template, B) cleavage of reversed forks by Artemis, XPF, or other

nucleases, C) cleavage of stalled forks by structure-specific endonucleases like MUS81, or D) collision of forks with topoisomerase-DNA complexes stabilized by topoisomerase inhibitors (34). While it is not well understood how seDSBs are repaired, I will go over a major pathway of seDSB repair, BIR and a subpathway of BIR, MMBIR.

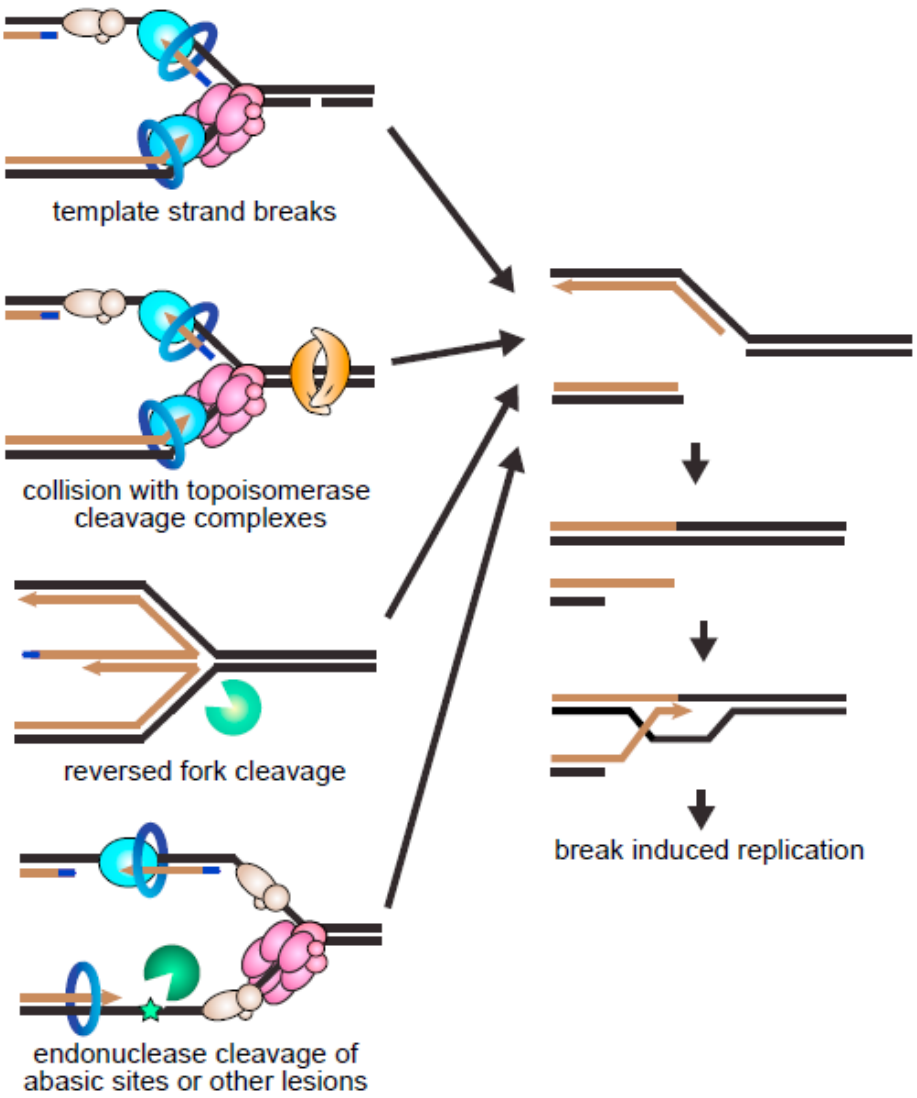

Figure 8. Sources of single-ended DSBs in mammalian cells. Reprinted from (34) with permission from Elsevier.

The single-ended nature of these DSBs precludes repair by direct end joining and necessitates recombination. As we discussed previously for HR, resection of 5' DNA at a DSB

exposes 3’ ssDNA that can invade a homologous template and be used as a primer for extension. Since seDSBs are often generated by fork collapse, there is often homologous DNA nearby in the form of a replicating sister chromatid. Several BIR steps are similar to HR, including resection, RPA binding, and Rad51 displacement of RPA that facilitates homology search and invasion (37). However, DNA synthesis proceeds using a migrating D-loop that continuously displaces the newly synthesized strand (37). This mode of synthesis leads to accumulation of a long stretch of newly synthesized ssDNA, making it susceptible to DNA damage and mutagenesis (38). Synthesis continues until the end of the chromosome or until another replication fork is encountered. To complete repair, the newly synthesized strand is utilized as a template, resulting in conservative inheritance (38). Several polymerases, including Pol ε, Pol α, and Pol δ, take part in BIR. Pol δ is thought to be the primary polymerase taking part in leading strand synthesis, whereas Pol α promotes initiation of leading strand synthesis and lagging strand synthesis (38). In contrast to HR, BIR is highly error-prone, as more frameshift, template-switching, and misincorporation errors take place, likely because of slippage and disassociation of Pol δ from the template (38).

There are both Rad51-dependent and Rad51-independent pathways of BIR, and both have been best studied in yeast. The Rad51-dependent pathway requires longer stretches of homology, is more efficient, and requires Rad55, Rad54 and Rad57. The Rad51-independent pathway depends on Rad59, the Mre11-Rad50-Xrs2 complex, and on the chromatin remodeler complex Rdh54 Swi2/Snf2. Both pathways require Rad52. Rad51-independent BIR is thought to occur via Rad52-mediated annealing of small regions of homology on broken DNA ends that can arise from replication, transcription, or secondary DNA structures.

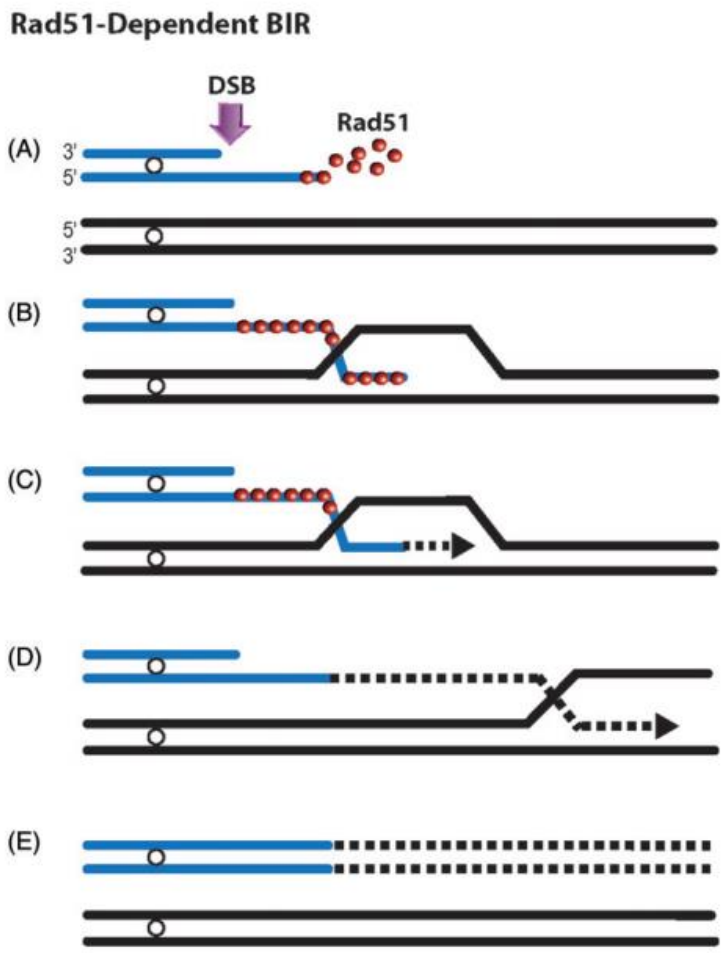

Figure 9. Rad51-dependent break-induced replication. Reprinted from (37) with permission from Taylor and Francis.

The preference of Rad51-independent BIR for short stretches of homology has led to the suggestion that it is similar to the MMBIR pathway. MMBIR is Rad51-independent, Rad52-dependent, and contributes to segmental duplications caused by replication stress (37). This MMBIR, Rad51-independent pathway was also found to be engaged at telomeric breaks and at chromosome fragile sites (CFSs) (37). Additionally, it is thought to contribute to complex genomic rearrangements (CGRs) that are observed in a number of genetic neurological diseases (39). One type of CGR, chromoanasynthesis, is characterized by chromosomal rearrangements in addition to copy number gains (duplications, triplications, and quadruplications) with

microhomology at their breakpoints (39). Another type of CGR, chromothripsis, is common in cancers and involves chromosome ‘shattering’ that is reflected in a large number of rearrangements restricted to a single chromosome (39). Regardless of the outcome, current MMBIR models involve a single DNA end that anneals with microhomology repeatedly in different genomic regions, effectively switching template strands and resulting in a CGR.

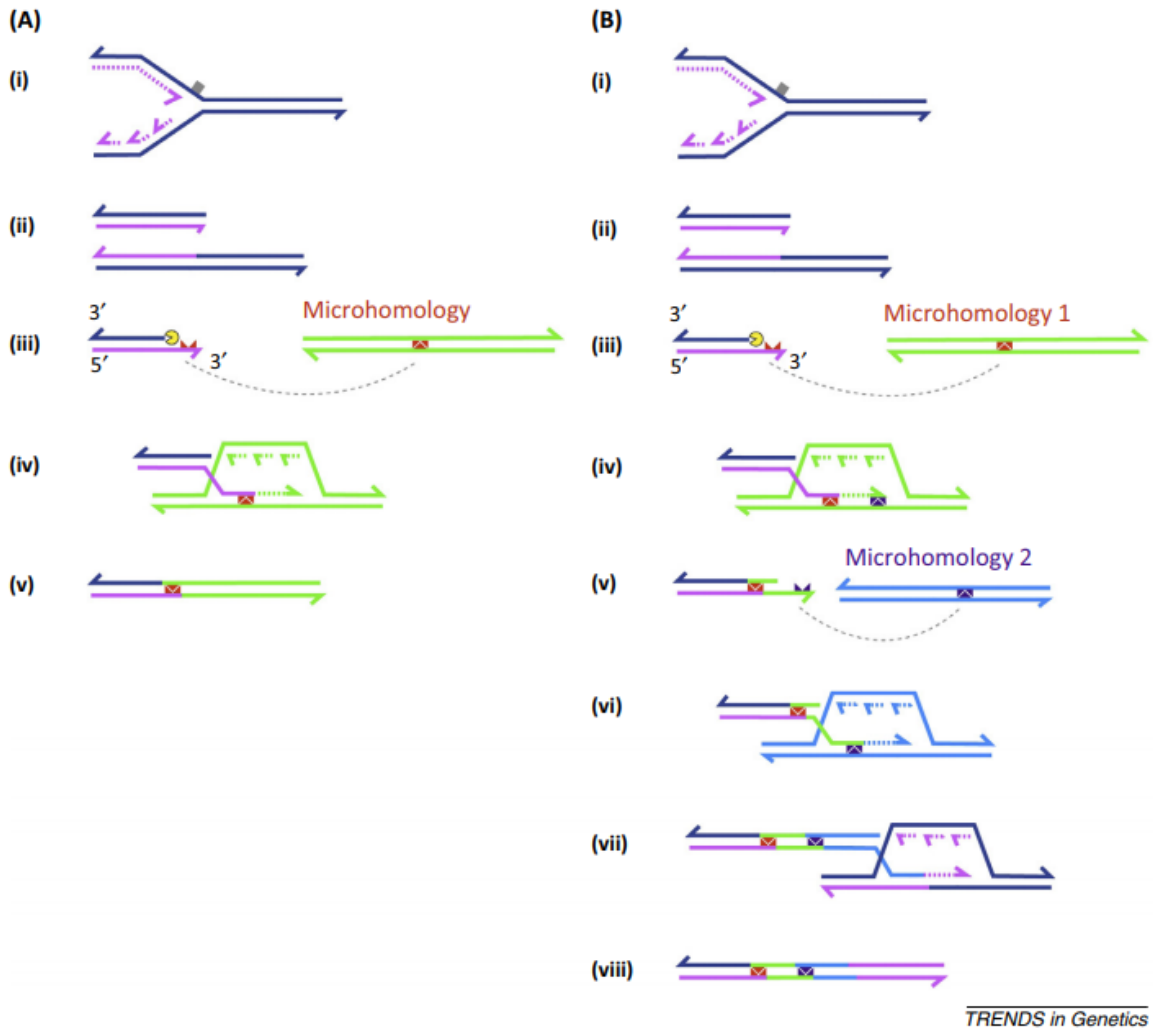

Figure 10. Schematic of microhomology-mediated break-induced replication. Chromosomal rearrangement outcomes are shown. Reprinted from (40) with permission from Cell Press.

Importantly, Rad51-independent BIR/MMBIR is induced by replication stress, as observed in a cyclin E overexpression model that led to replication fork collapse, DSBs, and

repair which led to tandem duplications and chromosomal rearrangements (41). Similarly, deregulated origin licensing that leads to rereplication and replication fork collapse induced Rad51-independent BIR/MMBIR (42). MMBIR is also a mechanism of repair used collapsed replication forks at chromosomal fragile sites (CFSs), locations in the human genome that frequently exhibit chromosome breaks during replication stress (43).

The limitations of current models make it difficult to distinguish between Rad51-independent BIR and MMBIR, and whether they represent the same pathway is unknown. Additionally, the prevalence of DNA end-joining by NHEJ and MMEJ in mammals make distinguishing between BIR, MMBIR, NHEJ, and MMEJ difficult. The lack of mammalian systems for studying replication fork breakage and repair in order to determine the genetic requirements of these pathways is a major obstacle for CGR study in cancers and genetic disease.

1.2.2 **Replication fork reversal, protection, and restart**

Stabilizing stalled replication forks and restarting them efficiently is necessary for genome stability. A primary intermediate of restarting forks is the reversed fork, in which nascent DNA strands are annealed to form two important structures: 1) a four-way structure that resembles a Holliday junction (HJ), and 2) a seDSB. Fork reversal can promote genome stability in several different ways. First, by putting template strand lesions into the context of dsDNA, repair is promoted (35). Second, as we have gone over previously, endonuclease cleavage can lead to seDSB and BIR/MMBIR. Third, if the nascent strands anneal, a new primer-template junction is formed that can replicate past the lesion (35). And finally, a converging fork can replicate the region. In these ways, fork reversal is an important mechanism of maintaining genome stability.

Fork reversal first involves the annealing of the two nascent strands, followed by restart of the reversed fork. The annealing of the two nascent strands unsurprisingly requires the RAD51 recombinase, but also requires a DNA translocase, of which there are three, HLTF, SMARCAL1, and ZRANB3 (35). The contribution of these factors to fork reversal is still being explored, but SMARCAL1 appears to act early on in fork reversal and primarily at leading strand gaps, whereas HLTF is activated by lagging strand gaps (34).

Once the reversed fork has been established, the exposed nascent strands of the fork typically undergo some amount of resection, in order to expose ssDNA that can either activate translocases to reestablish an active fork or switch templates, both of which restart replication (34). Unsurprisingly, the same group of nucleases that take part in resection during HR (MRE11, CtIP, EXO1, and DNA2) participate in resection of reversed forks (34,44). Importantly, they can prevent the accumulation of DSBs by promoting HR during replication. This is thought to be by controlled resection that enables fork restart, which has been conclusively demonstrated in the case of DNA2 in cooperation with the Werner (WRN) helicase (34). Exposed 3' overhang of the reversed fork can be coated by RAD51, which, because of homology of the nascent strand with parental DNA, could facilitate annealing with sequences ahead of the fork and establishment of a D-loop that can restart replication. Alternatively, the 3' overhang can be coated with RPA, which is recognized by the SMARCAL1 translocase, which uses an ATP motor to drive branch migration and reestablishment of an active fork (34). CtIP and MRE11 are known to be critical for fork restart, by removing Ku from seDSBs that exist at collapsed or reversed forks (45). Resection by MRE11 and CtIP is limited by Rad51, and more extensive resection is performed by EXO1 and DNA2 (44). How the extent of resection affects ssDNA coating by RPA/RAD51, template switching and/or reestablishment of the fork, and homology usage in restart pathways

(analogous to resection regulation in overt DSBR by MMEJ and HR) is not well-understood. Additionally, the coordination of resection with other factors reported to be involved in fork restart, including PARP1 and the helicase RECQ1, has not been well-explored.

While controlled resection often promotes fork restart and genomic stability, extensive resection and degradation of stalled forks can be detrimental to cells and cause chromosomal aberrations. Prevention of this extensive resection is termed replication fork protection. BRCA1, BRCA2, and some of the Fanconi Anemia (FA) group proteins were discovered to be required for replication fork protection. Replication tracts that are stalled with hydroxyurea (an inhibitor of ribonucleotide reductase that depletes nucleotide pools) were initially observed to be degraded when BRCA2 was absent (46). Tracts were also degraded when Rad51-stabilization-defective mutant BRCA2 was present, which did not affect HR, indicating that the functions of BRCA2 in fork protection and HR were separable (46). The nucleases responsible for fork degradation in the absence of BRCA2 were found to be CtIP, MRE11 and EXO1, and degradation led to chromosomal aberrations (46). Similar findings were observed for BRCA1 and FANCD2 (47). These findings have led to a model where extensive degradation of stalled forks in BRCA-deficient and FA-deficient cancer cells contributes to their chromosomal rearrangement phenotypes.

Based on the observation that BRCA2 stabilizes Rad51 for fork protection, it is likely that the role of HR proteins in this pathway is in preventing the degradation of ssDNA through Rad51 stabilization. Since the primary source of long stretches of ssDNA at replication forks is after replication fork reversal, which occurs frequently at stalled forks in order to repair lesions that block replication, this function of BRCA2 and Rad51 was thought to be important for reversed fork stabilization only. This is indeed one of the functions of BRCA2-Rad51, as

observed recently. When forks are persistently stalled, forks are reversed by the SMARCAL1 helicase, where BRCA2 stabilizes Rad51 onto nascent ssDNA, which protects it from degradation by MRE11, as expected (48). Surprisingly, Rad51 exhibited an additional function, as it was shown to bind not only to reversed forks, but also to ssDNA gaps at replication fork junctions, which was promoted by BRCA2 (48). Rad51 binds directly to Pol α, and facilitates Pol α and δ binding to stalled forks, likely promoting fork restart and preventing fork reversal (48).

BRCA1 has very recently been shown to complex with BARD1 for fork protection. The BRCA1-BARD1 complex interacts with RAD51, which promotes RAD51 accumulation at stalled replication forks (49). Genetic variants of BRCA1 and BARD1 were identified in human cancer patients, and were demonstrated to have defective nascent strand protection but HR proficiency, again separating the functions of replication fork protection from HR (49). Whether this pathway is distinct from BRCA2-dependent pathways of fork protection is unknown, but it is clear that replication fork protection by a variety of HR and FA factors is critical for genome stability and cancer prevention.

Interestingly, these extensively resected forks can still restart. However, restart after degradation leads to chromosomal aberrations and genomic instability (46). Recent studies have suggested that this pathway of restart is dependent on MUS81 and POLD3 and is a BIR/MMBIR-like pathway (44). Interestingly, this pathway is important for fork restart in BRCA2-deficient cells but not BRCA1-deficient cells (44). We will discuss the connection between this fork degradation phenotype, mutational signatures, and the efficacy of PARP inhibitors in BRCA-deficient cancers in a later section.

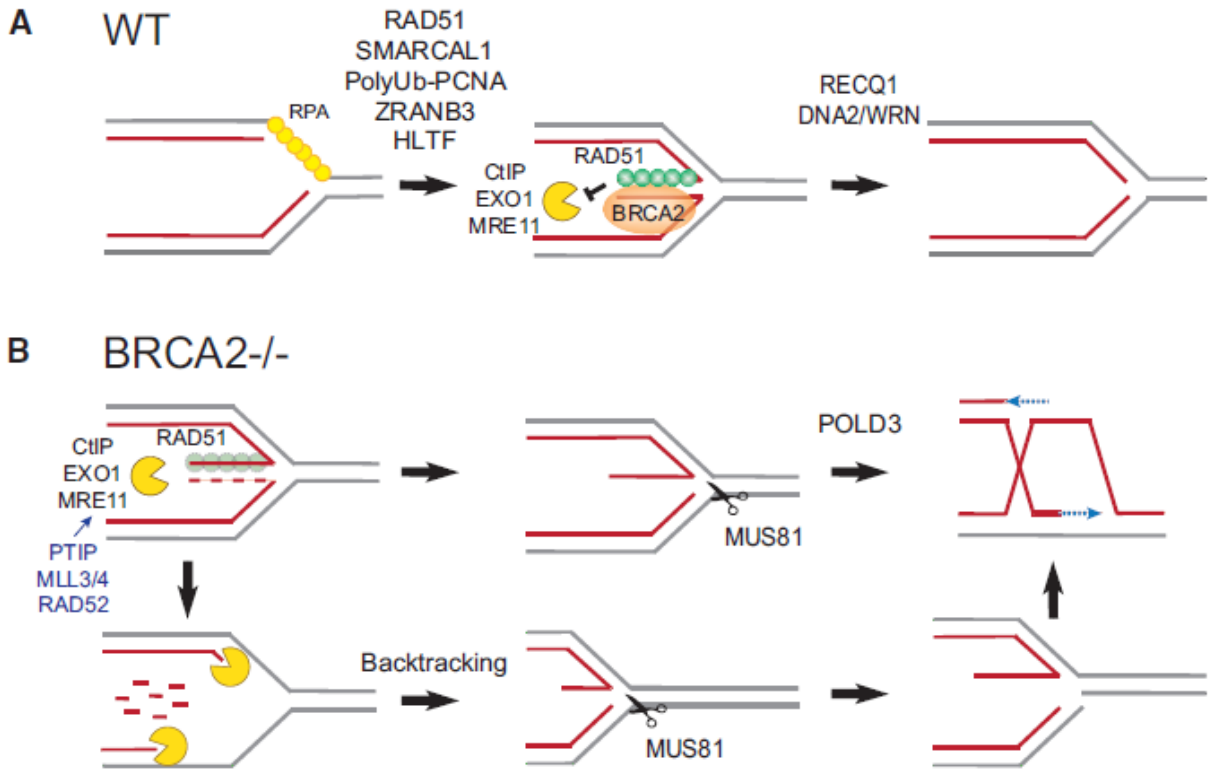

Figure 11. Mammalian fork protection and restart in WT and BRCA2-deficient cells. Reprinted from (35) with permission from Elsevier.

1.3 Ionizing radiation in genome damage and repair

Ionizing radiation (IR) is used for radiation therapy (RT), a primary method of cancer treatment. Close to half of all cancer patients will receive some form of RT as a part of their overall therapeutic plan (50,51). The main principles of RT are twofold: 1) targeting of IR to the tumor volume can locally induce genome damage to kill cancer cells and spare healthy tissues, and 2) deficiencies in DNA repair and high rates of replication sensitize cancer cells to IR, whereas normal cells are able to repair IR-induced damage. The effectiveness of these principles can be enhanced by understanding the DNA repair phenotype of an individual cancer, and combining RT with chemical agents that target effectors that participate in the DNA damage response (DDR) (50). The toxic effect of DDR inhibitors that are administered systemically is

limited by the redundant nature of elements of the DDR in normal cells, whereas cancer cells that are deficient in one or more DNA repair pathways are unable to repair damages and die (50).

While DNA damage is continually induced by oxidative stress, these oxidative lesions are distributed throughout the genome, and single lesions can be repaired with relative ease. Since IR involves the linear passage of energy through a cell, energy is deposited linearly when is passes through or nearby a DNA molecule. The proportion of DNA lesions induced by IR that are within a defined region of the DNA helix is therefore higher than an equal number of DNA lesions induced by oxidative stress. These sites of IR-induced damage localized to a small region of DNA are termed clustered damages, and are characteristic of IR (52).

How much energy a given type of IR deposits within a given length is called the linear energy transfer (LET). X-rays and γ-rays are low-LET, whereas particle radiation is high-LET. Low LET IR deposits roughly 30% of its energy as clustered damages, whereas high-LET IR deposits around 90% of its energy as clustered damages (53). Importantly, clustered DNA lesions induced by IR are difficult to repair (52). The damages induced by these types of IR is summarized in Table 1.

DSBs are thought to be the most cytotoxic DNA lesion induced by IR. These DSBs are often complex, as they have 3'phosphoglycolate or 3'-phosphate ends, single-stranded overhangs, and nearby base lesions or abasic sites. Complex DSBs are also more difficult to repair than clean DSBs, which contributes to the effectiveness of IR in cell killing. Secondary DSBs can also be generated by the attempted repair of closely spaced base lesions and/or SSBs.

IR-induced lesions in DNA	Number/Gy/cell	Number/Gy/cell
	γ-radiation	$^{12}C^{6+}$ ions (31.5 keV/μm)
5,6-thymine glycol	582	372
5-(hydroxymethyl)-2′-deoxyuridine	174	72
5-formyl-2′-deoxyuridine	132	66
FapyG	234	132
8-oxo-7,8-dihydro-2′-deoxyguanosine	120	60
SSBs	1000	

Table 1. Estimated quantity of DNA lesions generated by ionizing radiation. Adapted from (52) with permission from Elsevier.

Cell killing by different forms of IR, which is termed relative biological effectiveness (RBE), is roughly proportional to DSB induction, which is dependent on LET. This concept of LET and RBE is shown in Figure 12. LET values of different types of IR is shown in Table 2.

Type of Radiation	**Energy**	**LET (keV/μm)**
X-rays	250 kV	3
	3 MV	0.3
Cobalt-60	1.17–133 MV	0.3
Beta particles	10 kV	2.3
	1 MV	0.25
Neutrons	2.5 MV	20
	19 MV	7
Protons	2 MV	16
α-particles	5 MV	100

Table 2. LET values for different types of ionizing radiation. Adapted from (52) with permission from Elsevier.

While repair of individual lesions induced by IR has been well studied, repair of clustered DNA damage is not well understood. Mechanisms previously discussed are used to repair single base lesions (BER), single-strand breaks (SSBs), and DSBs (NHEJ, HR). Notably, the contribution of MMEJ to repair of IR-induced DNA lesions is has not been appreciated. Understanding the repair of IR-induced DSBs and clustered lesions is critical for proper

application of RT and chemotherapy, as well as a variety of other areas, including space exploration, workplace exposures, and nuclear power plant disasters.

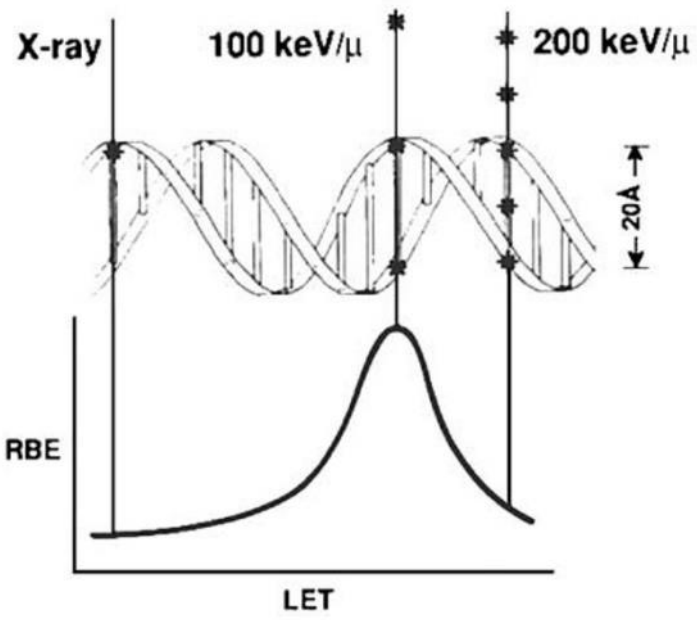

Figure 12. Relationship between Linear Energy Transfer and Relative Biological Effectiveness. At peak RBE, the average distance between ionization events is roughly the diameter of the DNA double-helix, leading to a high number of DSBs. Reprinted from (53) with permission from Nature Journals.

1.4 DNA repair in homologous recombination-deficient tumors

Germline mutations in BRCA1 and BRCA2 are associated with the development of breast, ovarian, and other cancers (54). As discussed previously, BRCA1 and BRCA2 are both involved in HR and replication fork protection. HR is an error-free process, and when HR is defective, alternative DNA pathways are engaged to repair DSBs and restore DNA replication. The other modes of DSB repair, NHEJ and MMEJ, either join DNA ends directly without the use of sequence homology or use small stretches of homology on both sides of the break to stabilize an annealed intermediate, deleting the intervening sequence. Use of these alternative pathways leads to accumulation of mutations, including small insertions and deletions. It is possible that

increased use of error-prone pathways drives cancer initiation and progression, although diverse roles of BRCA1/2 in the cell could potentially be responsible for pathogenesis.

Two groups independently described the hypersensitivity of BRCA1/2-deficient cells to inhibitors of the DNA damage sensor and signal transducer PARP1 (PARPi) (55,56). This sensitivity suggested a novel treatment strategy for HRD breast and ovarian cancers, and led to the testing of PARPi in clinical trials. The effectiveness of PARPi in HRD tumors was originally thought to be because of persistent SSBs that led to fork collapse and DSBs that could not be repaired via HR (57). It is now thought that PARPi prevent autoPARylation, which prevents PARP1 release from DNA, 'trapping' it (57). Trapped PARP1 is considered to be a DNA lesion, similar to inhibited Topoisomerase II-DNA adducts. Support for this model comes from the observations that PARP1-deficient cells are resistant to PARPi and that the amount of PARP1 trapping is a better predictor of cytotoxicity in BRCA-deficient cells that inhibition of PARylation (57). Several different PARPi have been developed; all trap PARP1 to different extents.

In vitro observations of PARPi efficacy have been strongly supported by clinical trials results; several PARPi - olaparib, rucaparib, and niraparib - have now been approved for cancer therapy in various settings (58). In controlled disease settings, olaparib was first approved in 2014 for maintenance therapy in platinum sensitive, BRCA1/2-mutant ovarian cancers that are in remission after chemotherapy (58). Further investigation led to the approval of olaparib for maintenance therapy of ovarian cancers regardless of BRCA1/2 mutation status in 2017 (58). Niriparib was approved for similar indications in 2017, although the effect of progression-free survival was highest in BRCA1/2 mutants, intermediate in BRCA1/2 wild-type patients that had HRD (as diagnosed by the next-generation sequencing (NGS)-based myChoice), and minor in

patients without HRD (58). Similar data was reported for rucaparib in maintenance therapy for ovarian cancer, which was approved in April 2018 (58). In relapsed disease settings, PARPi have also shown a significant clinical impact. The FDA approved olaparib in 2014 as monotherapy for BRCA1/2 mutant, advanced ovarian cancer (58). Rucaparib was approved for similar applications in 2016 (58). Talazoparib and veliparib are in late-phase trials for newly diagnosed advanced ovarian and other cancers (58).

For breast cancers, olaparib has been approved for monotherapy in patients with germline BRCA1/2 mutant, HER2-negative, metastatic disease (58). Talazoparib has exhibited a similar benefit in these patients in phase III trials (58). Maintenance therapy for BRCA1/2-mutant breast cancer patients with olaparib is currently being tested, and clinical testing of PARPi as monotherapy and combination therapy in the neoadjuvant setting is also underway (58). Positive results have been demonstrated for veliparib with carboplatin in triple-negative breast cancers, although veliparib with carboplatin and paclitaxel did not show a benefit in pathological complete response (58). Monotherapy with talazoparib in the neoadjuvant setting has been promising for BRCA1/2-mutant, HER2-negative breast cancers, rationalizing targeting of these tumors with PARPi early in disease progression (58).

1.4.1 Resistance to PARPi

Importantly, chemotherapy with PARPi can lead to the acquisition of resistance to PARPi, like most chemotherapeutic strategies (57). There are several possible mechanisms of resistance that have thus far been identified. These mechanisms center around restoration of HR, which when functional can effectively repair trapped PARP1-DNA lesions. These can be mutations in BRCA1 or BRCA2 that revert the original mutation to produce a functional protein, or disruption of 53BP1 or REV7 (57). Additionally, loss of PARP1 itself leads to resistance of

PARPi (57). These mechanisms of PARPi resistance can also lead to resistance to platinum agents (57). An important aspect of the clinical development of PARPi applications is combination therapies that minimize the development of resistance and treatment plans that account for the similarities in mechanisms of resistance to PARPi and platinum agents.

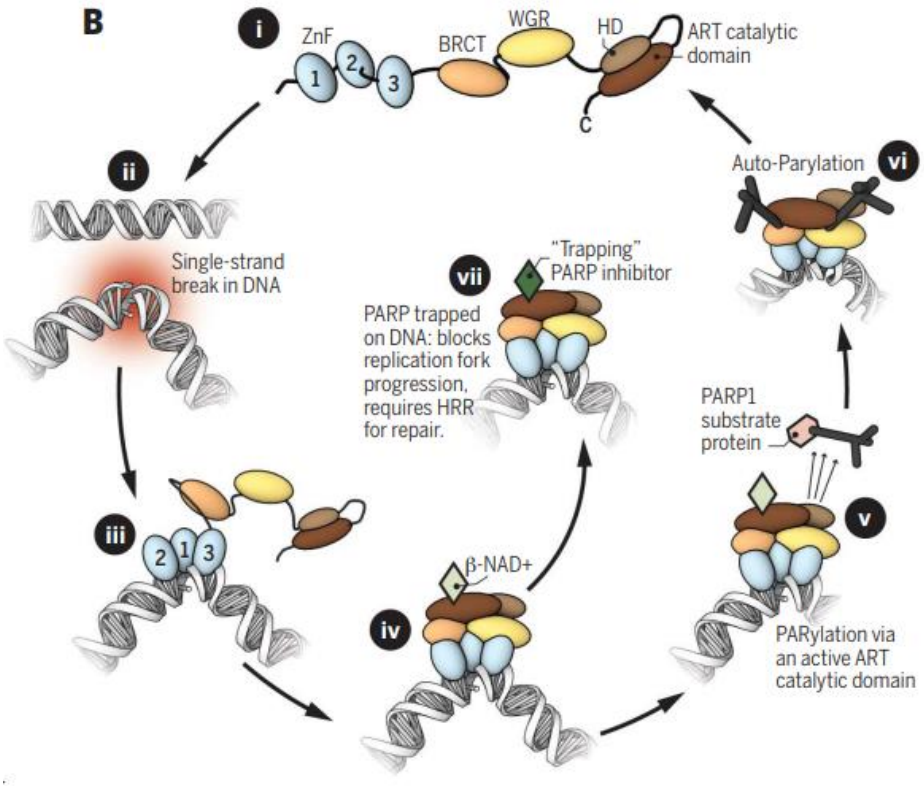

Figure 13. Mechanism of cell killing by PARP1 inhibition. PARP1 (i) is recruited to SSBs (ii), where it is activated to catalyze the addition of ADP-ribose polymers to itself and a variety of other substrates. Without inhibition, PARP1 auto-PARylation results in its release (vi), however, when PARP1 is inhibited it cannot auto-PARylate and it remains trapped on DNA. Reprinted from (57) with permission from Science.

1.4.2 Application of PARPi

Detection of BRCA1/BRCA2 mutations, both germline and somatic, through NGS has typically been used as the predictive biomarker of PARPi sensitivity, and NGS has been approved as a companion diagnostic in several scenarios (58). However, the exact effect of

BRCA1/2 mutations on HR is not well understood, and additional breast cancer susceptibility genes that confer PARPi sensitivity have been identified which have uncertain effects on HR capacity (58). Discovery of functional biomarkers of HR and other DDR pathways that accurately predict PARPi sensitivity is a critical goal for proper application of PARPi (58).

To this end, several distinct approaches have been considered, including sequencing of panels of PARPi-sensitivity-related genes, transcriptomic approaches, platinum sensitivity, immunohistochemical panels of HR proteins, and whole-genome sequencing (WGS) (58). Cancer genome sequencing projects, including those undertaken by Wellcome Trust Sanger Institute, have uncovered mutational signatures in human cancers, including a specific mutational signature, signature 3, that is specifically associated with BRCA1/2-mutant cancers, and occurs frequently in breast, ovarian, prostate, and pancreatic tumors (59). In addition to being associated with BRCA1/2 mutations, the signature is also associated with inactivation of BRCA genes through methylation, and mutations in other HR genes (60). This has led to the hypothesis that this signature is a more sensitive predictor of HR-deficiency, and thus PARPi sensitivity, than HR gene panel sequencing and other methods (61). Signature 3 includes single base substitutions in combination with large rearrangements that contain microhomology at their breakpoints, indicative of preferential use of alternative pathways for DNA repair in the absence of HR, likely MMEJ (59). While these mutational signatures indicate the collective use of DNA repair over the lifetime of the tumor, they do not indicate when these mutations take place and what repair pathways are active currently in the tumor. Therefore, it is possible that despite HR being inactivated for much of the tumor lifetime, cells with signature 3 could be HR-proficient, or could easily revert from HR-deficiency to proficiency. Based on the problems facing each

possible method of HR-deficiency diagnosis, it is likely that a combination of approaches will emerge as the most effective solution (58).

1.4.3 Mutational Signature in Human Cancers

Cancers acquire somatic mutations and copy number alterations as they progress. It is now clear that these mutations and structural alterations are in part due to altered DNA repair capacity of tumors (62). Detection of specific patterns of mutations and rearrangements can identify changes in DNA repair in tumors that can inform a precision medicine approach to cancer therapy (62).

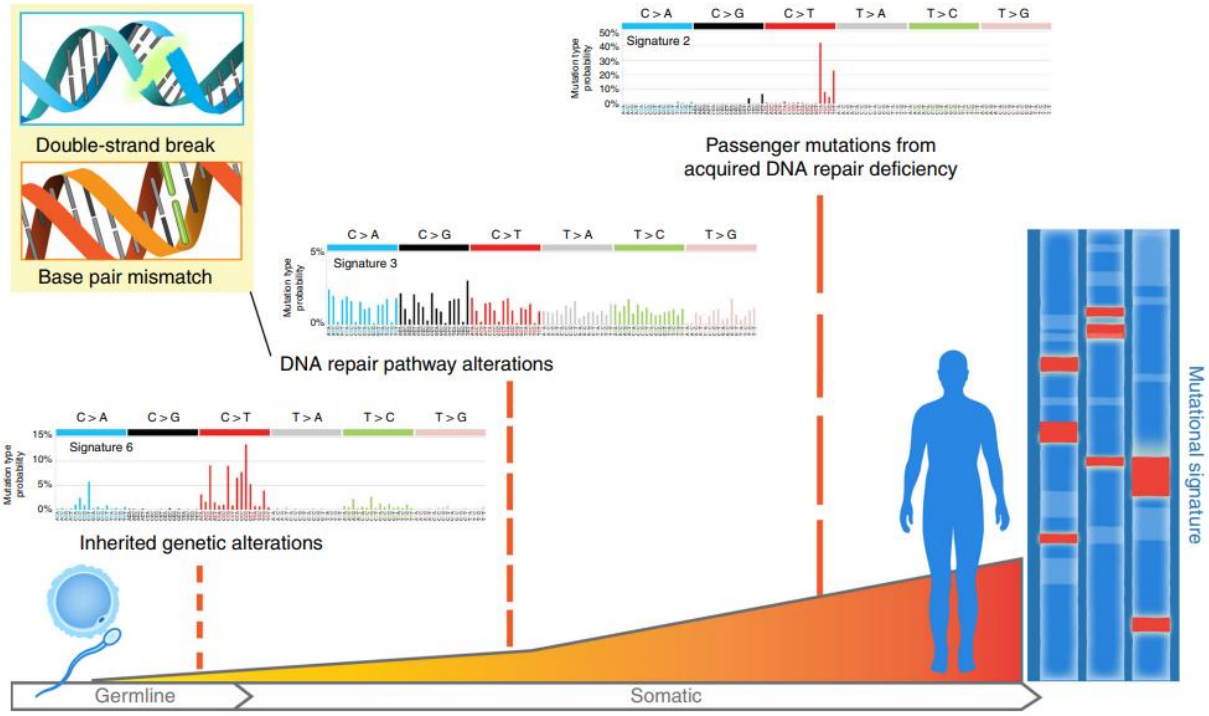

Figure 14. Mutational signatures in human cancer. A cancer's mutational signature is a record of DNA damage and repair that depends on a variety of factors. Reprinted from (62) with permission from Nature Journals.

The advent of genomic sequencing capabilities and tumor database projects have made statistical identification of these mutational signatures and their association with other tumor

features possible. Array-based comparative genomic hybridization and single-nucleotide polymorphism technologies have been used to identify copy number changes, which was used to define initial signatures of HR-deficiency by telomeric allelic imbalances, large-scale state transitions, and loss of heterozygosity (LOH) (58). Currently, WGS of human tumors has made it possible to characterize tumors based on single-nucleotide mutations. The six possible single base substitutions (SBS), when placed in the context of the preceding and following bases, define 96 possible mutations. By extracting the number of each mutation type occurring in each tumor, a matrix containing the distribution of mutation types in human cancers can be created. Using a mathematical framework termed non-negative matrix factorization (NMF), distinct mutational signatures that occur commonly in human cancers can be found (59). This process was initially performed by Alexandrov et al. in a seminal paper that identified 30 different mutational signatures in over 7000 cancers (59). Signature associations included age, exposures, and DNA repair deficiencies. Several defective DNA repair pathways have now been discovered to be associated with specific mutational signatures, including HR, mismatch repair (MMR), nucleotide excision repair (NER) and APOBEC cytosine deaminases (62). These defective DNA repair pathways are typically inherited familial syndromes, but can be a result of somatic mutations. Interestingly, this study and similar studies identified mutational signatures in 'atypical' malignancies at a low frequency, indicating that germline mutations in DNA repair genes may predispose carriers to increased cancer rates in several different tissues, e.g non-breast non-ovarian cancer with BRCA1/2 mutations (63). In addition to base substitutions, signatures have now been updated to include the contributions of insertions, deletions, inversions, tandem duplications, and clustering of these structural changes (60). It is now clear that Signature 3 (HR-deficiency-associated SBS signature) is associated with Rearrangement Signatures 3 (small

tandem duplications) and 5 (deletions less than 1 MB) (60). These duplications and deletions have significantly elevated microhomology at their junctions, which implicates preferential usage of MMEJ in these tumors as an alternative to HR (60).

1.4.4 MMEJ and HR-deficiency

The association of Rearrangement Signatures 3 and 5 (which have microhomology at breakpoint junctions) with HR-deficiency raised the possibility of MMEJ taking on an increased role in DSBR in HR-deficient cells. Several recent papers have explored the particular importance of POLQ in DNA repair in HRD cancer cells. Initially, D'Andrea and colleagues found that POLQ expression was upregulated in epithelial ovarian cancers (EOCs) and correlated positively with several HR factors (24). When they depleted POLQ, HR efficiency and RAD51 foci formation increased, and depleted cells were hypersensitive to genotoxic agents, suggesting POLQ both inhibits HR and contributes to genome stability in HR-proficient cells (24). They discovered that POLQ binds directly to RAD51 through the 847-894 amino acid region (24). Additionally, they showed POLQ has activity for replication stress-mediated DNA structures, and found that POLQ contributed to both replication progression and fork restart (24). POLQ expression was found to inversely correlate with HR activity, and depletion of POLQ was synthetically lethal in BRCA1-deficient tumor cells (24). POLQ promoted MMEJ in these tumors, and formed foci that were dependent of PARP1 activity (24). This work identified POLQ as a potential therapeutic target for HRD cancers.

Shortly thereafter, the group of Agnel Sfeir published a study that demonstrated a role for POLQ in chromosomal translocations, and the absence of insertions and microhomology at translocations that did form in POLQ-knockout cells (26). POLQ accumulated at laser-induced DNA breaks, and colocalized with the DSB marker γH2AX at these breaks, which was

dependent on PARP1 activity (26). POLQ was demonstrated to have a role in suppressing HR at telomeres in this work, by counteracting the accumulation of Rad51 foci (26). Depletion of POLQ in BRCA1/2-deficient cells led to the accumulation of chromosome aberrations, indicating that POLQ is required for genomic stability and survival of these cells (26). Sfeir followed up this work in 2017 by demonstrating a clear mechanism for POLQ competition with HR for strand break repair. They examined the effects of the helicase and polymerase domains, as well as the Rad51-interacting motif, on POLQ-mediated repair. The helicase and polymerase domains, but not the Rad51-interacting motif, were found to be necessary for survival of BRCA1-deficient cells (64). They also found that these domains but not the motif were required for translocations (64). Depletion of POLQ was also found to enhance the proportion of genome editing events mediated by HR (64). Then they demonstrated that the helicase domain of POLQ dissociates RPA from ssDNA, promoting MMEJ over HR (64).

BRCA1/2 have also been shown to have direct roles in suppressing microhomology-based repair pathways. BRCA2 was observed to promote HR over MMEJ and NHEJ by stabilizing RPA on ssDNA (65). BRCA1 was shown to suppress tandem duplications that arise via a replication-restart mechanism that is terminated by either canonical end-joining or MH-mediated template switching (66). These tandem duplications occur frequently in rearrangement signature 3 (non-clustered rearrangements with 1-10kb tandem duplications), which is associated with BRCA1 deficiency.

An unbiased CRISPR screen for DNA repair factors synthetic lethal with BRCA2 confirmed the relationship of BRCA2 with POLQ. POLQ knockout produced the strongest effect, although knockout of long-patch BER and MMEJ factors also produced significant cell killing (67). XRCC1, PARP1, FEN1, LIG1 were among the highest scores in these pathways

(67). Interestingly, LIG3 and POLB did not have a strong effect, indicating that XRCC1's effect on survival in this context is not through its role in SSBR/BER. How exactly XRCC1 mediates DNA repair in HR-deficient cells is unknown and the subject of significant interest.

These studies have collectively established suppression of microhomology-based repair mechanisms by HR factors, and rationalize targeting of MMEJ factors, particularly POLQ, for cancer therapy. Targeted integration of donor DNA via HR at CRISPR-induced DSBs has also been shown to benefit from POLQ depletion. To this end, several companies and scientific groups are developing POLQ inhibitors. However, a detailed mechanism of POLQ participation in MMEJ with factors other than PARP1, including XRCC1, MRE11, CtIP, and Lig1/Lig3 remains elusive. How these factors cooperate and form repair complexes in HRD tumor cells is a critical question that will impact future chemotherapeutic development.

1.5 XRCC1 in strand break repair and disease

While we have discussed XRCC1's role in SSBR and MMEJ at a superficial level in previous sections, it is worth examining XRCC1 in more detail. After its discovery by Larry Thompson, XRCC1 was quickly established as a close partner of Ligase 3 and POLB, and a critical component of SSBR (68,69). XRCC1-deficient cells were also found to be sensitive to alkylating agents, UV radiation, and displayed increased levels of sister chromatid exchange (SCE) (70). XRCC1 knockout mice are embryonic lethal, indicating that XRCC1 is required for development.

1.5.1 Structure of XRCC1

The human XRCC1 gene is located on chromosome 19q13.3. Human XRCC1 is a 633 amino acid (aa) protein, composed of three conserved domains, a nuclear localization signal (NLS), and a PAR-binding motif (PARBM). The N-terminal domain (NTD) spans from 1-188

aa, the BRCT1 domain spans from 315-403 aa, and the BRCT2 domain spans from 536-633 aa. Two unstructured linker regions span from 183-315 aa and 403-538 aa. The XRCC1 NLS is located from 239-266 aa, and the PARBM is in the BRCT1 domain from 379-400 aa. The NTD facilitates XRCC1's direct interaction with POLB, which is regulated by the oxidation state of the NTD, suggesting that redox levels in the cell can regulate SSBR at this level (71). The first unstructured linker domain contains an RIR-like motif that mediates a weak interaction with PNKP, and may facilitate an interaction with PCNA (72). The BRCT1 domain provides a surface for multiple protein-protein interactions, including with APE1, various DNA glycosylases, Polα-primase, and PAR (73-75). The PARBM in this domain makes it likely that PARylation regulates some or all of these interactions. The second linker domain contains a forkhead-associated (FHA) domain, which mediates interactions with APLF, APTX, and PNKP (76,77). Finally, the BRCT2 domain of XRCC1 mediates its strong interaction with LIG3, stabilizing LIG3 levels (78). XRCC1 can also homodimerize and form a heterotetramer with LIG3, although the biological significance of these multimers is not known (79).

1.5.2 Post-translational modification of XRCC1

Post-translational modifications, such as phosphorylation, ubiquitination, acetylation, and PARylation can regulate protein function by modulating protein-protein interactions, functional activity, or degradation, among others (80). XRCC1 has several serine/threonine residues that are possible substrates for S/T kinases, many of them in the second linker region. Reported examples of XRCC1 phosphorylation include phosphorylation by checkpoint kinase 2 (CHK2) on Thr284 (81), which promotes BER, and phosphorylation by DNA-PK at Ser371 (in the BRCT1 domain),

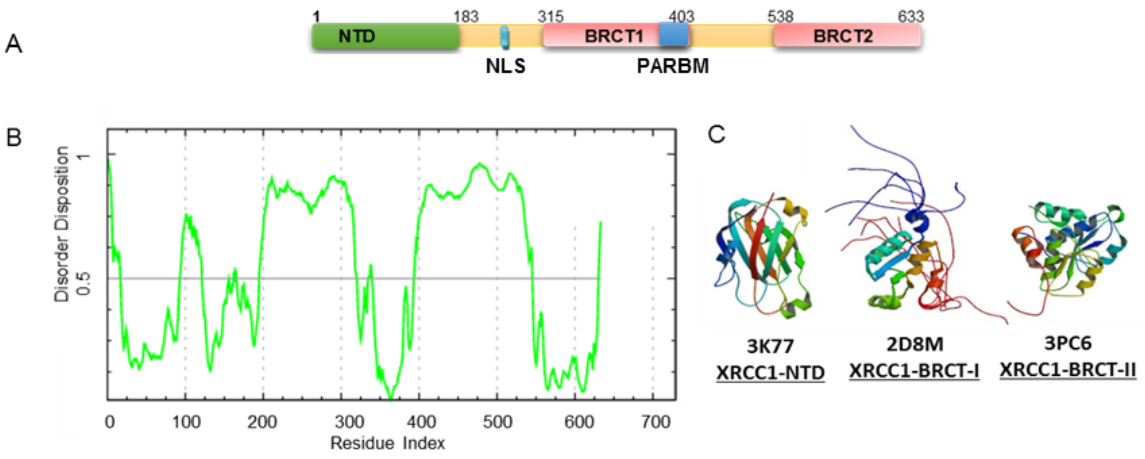

Figure 15. XRCC1 domain map. A) Map of XRCC1 with its domains and motifs labeled. B) PONDR plot of XRCC1 showing disorder in the two linker regions. C) Structural representation of the three domains of XRCC1.

which causes dissociation of XRCC1 dimers (82), although the function of this phosphorylation is unknown. The most well-studied XRCC1 PTM is its phosphorylation by casein kinase 2 (CK2) on nine residues in the second linker region, close to the BRCT2 domain. Ser518, Thr519, and Thr523 are the most well-studied of these residues. Phosphorylation of these residues by CK2 was shown to be required for interaction between XRCC1 and PNKP, APTX, and APLF, all of which interact with XRCC1 through its FHA domain (83-85).

1.5.3 LIG3-independent functions of XRCC1

A significant amount of work on XRCC1 has focused on its close connection to LIG3 and their combined function in SSBR/BER. However, recent evidence has identified LIG3-independent functions of XRCC1. Caldecott identified that XRCC1-dependent strand break repair in S-phase is unaffected by mutations that disrupt its interaction with LIG3, and that

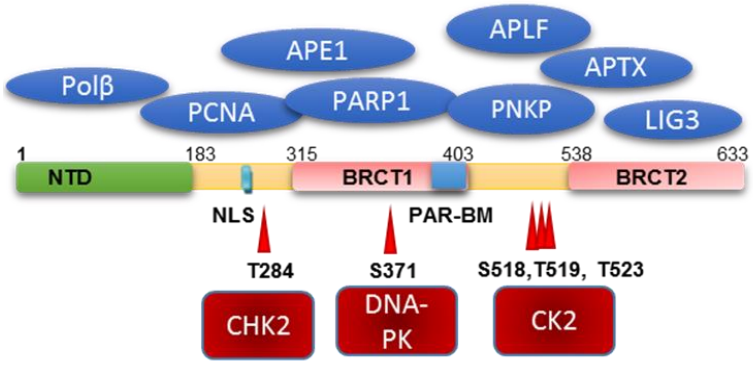

Figure 16. Interactions and phosphorylation sites of XRCC1.

XRCC1 form foci in S-phase that colocalize with Rad51, connecting it with HR (86). The BRCT2 domain of XRCC1 was found to be dispensable for cellular survival after treatment with alkylating agents (87), and similarly, LIG3-null cells are not sensitive to the same DNA-damaging agents that XRCC1-depleted cells are sensitive to (88). This may be explained by the participation of XRCC1, but not LIG3, in replication-associated BER, as Hanssen-Bauer et al. have identified large multiprotein complexes containing XRCC1, LIG1, glycosylases, and elements of the replisome (3). Caldecott et al. recently found that most cellular pAR is detected in S phase cells during DNA replication, and that PARP activation during DNA replication recruits XRCC1, implicating XRCC1 in Okazaki fragment ligation, although it was not shown whether LIG3 participates in this process (89). Interestingly, DNA-PKcs and PARP1 were demonstrated to recruit XRCC1 to stalled replication forks, where it facilitated fork restart, although the involvement of LIG3 was not studied (90). Although it is clear that XRCC1 has LIG3-independent functions, those functions are still being delineated.

1.6 Significance

The use of microhomology in DNA repair is an important area of investigation in cancer biology and genetics. High levels of DNA damage in cancer cells, due to oxidative stress and replication stress, in combination with aberrant DNA repair mechanisms, drives the

accumulation of mutations in cancer genomes (91). These mutations can confer selective growth advantages on cells, which leads to their clonal expansion and an increase in proliferative capacity (91). In the case of chemoradiotherapy for tumors, DNA repair can lead to the clonal survival and the emergence of therapeutic resistance (92). Therefore, understanding DNA repair mechanisms is critical both for understanding tumorigenesis and the proper application of chemoradiotherapy.

The error-prone nature of microhomology-mediated DNA repair mechanisms, which cause large deletions, insertions, and rearrangements, suggests a potentially large contribution to cancer evolution and therapeutic resistance (62). Indeed, recent studies have indicated that these mechanisms are important for cancer development and therapeutic survival (24-26). However, these mechanisms, and their activation in cancer cells and by ionizing radiation, are not well understood.

We have focused our studies on two areas: 1) mechanisms of error-prone repair after IR and 2) mechanisms of error-prone repair in HR-deficient cells. The focus within each of these studies is on the scaffolding protein XRCC1. These studies unveil that XRCC1 has unexpected roles in the regulation of microhomology-mediated end joining after IR and in HR-deficient cancers. We hope that this knowledge will contribute to the proper application of existing chemoradiotherapy, and potentially aid in the development of MMEJ-targeted therapies in the future.

1.7 Goals and Hypotheses

The two major goals of this dissertation were 1) to characterize the contribution of MMEJ to repair of IR-induced DSBs, and 2) understand the contribution of XRCC1 to MMEJ in BRCA2-deficient cancer cells.

Our working hypothesis for the first project was that MMEJ contributes significantly to the repair of IR-induced DSBs via formation of XRCC1 repair complexes. To test this, our group developed a novel DSB substrate with blocked termini that could be used to distinguish MMEJ repair from NHEJ *in cell.* This substrate could also be used to measure MMEJ activity of protein complexes *in vitro*. We used these powerful techniques to characterize the impact of IR on MMEJ, as well as the effect of a critical post-translation modification of XRCC1 on MMEJ complex formation and activity.

Our working hypothesis for the second project was that XRCC1 plays a critical role in BRCA2-deficient cells by mediating MMEJ. Using an isogenic set of U2OS cells, one with an inducible shRNA cassette targeting BRCA2, we were able to study the effect of XRCC1 depletion on WT and HR-deficient cells. Using a variety of cellular and *in vitro* techniques, we documented a distinct impact of XRCC1 on survival, DNA repair and replication in HR-deficient cells.

2. METHODS AND REAGENTS*

This section contains all the reagents and protocols employed to carry out the data in this dissertation.

2.1 Buffers

Enzymatic reactions carried out were performed using buffers supplied with purchased enzymes.

2.2 Antibodies

2.2.1 Primary Antibodies

Mouse monoclonal ANTI-FLAG® M2-Peroxidase (HRP) antibody (A8592, Sigma), mouse monoclonal ANTI-FLAG® M2 antibody (F1804, Sigma), rabbit polyclonal anti-DYKDDDDK tag antibody (#2368, Cell Signaling Technology), mouse monoclonal anti-6X His tag® antibody (ab18184, Abcam), mouse monoclonal anti-XRCC1 antibody (#MS-434-P0, Thermo Scientific), rabbit polyclonal anti-phospho-XRCC1 (S518/T519/T523) antibody (A300-059A, Bethyl Laboratories, Inc.), rabbit polyclonal anti-PARP-1 Antibody (H-300) (sc-25780, Santa Cruz Biotechnology), mouse monoclonal anti-PADPR antibody (ab14459, Abcam), mouse monoclonal anti-DNA Ligase 3 antibody (custom made), rabbit polyclonal anti-Mre11 antibody (#4895, Cell Signaling Technology), rabbit polyclonal anti-CtIP antibody (ab70163, abcam),

*Parts of this chapter are reprinted with permission from "Microhomology-mediated end joining is activated in irradiated human cells due to phosphorylation-dependent formation of the XRCC1 repair complex" by Dutta A, Eckelmann B, Adhikari S, Ahmed KM, Sengupta S, Pandey A, *et al.*, 2017. *Nucleic Acids Research*, 45, 2585-99, Copyright 2017 by Oxford University Press. Parts of this chapter are reprinted with permission from "XRCC1 promotes replication restart, nascent fork degradation and mutagenic DNA repair in BRCA2-deficient cells" by Eckelmann B, Bacolla A, Wang H, Ye Z, Guerrero EN, Jiang W, *et al.*, 2020. *Nucleic Acids Research Cancer*, 2, 3, Copyright 2020 by Oxford University Press.

1. Whole Cell Lysis Buffer:	1X Tris-buffer saline (TBS) solution (50 mM Tris-HCl pH 7.5, 150 mM NaCl), 1% Triton X and one tablet of Pierce™ protease inhibitor cocktail (Thermo Scientific) per 10 ml.
2. Cytoplamic Extraction Buffer:	10 mM Tris-HCl pH 7.9, 0.34 M Sucrose, 3 mM $CaCl_2$, 2mM $MgCl_2$, 0.1 mM EDTA, 1 mM DTT, 0.1% Nonidet P-40, and one tablet Pierce™ protease inhibitor cocktail per 10 ml.
3. Nuclear Extraction Buffer:	20 mM HEPES (4-(2-hydroxyethyl)-1-piperazineethanesulfonic acid) pH 7.9, 3 mM EDTA, 10% Glycerol, 150 mM potassium acetate, 1.5 mM $MgCl_2$, 1.5 mM DTT, 0.5% Nonidet P-40, and one tablet Pierce™ protease inhibitor cocktail per 10 ml.
4. Chromatin Extraction Buffer:	150 mM HEPES pH 7.9, 1.5 mM $MgCl_2$, 10% Glycerol, 150 mM potassium acetate, and one tablet Pierce™ protease inhibitor cocktail per 10 ml.
5. FLAG Co-IP Wash Buffer:	1X TBS, 0.5% Triton X
6. 10X Annealing Buffer:	100 mM Tris-HCl, pH 7.5–8.0, 500 mM NaCl, 10 mM EDTA
7. 10X Plasmid Recircularization Assay Buffer	20mM $MgCl_2$, 600mM NaCl, 500mM HEPES, 20mM DTT, 10 mM ATP, 10mM dNTP, 500 µg/ml BSA
8. 10X CK2 Kinase Buffer:	250 mM MOPS, pH 7.5, 1.5 M NaCl, 50 mM $MgCl_2$, 50 mM $MnCl_2$, 2.5 mM DTT

Table 3. Buffers

mouse monoclonal anti-Nbs1 antibody (GTX70224, Genetex), rabbit monoclonal anti-phospho-Histone H2A.X (Ser139) (20E3) (#9718, Cell Signaling Technology), mouse monoclonal anti-phospho-Histone H2A.X (Ser139) antibody (#05-636, EMD Millipore), mouse monoclonal anti-β-Actin (A5316, Sigma), rabbit monoclonal anti-XRCC1 antibody (ab134056, Abcam), rabbit polyclonal anti-DNA polymerase Beta antibody (18003-1-AP, Proteintech), rabbit polyclonal anti-DNA polymerase Theta antibody (ab80906, abcam), mouse monoclonal anti-BRCA1

antibody (D-9) (sc-6954, Santa Cruz Biotechnology), mouse monoclonal anti-BRCA2 antibody (2B) (OP95, EMD Millipore), mouse monoclonal anti-FEN1 antibody (B4) (sc-28355, Santa Cruz Biotechnology), mouse monoclonal anti-BrdU antibody (IIB5) (ab8152, Abcam), and mouse monoclonal anti-β-Actin (A5316, Sigma).

2.2.2 Secondary Antibodies

Secondary antibodies for Western Blotting were from GE Healthcare (anti-mouse, NA9310V; anti-rabbit, NA934V). Secondary antibodies for immunofluorescence were from Invitrogen (Alexa Fluor, anti-rabbit 594, A11037; anti-mouse 594, A11005; anti-rabbit 488, A11008; anti-mouse 488, A11001).

2.3 siRNAs

Target	siRNA sequence (sense, antisense) (5'-3')
XRCC1	(ACACACACACGAUGCAUUUUU, AAAAAUGCAUCGUGUGUGUGU)
Ligase 3	(CCACAAAAAAAAUCGAGGATT, UCCUCGAUUUUUUUUUGUGGTG)
CtIP	(GCUAAAACAGGAACGAAUC, GAUUCDUUCCUDUUUUAGC)
Ligase 1	(GGCAUGAUCCUGAAGCAGATT, UCUGCUUCAGGAUCAUGCCTT)
Pol Q	(CCUUAAGACUGUAGGUACUUU, AGUACCUACAGUCUUAAGGUU)
FEN1	(AUCAAAGACAUACACGGGCUUGAUG, UCAAGCCCGUGUAUGUCUUUCAUUU)
BRCA1	CAGCAGTTTATTACTCACTAA (target sequence)
BRCA2	TTGGAGGAATATCGTAGGTAA (target sequence)
ctrl	MISSION siRNA Universal Negative Control #1 (Sigma)
Nbs1	(CCAACUAAAUUGCCAAGUAUU, AAUACUUGGCAAUUUAGUUGG)

Table 4. siRNA sequences

2.4 Drugs and Small Molecule Inhibitors

DNA-PK inhibitor, NU7741 (Tocris Biosciences, Bristol, UK), CK2 inhibitor, CX-4945 (Abcam, US), Mre11 exonuclease inhibitor, Mirin (Sigma-Aldrich, US), Mre11 endonuclease inhibitor, PFM03 (John Tainer Lab, MD Anderson Cancer Center, Houston, TX), PARP1 inhibitor, Rucaparib (Selleck Chemicals), ATR inhibitor, VE-821 (Sigma-Aldrich, US), hydroxyurea (Sigma-Aldrich, US).

2.5 Plasmids

Primers for subcloning were purchased from Sigma. XRCC1^{WT}-6XHis-pCD2E and CK2 non-phosphorylatable mutant XRCC1^{CKM}-6XHis-pCD2E were gifts from Keith Caldecott Lab at University of Sussex, UK. XRCC1 cDNA sequence was PCR amplified from XRCC1-pCDNA4 using Platinum® Pfx DNA Polymerase (ThermoFisher Scientific) and subcloned in p3X-FLAG-CMV14 at XbaI and ClaI restriction endonuclease sites.

Forward primer: 5'-CCCATCGATATGCCGGAGATCCGCCTCCG-3'

Reverse primer: 5'-CCGTCTAGAGGCTTGCGGCACCACCCCATA-3'

Similarly, XRCC1^{CKM} was subcloned similarly from XRCC1^{CKM}-6XHis-pCD2E in p3X-FLAG-CMV14 vector using same set of primers and identical PCR amplification protocol. pEGFPN1 was used as a backbone to generate linearized plasmid substrate, pNS for *in cell* and *in vitro* repair assays. Myc-POLQ-FLAG construct was purchased from Addgene (deposited by Agnel Sfeir, plasmid #731132).

2.6 Cell culture

U2OS cells, A549, and HEK293 cells were grown in Dulbecco's High Glucose Modified Eagles Medium (DMEM) with 4 mM L-Glutamine, without Sodium Pyruvate (Hyclone, GE

Healthcare Life Sciences), supplemented with 10% fetal bovine serum (Hyclone, GE Healthcare Life Sciences) and 1X Penicillin-Streptomycin Solution (Corning cellgro®) at 37ºC in presence of 5% CO_2 in a CO_2 incubator. Cells were washed with Dulbecco's phosphate buffered saline (DPBS, Hyclone, GE Healthcare Life Sciences). Cells were trypsinized using Trypsin-EDTA solution (Sigma-Aldrich). Stable XRCC1-HEK293 cells were grown in DMEM selection media containing zeocin (Invitrogen) and G418 sulfate solution (Corning cellgro®), respectively. Inducible BRCA2-shRNA-expressing U2OS (B2) and inducible scrambled-shRNA-expressing U2OS (scr) cell lines were a gift from Ryan Jensen (Yale University). They were cultured in 2 μg/ml puromycin (Invivogen), and shRNA expression was induced with 10μg/ml doxycycline for 72 hrs. U2OS-EJ2 cells were a gift from Jeremy Stark (City of Hope). They were cultured in 2 μg/ml puromycin (Invivogen).

2.7 Irradiation

The cells were irradiated with an RS2000 (Rad Source Technologies, Inc., Suwanee, GA) 160 kVp X-ray source. Tissue culture plates or chamber slides containing cells were placed in shelf 3, circle 4, where the dose rate is 2.0 Gy/min and the uniformity of dose across the field in horizontal plane is >95%. After irradiation the plates or slides were immediately returned to their incubators.

2.8 Recombinant proteins

Recombinant XRCC1, Mre11, XRCC1 domains, Mre11 domains, DNA Ligase 3α and XRCC1/DNA ligase 3α complex were purified by Pavana Dixit at Mitra Lab from cell pellets from Miaw-Sheue Tsai's lab, Lawrence Berkeley National Laboratory, Berkeley, CA.

2.9 Protein extraction

2.9.1 Whole cell lysis

Cells were washed with DPBS and harvested with a cell scraper. The cells were pelleted at 800 rpm, 4ºC for 5 min and lysed with whole cell lysis buffer (500 µl per 10 cm plate) by vortexing for 15 min and centrifuged at 14000 rpm, 4ºC for 15 min, after which the supernatant was retrieved.

2.9.2 Nuclear fraction isolation

After pelleting, cells were resuspended in cytoplasmic extraction buffer (500 µl per 10 cm plate) and mixed by pipetting 10-15 times. The suspension was briefly vortexed and centrifuged at 3500 g. Supernatant (cytoplasmic fraction) was discarded. The nuclear pellet was resuspended in whole cell lysis buffer (300 µl per 10 cm plate), centrifuged at 14000 rpm, 4ºC for 15 min, after which the supernatant was retrieved.

2.10 Co-immunoprecipitation

Protein concentration of whole cell lysates from appropriate cells were measured through Bio-rad protein assay. ANTI-FLAG® M2 affinity gel beads (Sigma-Aldrich) were washed with cold 1X TBS buffer and mixed with whole cell lysate (10 µl per 1 mg of total protein). The volume was adjusted with 1X TBS to keep the final concentration of Triton-X 0.5%. The beads were incubated 3 hrs at cold room to carry out the co-IP. The beads were washed with FLAG co-IP wash buffer 3 times for 5 min each. The beads were eluted with 2X LDS dye and heated for 1 min at 95ºC.

2.11 Protein transfer and Western Blotting

Protein or co-IP samples were loaded along with Precision Plus Protein™ Dual Color Standards (Bio-rad) in NuPAGE Novex 4-12% Bis-Tris Protein Gels (Invitrogen) or Criterion™ XT Bis-Tris gels (Bio-rad), and gel electrophoresis was carried out in 1X NuPAGE running buffer (Invitrogen) or MOPS-XT buffer (Bio-rad), respectively. Protein transfer from SDS-PAGE gels to nitrocellulose membrane (Invitrogen) were carried out in 1X NuPAGE transfer buffer (Invitrogen) or 1X Tris-Glycine transfer buffer (Invitrogen) respectively. After transfer, nitrocellulose membranes were blocked with 5% skim milk (Fisher Scientific) solution in 1% Tris-Buffered Saline and Tween 20 (TBST) buffer (Invitrogen). This was followed by blotting with appropriate primary and secondary antibodies. Washing was done with 1% TBST.

2.12 Immunofluorescence

U2OS/A549 cells were grown in 8 chamber slides and after appropriate treatment, they were fixed with 4% paraformaldehyde for 15 min, followed by permeabilization with 0.5% Triton-X solution in DPBS for 15 min. Blocking was performed with 3% BSA solution in DPBS with 0.2% Triton-X for 1 hour. The samples were incubated overnight with appropriate primary antibodies diluted in DPBS with 0.2% Triton-X. Cells were then washed 3X with DPBS with 0.2% Triton-X and incubated with conjugated secondary antibody for 1 hr. Cells were again washed 3X with DPBS with 0.2% Triton-X after which the slides were air-dried. The slides were mounted with mounting media with DAPI (Duolink) and coverslip. The samples were observed under 60X oil-immersion lens in Nikon upright bright-field/fluorescent microscope or inverted Zeiss microscope and images were captured from five random fields for each sample. The images were merged and analyzed with ImageJ software.

2.13 Proximity Ligation Assay

Proximity ligation assay (PLA) is an immunochemistry-based technique for detecting *in situ* protein-protein interaction or co-localization. For each assay, two primary antibodies raised in different species were used. PLA was performed with the Duolink kit (Olink Bioscience) following the manufacturer's protocol using buffers and reagents provided in the kit. U2OS/HEK293 cells grown in 8 chamber slides with appropriate treatment were fixed with 4% paraformaldehyde and permeabilized with 0.5% Triton-X solution in DPBS. The cells were blocked with blocking solution (Duolink) for 30 mins at 37ºC in a CO_2 incubator. Appropriate primary antibodies were diluted in Antibody Diluent Solution (Duolink) and added to the wells and incubated overnight at 4ºC. Then, wells were washed 2X with PLA Wash Buffer A (Duolink) for 5 min. The samples were incubated with Duolink plus and minus probes diluted appropriately in Antibody Diluent Solution and incubated for 1 hr at 37ºC in a CO_2 incubator. The samples were again washed 2X with Wash Buffer A and ligation was carried out by incubating the samples with 0.3 µl Ligase per well diluted in 30 µl 1X Ligation Stock (Duolink) for 30 mins at 37ºC in a CO_2 incubator. The samples were again washed and Amplification was carried out by addition 0.2 µl Polymerase diluted in 30 µl 1X Amplification Stock (Duolink) and incubating 2 hrs at 37ºC in a CO_2 incubator. Amplification step was carried out in the dark and slides were protected from light thereafter. Finally, slides were washed with Wash Buffer B (Duolink) 2X for 10 min and 1X with 0.01X Wash Buffer B for 1 min. The slides were air dried and mounted with mounting media with DAPI (Duolink) and coverslip. The slides were observed under 60X oil-immersion lens in Nikon upright bright-field/fluorescent microscope or inverted Zeiss microscope and images were captured from five random fields for each sample. The images were merged and analyzed with ImageJ software.

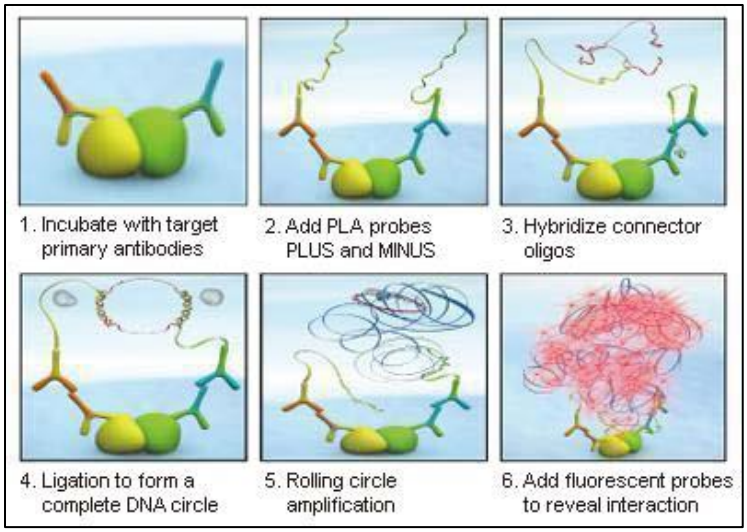

Figure 17. Cartoon depicting Proximity Ligation Assay (Sigma-Aldrich, Duolink PLA). Reprinted with permission from Sigma-Aldrich.

2.14 *In Cell* Plasmid Recircularization Assay

100 ng of the repair substrate, pNS was transfected in exponentially growing control or appropriately treated U2OS/A549 cells using Lipofectamine 2000 and incubated overnight. Next day the cells were checked for GFP expression and plasmids were isolated using Qiagen plasmid miniprep kit. 5 µl of plasmid extract was transfected in XL10-gold ultracompetent cells using manufacturer's protocol and plated in 50 µg/ml Kanamycin containing LB-agar plates. The bacterial plates were sent to GENEWIZ (South Plainfield, NJ) for sequencing of randomly chosen 40 colonies using CMV-F primer. Relative percentage of repaired joints by MMEJ or NHEJ was plotted and statistical analysis was performed by two-tailed Fisher's exact t test using Prism software.

2.15 *In Vitro* Plasmid Recircularization Assay

Exponentially growing U2OS cells transiently expressing XRCC1-FLAG were treated with drugs/inhibitors/siRNAs as indicated and/or irradiated with 3 Gy X-rays. After 1 hour, the cells were harvested along with untreated cells for nuclear extraction. XRCC1-FLAG co-IP was

performed by incubating 1.5 mg of nuclear extract with FLAG-M2 agarose beads for 2 h at 4°C. The beads were directly incubated 30 mins with 5ng pNS in a reaction buffer containing 2mM $MgCl_2$, 60mM NaCl, 50mM HEPES, 2mM DTT, 1 mM ATP, 1mM dNTP and 50 µg/ml BSA under mild shaking. This was followed by addition of 14 ng XRCC1-DNA ligase 3α recombinant protein complex in the reaction mix and incubation overnight at 16°C. The beads were spun down and 5 µl of the reaction mix was transformed in XL10-gold ultracompetent cells and sequence analysis of colonies were performed as discussed earlier. Number of colonies obtained from each experiment was plotted and statistical analysis was performed by two-tailed Fisher's extact t test using Prism software. The beads were eluted with 2X LDS loading buffer and analyzed by western blotting.

2.16 γH2AX Foci Formation Assay

U2OS cells with appropriate siRNA treatment were plated in 8-chamber slides and incubated overnight. Next day the cells were treated with appropriate drugs (hydroxyurea for 3h), or inhibitors (NU7441 for 1hr, Rucaparib and CX4945 for 2 hr) prior to X-ray irradiation. After 1 hour incubation the cells were fixed with 4% paraformaldehyde for 15 minutes, followed by permeabilization with 0.5% Triton-X solution in DPBS for 15 min. Blocking was performed with 3% BSA solution in DPBS for 1 hour. The samples were incubated with anti-phospho-serine H2A.X antibody diluted 1:500 in DPBS with 0.2% Triton-X for 2 hrs at room temperature. After washing 3X with DPBS with 0.2% Triton-X, the cells were incubated with conjugated secondary antibody (1:500). After washing, the slides were dried for 5-10 mins in a 37°C incubator and mounted with mounting media containing DAPI (Duolink) and coverslips. The samples were observed under 60X oil-immersion lens in Nikon upright bright-field/fluorescent or an inverted Zeiss microscope and images were captured from five random fields for each sample. The images

were merged and foci were counted through ImageJ software. Mean number of γH2AX foci per cell were plotted.

2.17 Clonogenic Assay

U2OS cells were transfected with 100nM control siRNA or XRCC1 siRNA and incubated 72 hrs. Cells were treated with 10 μM NU7441/ DMSO for 1hr, and thereafter exposed to different dose of X-rays (0, 3, 6, 9 Gy). Or cells were treated with hydroxyurea (3 mM) or VE-821 (ATRi) (3 μM) for 8 hr. The cells were trypsinized and 300 cells from each sample were plated in quadruplicate in 6 well plates. The NU7441 pre-treated cells were replated in DMEM containing 10μM NU7441. After 10 days the plates were harvested and the colonies were stained with 0.5% crystal violet solution in 50/50 methanol/water for 15 mins. The plates were washed gently in water and air-dried for counting the colonies.

2.18 EJ2 Assay and Flow Cytometry

For EJ2-MMEJ assay, we followed Jeremy Stark's published protocols for cell treatment, depeletion with siRNA, DSB induction by ISceI transfection, and cell harvesting. Flow cytometry was performed using a BD FACS LSRII with assistance from David Haviland and data were analyzed using Flowing Software (Perttu Terho, Turku Centre for Biotechnology).

2.19 Comet Assay

Neutral comet assay was performed using the Trevigen CometAssay Kit (4250-050-K) according to manufacturer's protocol. At least 50 random comets for each sample were analyzed using CaspLab software.

2.20 Single-Strand Nick Ligation Assay

Annealed oligomers, one containing a nick, labeled with Cy3 fluorescent dye were mixed with IP complexes in 1x T4 ligation buffer and the mixture was incubated in a water bath at

30°C for 20 min, followed by incubating with 2x TBE sample buffer at 100°C for 3 min and on ice for another 3 min. Oligomers were separated by denaturing urea polyacrylamide gel electrophoresis, and Cy3 fluorescence was detected by a Typhoon FLA 7000 system.

2.21 DNA Fiber Analysis

Cells were labeled with 50 μM CldU (Sigma), exposed to hydroxyurea (4 mM), and labeled with 50 μM IdU (Sigma) as indicated in the figures. DNA fibers were spread as described by Jackson and Pombo, and fiber tracts were detected using anti-IdU (BD Biosciences, 347580) and anti-CldU (Novus Biologicals, NB500-169) primary antibodies and Alexa Fluor 488 and 555 secondary antibodies (Invitrogen). Fibers were imaged at 60x magnification with oil immersion using a Zeiss microscope and analyzed with ImageJ.

2.22 Statistical Analyses

All statistics were performed using Prism software. Fiber assay distributions were analyzed using the Mann-Whitney U test. PLA foci distributions, comet assay distributions, MMEJ in vitro assay, EJ2 repair events, and clonogenic survival assay were analyzed using student's t-test. Foci formation and in cell MMEJ assay results were analyzed using Fisher's exact test.

3. MICROHOMOLOGY-MEDIATED END JOINING IS ACTIVATED IN IRRADIATED HUMAN CELLS DUE TO PHOSPHORYLATION-DEPENDENT FORMATION OF THE XRCC1 REPAIR COMPLEX*

3.1 Introduction

About half of all cancer patients are treated with IR, either alone or in combination with surgery and/or chemotherapy (50). However, invariable development of resistance to radiotherapy in recurrent cancers warrants comprehensive understanding of the repair of IR-induced DNA damage, which promotes tumor cell survival. IR induces clustered damage in the genome, including highly cytotoxic DSBs, together with an excess of closely spaced SSBs, AP sites and oxidized bases (93). In dividing cells, DSBs can be repaired accurately in the S/G2 phase via HR, which requires resection at the 5' DSB termini to generate 3' overhangs, followed by invasion of the homologous sequence in the undamaged sister chromatid (94). However, NHEJ, which involves ligation of blunt ends, is the predominant pathway for DSBR, independent of cell cycle phase (8). Although NHEJ can be error-prone at complex DSBs (95) as a result of end resection and/or gap filling prior to ligation (96), the binding of Ku limits end resection at DSB ends, preventing significant loss of nucleotides (97). A recently characterized, highly error-prone DSBR process variously named backup NHEJ, alternative NHEJ, or alternative end joining (Alt-EJ), does not require NHEJ proteins but utilizes the BER/SSBR proteins including PARP1, XRCC1, and LIG1/LIG3 for joining the DSB termini (30,98,99). Significant diversity in Alt-EJ has been observed, with several sub-pathways differing in their

*Parts of this chapter are reprinted with permission from "Microhomology-mediated end joining is activated in irradiated human cells due to phosphorylation-dependent formation of the XRCC1 repair complex" by Dutta A, Eckelmann B, Adhikari S, Ahmed KM, Sengupta S, Pandey A, *et al.*, 2017. *Nucleic Acids Research*, 45, 2585-99, Copyright 2017 by Oxford University Press.

requirement for preexisting or de novo microhomology (100), while a few reports have described microhomology-independent processes for Alt-EJ (101,102).

MMEJ carries out DSB joining via annealing of short microhomology sequences (5–25 bases) to the complementary strand spanning the break site (100). The consensus requirement for MMEJ is the initial resection of DSB ends by MRE11/RAD50/NBS1 (MRN) and CtIP, analogous to that observed in HR, in order to generate a 3' ssDNA overhang that helps search for microhomology sequences across the DSB (103). After annealing of the microhomology sequences, any resulting flap segments are removed by the endonuclease activity of CtIP or flap endonuclease 1 (FEN-1), followed by gap-filling in both strands by a DNA polymerase, such as DNA polymerase θ or λ, and finally ligation of the nicks by LIG1/3 (104). However, how these steps are regulated is not understood. In any event, MMEJ results in loss of one microhomology sequence and the intervening region, which leads to deletions of variable size. MMEJ, active in both normal and cancer cells (98), could serve as a backup pathway to NHEJ (105). However, recent studies have suggested that it could be a dedicated pathway in cancer cells, particularly those with deficiencies in HR activity (24,106). Whole-genome sequence data from large cohorts of cancer patients has suggested a significant contribution of MMEJ to the genomic instability in cancer cells, via deletion, insertion, inversion, and complex structural changes (107,108).

In the present study, we investigated the contribution of MMEJ to repair of IR-induced DSBs. Strand breaks generated by IR have non-ligatable termini containing 3' phosphate (P) and/or 3' phosphoglycolate (109), which need to be removed to generate the 3' OH terminus required for repair synthesis and ligation. Incidentally, the proportion of 3' P termini at IR-induced strand breaks in synthetic oligonucleotides increases under hypoxic and anoxic conditions (110). To assess the relative contribution of MMEJ versus NHEJ at IR-induced DSBs,

we developed an in cell assay based on circularization of a linearized GFP reporter plasmid containing 3' P termini, followed by sequence analysis of the repaired joints. After documenting that in cell circularization of this novel substrate recapitulated the requirements for NHEJ and MMEJ in the cellular genome, we observed that MMEJ activity is low relative to NHEJ in untreated cells, as expected. However, MMEJ activity was significantly enhanced after radiation treatment. We then focused on the scaffold protein XRCC1, which interacts with both SSBR proteins and MRN, all of which are recruited at IR-induced clustered damage sites. We tested the hypothesis that XRCC1, via phosphorylation by CK2, forms a repair-competent complex to carry out MMEJ. Finally, our observation that the XRCC1-IP can perform MMEJ in vitro, similar to what our group observed previously with BER complexes (111), could allow us to identify undiscovered factors involved in MMEJ.

3.2 Results

3.2.1 In Cell Plasmid Recircularization Assay

The mechanisms of DSBR in the mammalian genome are commonly investigated through generation of site-specific DSBs by an ectopic meganuclease such as I-SceI (112). Although this strategy can quantitatively characterize HDR versus NHEJ at specific genomic loci, the induced DSBs do not resemble the complex strand breaks induced by ionizing radiation, which include SSBs, oxidized bases, and DSBs with non-ligatable termini (52). To explore how radiation-induced DSBs are repaired in the genome, we used circularization of a reporter plasmid, linearized with nonligatable 3'P termini, as a model system for analyzing DSB repair via NHEJ or MMEJ. We followed the repair, i.e. circularization of the linearized GFP reporter plasmid, pNS, in transfected human cells from which the plasmid population was recovered and screened in E. coli. The plasmid molecules circularized in the human cell produced kanamycin

resistant colonies based on expression of the drug resistance gene in the plasmid (pEGFPN1). Noncircularized plasmid molecules recovered from the human cells could not be circularized in E. coli because these are promptly degraded by the RecB/C nuclease. Linearized plasmid was shown to have > 103-fold lower transformation efficiency than the circular plasmid in wild-type E. coli used in our experiments. To ensure that we eliminated any chance of recovering drug resistant E.coli colonies resulting from plasmid recircularization in the E. coli, we treated the plasmid extracted from transfected human cells with lambda exonuclease (NEB) to remove any linear plasmids. We observed no significant difference in the transformation efficiency or in the relative products of NHEJ versus MMEJ in untreated vs. lambda exonuclease-treated plasmid extracts, as we had expected. Finally, DSB repair via HDR was precluded because the plasmids lack the ability to replicate in human cells. Thus, each bacterial colony represented an individual DSB repair event in the human cell. Subsequent sequence analysis of the rejoined region in individual plasmids allowed us to evaluate the relative contribution of NHEJ and MMEJ to the repair of the DSB in pNS. In order to quantitate the relative contribution of MMEJ versus NHEJ, we introduced a pair of 5 nt long microhomology sequences flanking the DSB, following the current consensus on the requirement for MMEJ, as has been characterized by both in vitro and chromatin-based DSB repair assays in human and yeast cells (98,113,114).

We transfected human osteosarcoma U2OS cells or human lung carcinoma A549 cells at 70–80% confluency with linearized pNS, which expresses GFP only if circularized via DSB repair (end joining). Although GFP expression was observed as early as 6 h after transfection, we routinely harvested cells after overnight incubation (15 h) of the transfected cells before extracting the plasmid for transforming E. coli. At least 40 kanamycin-resistant colonies were randomly selected for sequencing using a CMV-F primer. NHEJ requires blunt termini with 5’P

and 3'OH, generated either by removal of the 3'P termini by PNKP (115), exonucleolytic degradation of a few terminal bases, or gap-filling synthesis, which leads to either error-free repair or that with a small deletion/insertion. On the other hand, MMEJ of our plasmid substrate

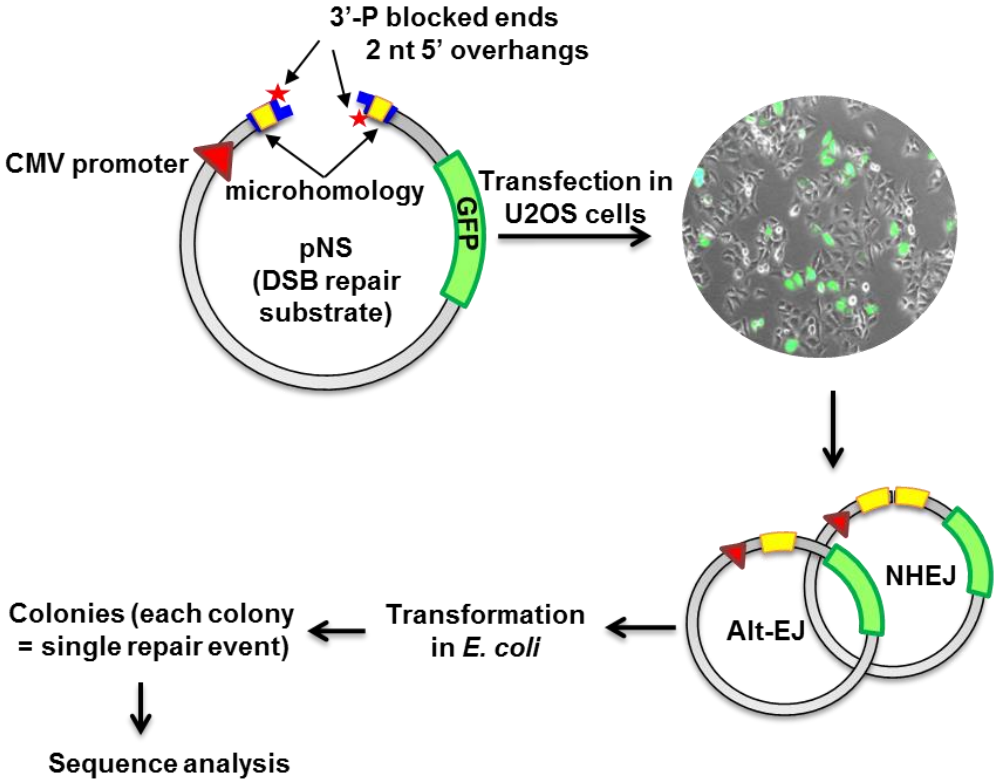

Figure 18. Schematic representing *in cell* repair of pNS to quantify MMEJ vs. NHEJ. Reprinted from (156) with permission from Oxford University Press.

would involve annealing at the microhomology sequence, resulting in a larger deletion with the loss of one microhomology sequence. We observed long non-specific deletions (>10 nt) in a small number of plasmid molecules, which were ignored because of their likely formation due to non-specific exo/endonucleolytic degradation at the DSB termini. Thus, the molecules with only a 1–3 nt insertion or 1–10 nt deletion were scored as products of NHEJ, while those with a deletion of one microhomology sequence (including the intervening sequence) were counted as products of MMEJ (Figure 19). In cell repair of pNS showed that NHEJ was the predominant

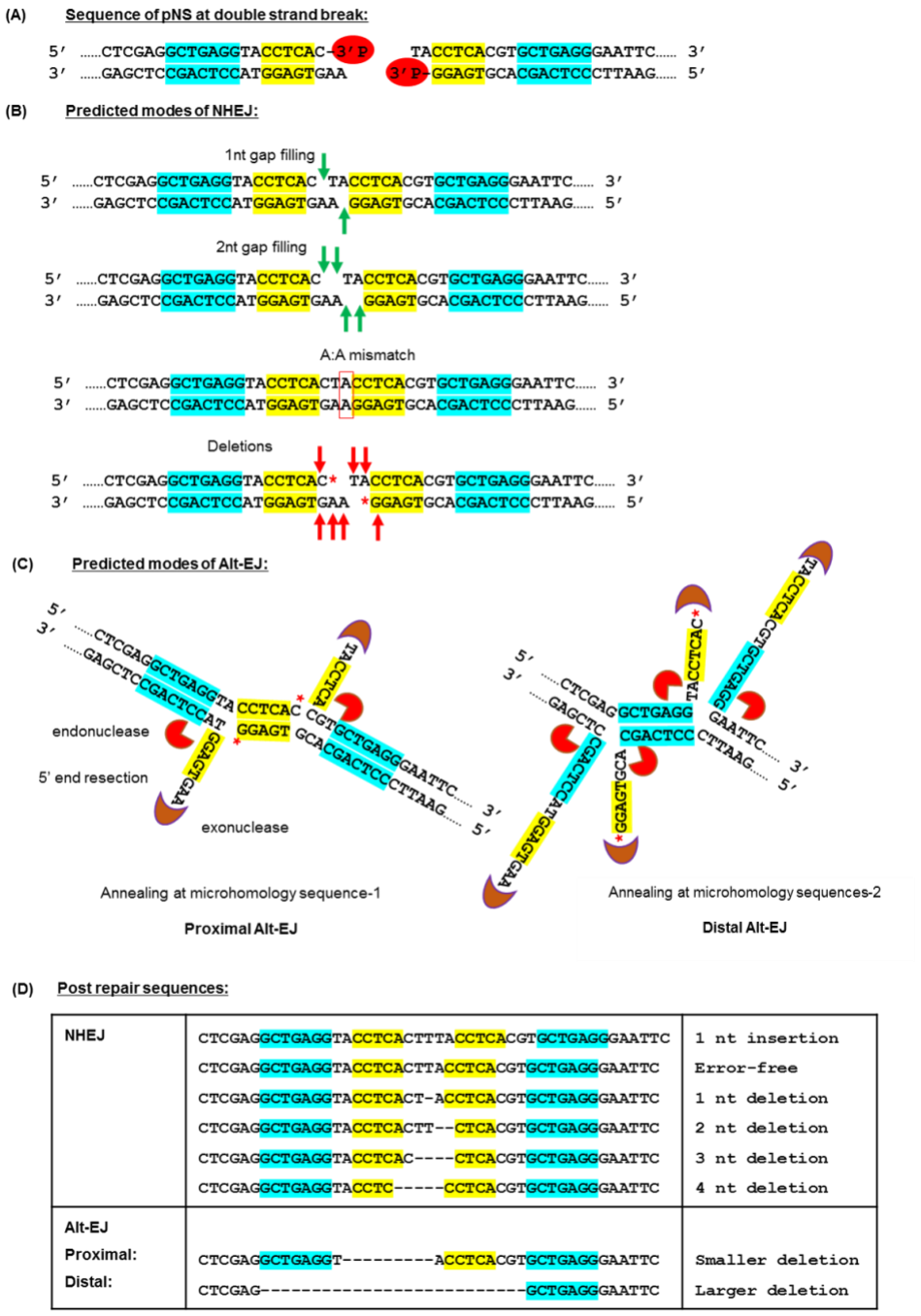

Figure 19. pNS sequence details. (A) Sequence of pNS. (B) Modes of NHEJ. (C) Modes of MMEJ. (D) Sequencing outcomes of repair. Reprinted from (156) with permission from Oxford University Press.

contributor to repair of pNS in both U2OS and A549 cells, while a small fraction of repair events (14% in A549 and 8% in U2OS) were of the MMEJ type (Figure 20). These results are in

general agreement with the published literature that NHEJ is the predominant contributor to DSB repair in the human cell genome relative to MMEJ (104).

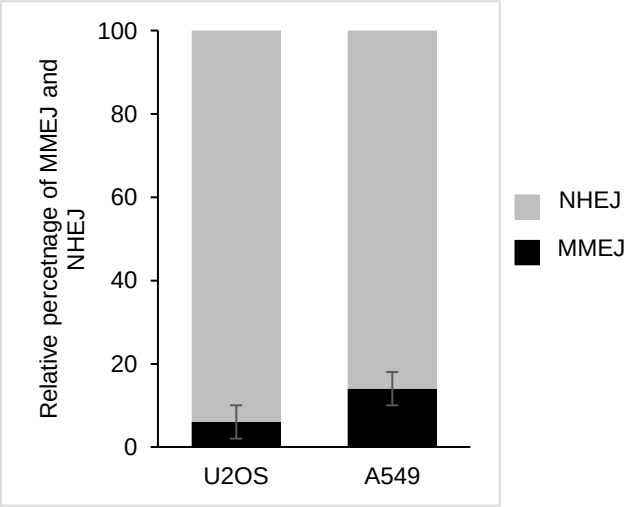

Figure 20. Relative percentage of NHEJ and MMEJ *in cell* in U2OS and A549 cells. Reprinted from (156) with permission from Oxford University Press.

3.2.2 MMEJ is Enhanced When End Cleaning is Inhibited

Because ligation requires removal of the 3' P at DNA termini by PNKP (116), we tested the effect of PNKP deficiency on MMEJ. We analyzed end joining of pNS in A549 cells in which PNKP was depleted via stable expression of its shRNA (117). The frequency of MMEJ in PNKP-depleted cells was 3-fold higher compared to that in the wild type (WT) cells, which was reversed by ectopic expression of WT-PNKP but not by the phosphatase-inactive mutant (Figure 21). These results strongly suggest that NHEJ involves 3' P removal by PNKP, as reported earlier (115), and that its deficiency promotes MMEJ-mediated DSB repair. Although it has been suggested that PNKP promotes MMEJ in vitro via its interaction with PARP1-XRCC1/LIG3 (101), our results indicate that it is dispensable during in cell MMEJ that utilizes microhomology.

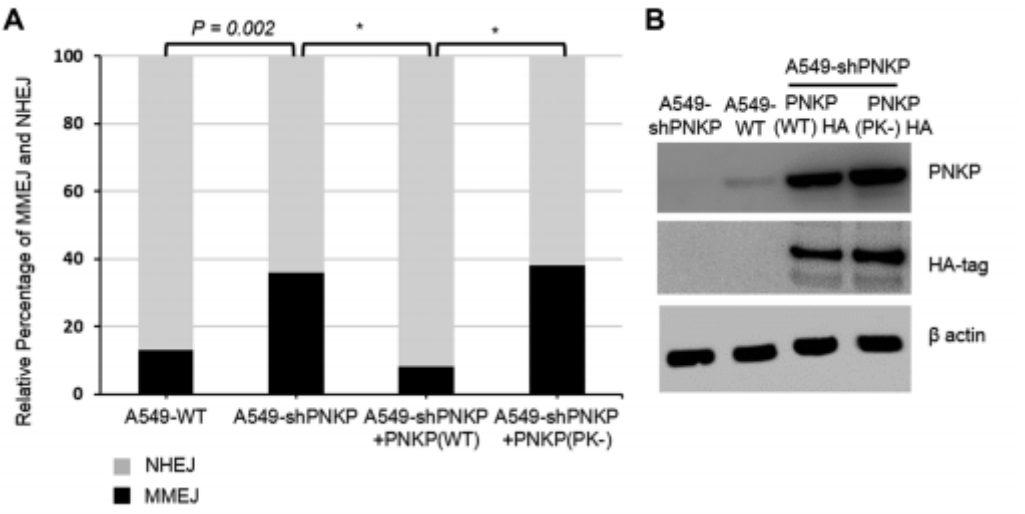

Figure 21. End-cleaning by PNKP promotes NHEJ. (A) In cell repair of pNS in WT A549 cells, shRNA-mediated PNKP-depleted cells, or in endogenous PNKP-depleted cells with transient expression of HA-tagged PNKP-WT or PNKP-phosphatase/kinase inactive (PK-) mutant. (B) Western analysis of extracts from cells in (A). Reprinted from (156) with permission from Oxford University Press.

3.2.3 MMEJ is Enhanced After Ionizing Radiation

We then asked whether MMEJ and NHEJ are affected in cells by radiation-induced activation of the DNA damage response signaling. We irradiated A549 and U2OS cells with various doses of X-rays immediately before transfection with pNS, and then analyzed sequences of the repaired plasmids. The contribution of MMEJ relative to NHEJ was enhanced ~5-fold after exposure to a 0.5 Gy or higher X-ray dose in both cell lines (Figure 22). These results are consistent with a previous report of induction of MMEJ in yeast and mammalian cells after irradiation, although its mechanism was not investigated (118).

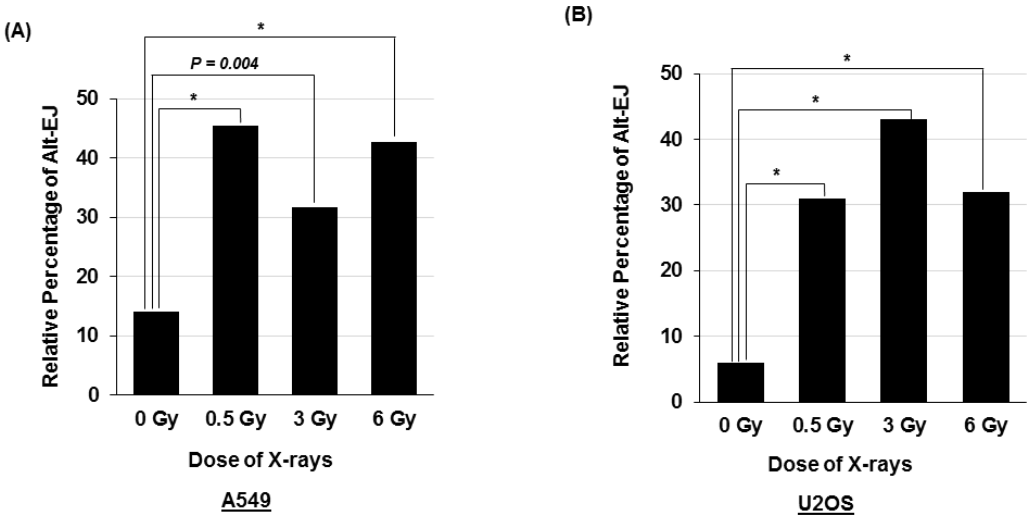

Figure 22. IR stimulates MMEJ. (A) *In cell* repair of pNS in control A549 cells and in cells preirradiated with various doses of X-rays, as indicated. (B) In cell repair of pNS in control U2OS cells and cells treated with different doses of X-rays, as indicated. Reprinted from (156) with permission from Oxford University Press.

3.2.4 MMEJ After Ionizing Radiation Requires XRCC1, PARP1, MRE11, and CtIP

We confirmed that MMEJ was not mediated by a variant NHEJ process, based on the result that MMEJ accounted for up to 95% of DSBR in U2OS cells when the cells were pretreated with the DNA-PK inhibitor NU7441. Furthermore, induction of MMEJ in preirradiated cells was absent if any of the known MMEJ factors, namely, XRCC1, PARP1, MRE11 and CtIP, were either depleted by treatment with cognate siRNA or inhibited by specific inhibitors (Figure 23).

3.2.5 XRCC1 is Recruited to DSBs for Repair After Ionizing Radiation

Based on our observation that MMEJ is compromised in XRCC1-deficient U2OS cells, and also on published reports documenting the involvement of XRCC1 in MMEJ-mediated DSBR (30,98,119), we tested if XRCC1 localizes to X-ray-induced DSBs in the genome.

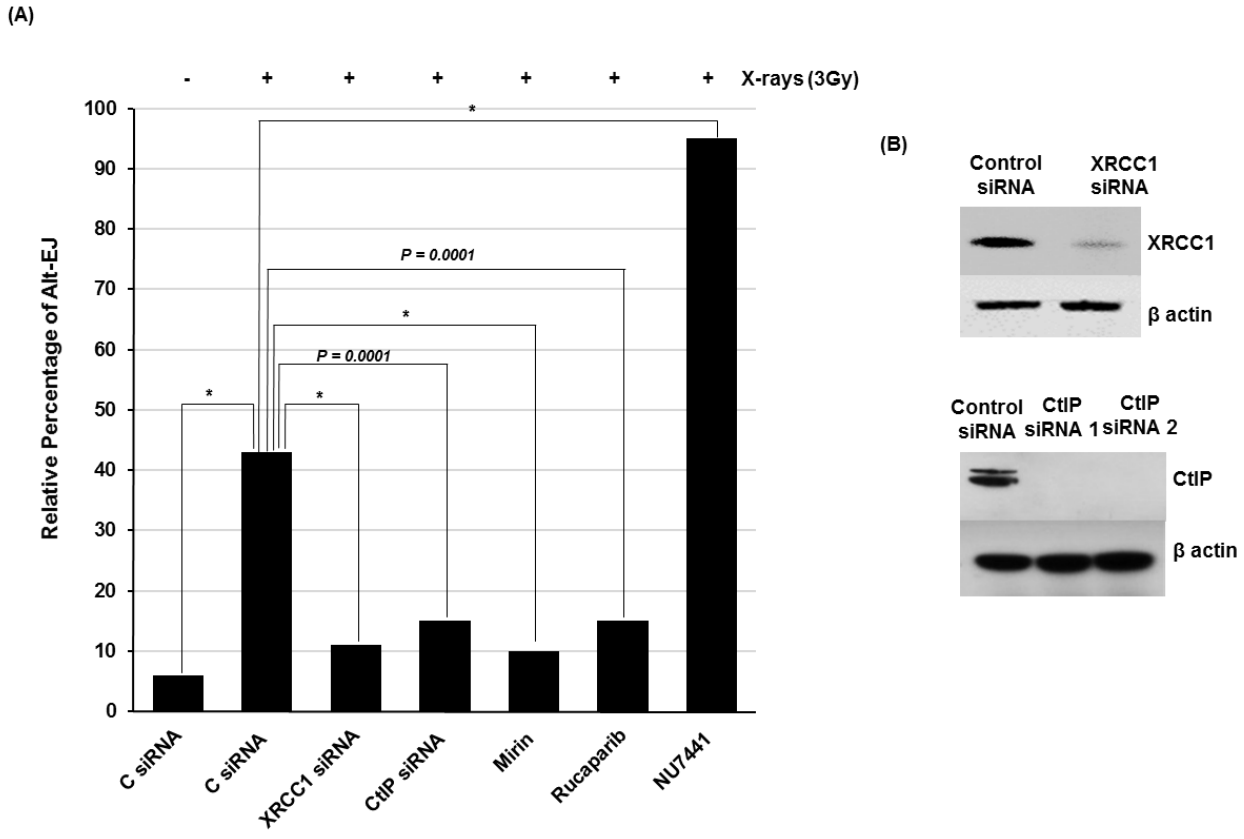

Figure 23. MMEJ after IR depends on XRCC1, CtIP, PARP1, and MRE11. In cell repair of pNS in control U2OS cells and cells treated with different doses of X-rays, XRCC1 siRNA (100 nM, 72 h), CtIP siRNA (100 nM, 72 h), rucaparib (10 μM), mirin (100 μM), or NU7441 (10 μM), as indicated. Reprinted from (156) with permission from Oxford University Press.

Proximity ligation assay (PLA) for XRCC1 and the DSB marker γH2AX confirmed that XRCC1 was recruited at DSBs in irradiated cell nuclei (Figure 24). Moreover, the number of PLA foci increased significantly after inhibition of DNAPK with NU7441, suggesting that XRCC1's involvement in DSB repair is more pronounced when NHEJ is inhibited (Figure 24). Significant reduction in the number of PLA foci showing XRCC4-γH2AX co-localization in NU7441-pretreated cells confirmed NHEJ inhibition (Figure 24).

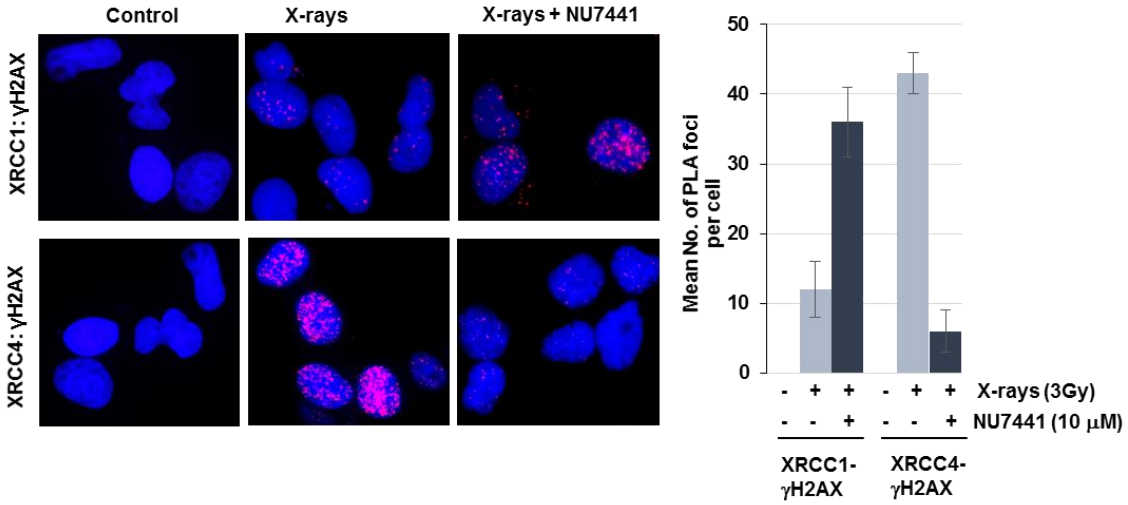

Figure 24. XRCC1 is recruited to DSBs after IR. PLA for XRCC1-γH2AX and XRCC4-γH2AX interaction in U2OS control cells, and in irradiated cells with or without 10 μM Nu7441. Quantification of the mean number of PLA foci per cell is shown in the right panel. Reprinted from (156) with permission from Oxford University Press.

Because we and others have observed that PARP1 is required for MMEJ (120), and assists recruitment of XRCC1 to SSBs (121), we asked if PARP1 regulates XRCC1 recruitment to DSBs. However, the number of XRCC1-γH2AX PLA foci were not reduced in irradiated cells pretreated with PARP1 inhibitor compared to that in control cells (Figure 25). This strongly suggests that while PARP1 stimulates MMEJ, it is not a rate-limiting factor for XRCC1 recruitment to DSBs, unlike SSB repair (122). Reduced auto-poly(ADP)-ribosylation of PARP1 in Rucaparib-treated cells confirmed PARP1 inhibition (Figure 25).

XRCC1's role in DSB repair was further confirmed by the increase in γH2AX foci level and their delayed disappearance in U2OS cells after combined depletion of XRCC1 and DNA-PK inhibition relative to DNA-PK inhibition alone (Figure 26). XRCC1-depleted cells also showed higher radiosensitivity than the control cells when treated with the DNAPK inhibitor (Figure 26). Together, these data indicate that XRCC1-mediated DSB repair is non-epistatic to

NHEJ. This conclusion is further supported by earlier studies showing DSB accumulation in the Arabidopsis genome after loss of XRCC1 (123).

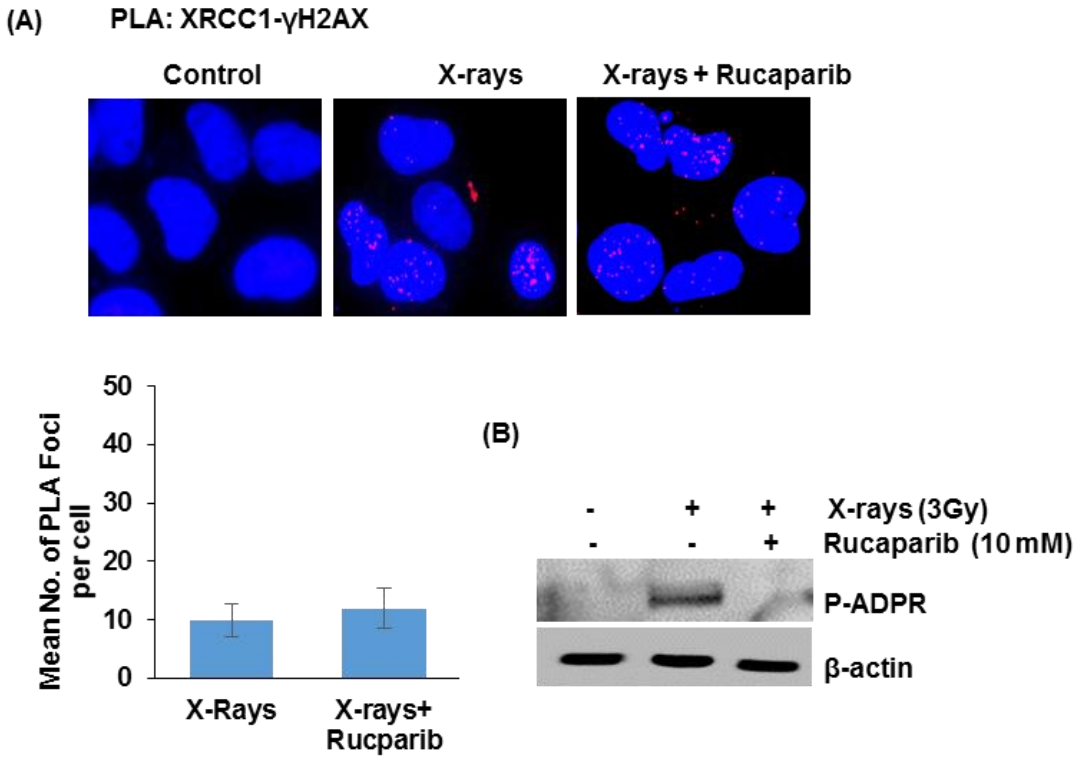

Figure 25. XRCC1 recruitment to DSBs is independent of PARP1 activity. (A) PLA for XRCC1-γH2AX interaction in control U2OS cells, and in irradiated cells with or without 10 μM rucaparib. Quantification of the mean number of PLA foci per cell is shown in the lower panel. (B) Western analysis for poly-ADP-ribosylated (ADPR) PARP1 of cell extracts from U2OS control cells, and irradiated cells with or without 10 μM rucaparib. Reprinted from (156) with permission from Oxford University Press.

3.2.6 CK2 Phosphorylation of XRCC1 Drives Formation of the XRCC1-MMEJ Complex

CK2-catalyzed phosphorylation of XRCC1 promotes SSBR by enhancing its interaction with LIG3 and PNKP (84,124). We tested if enhanced MMEJ activity in irradiated cells is also due to CK2 phosphorylation-dependent protein-protein interactions. FLAG-IP from U2OS cells

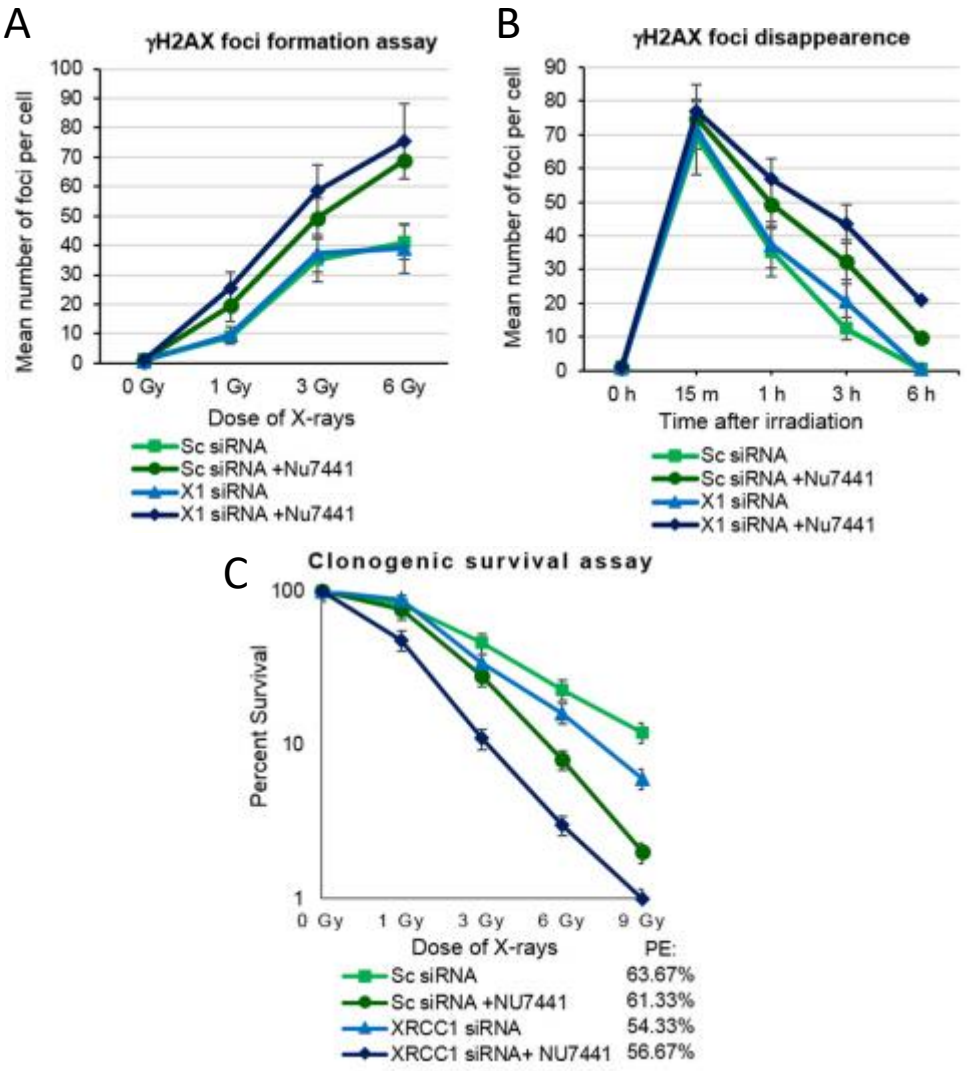

Figure 26. XRCC1 depletion affects DSBR and cell survival after IR. (A) γH2AX immunostaining in U2OS cells transfected with control siRNA or XRCC1 siRNA, with or without NU7441 treatment. Cells were fixed 1 h after irradiation with various doses of X-rays. (B) Kinetics of γH2AX foci disappearance in the same set of cells at different time points (15 min, 1, 3, 6 h) following treatment with 3 Gy X-rays. (C) Clonogenic survival analysis for the same set of U2OS cells treated with X-rays (0, 1, 3, 6, 9 Gy). Plating efficiency (PE) for each set of cells without irradiation is given. Reprinted from (156) with permission from Oxford University Press.

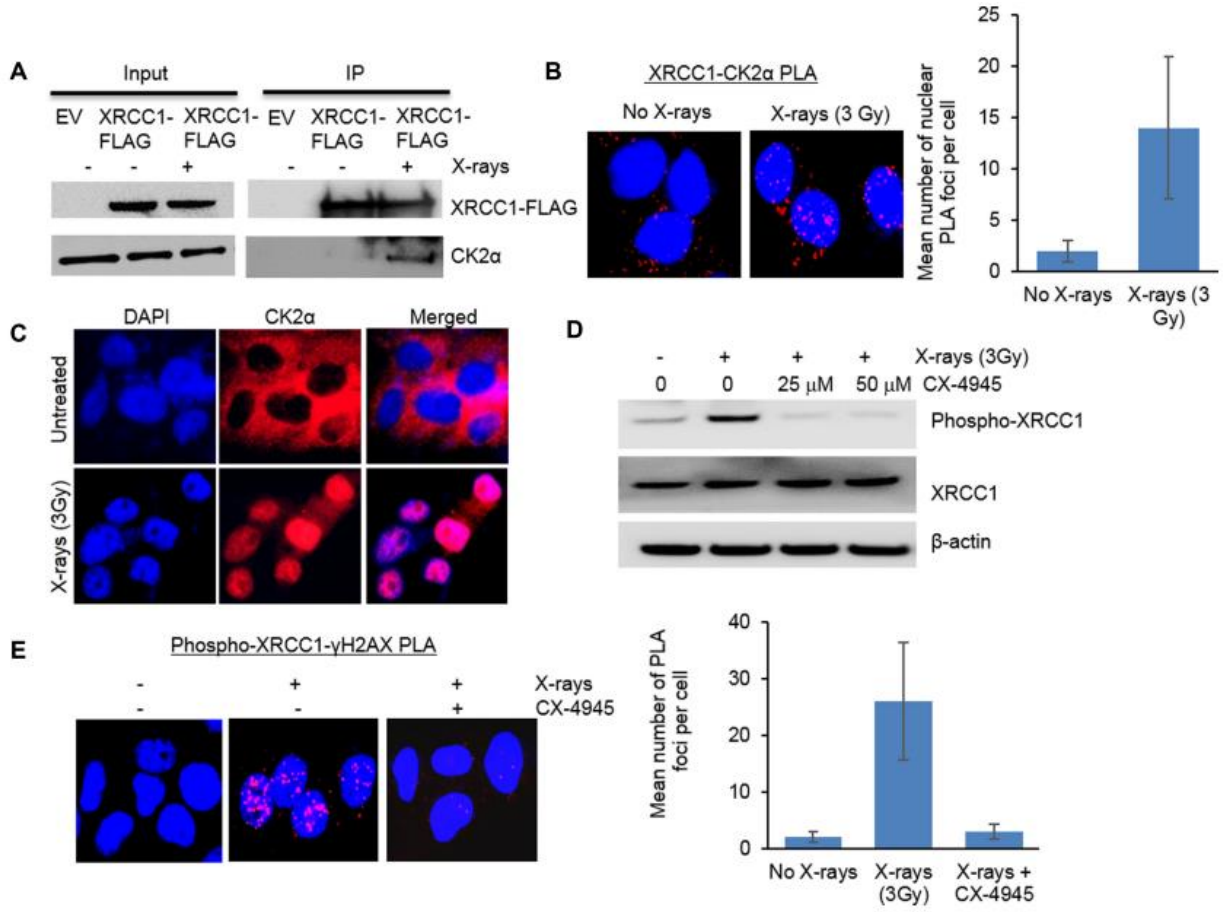

Figure 27. CK2 recruits XRCC1 to DSBs. (A) Western analysis of CK2αin XRCC1-FLAG IP with and without X-ray treatment. (B) XRCC1-CK2α PLA. (C) CK2α immunostaining in control and irradiated cells. (D) Western blot analysis of phosphorylated XRCC1 in U2OS control cells, irradiated cells, and cells treated with CX-4945 (25 μM, 50 μM) prior to irradiation. (E) PLA for phospho-XRCC1-γH2AX interaction in control cells, and irradiated cells with or without CX-4945 (50 μM) treatment. Reprinted from (156) with permission from Oxford University Press.

expressing ectopic XRCC1-FLAG showed a significant increase in CK2α level after irradiation with 3 Gy of X-rays, consistent with an increase in the number of nuclear PLA foci for XRCC1-CK2α (Figure 27). CK2 activated by stress signaling translocates to the nuclei after irradiation (125), where it colocalizes with γH2AX foci (126). We observed CK2α localization to the nuclei of irradiated U2OS cells, together with an increase in phosphorylation of XRCC1 at S518/T519/T523, which was reduced in cells pretreated with the CK2 inhibitor CX-4945 (Figure

27). Furthermore, the phospho-XRCC1-γH2AX PLA foci in irradiated cells indicated localization of phosphorylated XRCC1 at DSBs, which was blocked by CX-4945 (Figure 27).

The 3' ssDNA overhang, a prerequisite for stabilizing DSB termini via microhomology-dependent annealing in MMEJ, is generated by the end processing nucleases MRE11 and CtIP (103,127,128); however, their role in coordinating MMEJ is not clearly understood. Because we observed recruitment of XRCC1 at X-ray-induced DSBs, we tested the role of XRCC1 in assembling the MMEJ complex. We isolated IPs of endogenous XRCC1 or XRCC1-FLAG from nuclear extracts of control U2OS cells or those transiently expressing XRCC1-FLAG, and identified MRE11 and CtIP in the IPs (Figure 28). The levels of these proteins in the IPs increased after irradiation (Figure 28). The XRCC1 level in the U2OS nuclear extract also increased after irradiation; however, its interaction with MRE11 and CtIP was prevented in cells pretreated with CX-4945, which was further confirmed by PLA analysis (Figure 28).

We then analyzed FLAG-IP from U2OS nuclear extracts transiently expressing, at a comparable level, XRCC1-WT or non-phosphorylable XRCC1-CKM-FLAG (each of the eight primary serine/threonine CK2 target sites within the linker domain mutated to alanine). We observed a significant increase in MRE11 and CtIP levels in the XRCC1-WT-FLAG-IP but not in XRCC1-CKM-FLAG-IP isolated from irradiated cells (Figure 29). This confirmed that CK2-mediated phosphorylation of XRCC1 is critical for its interaction with both MRE11 and CtIP.

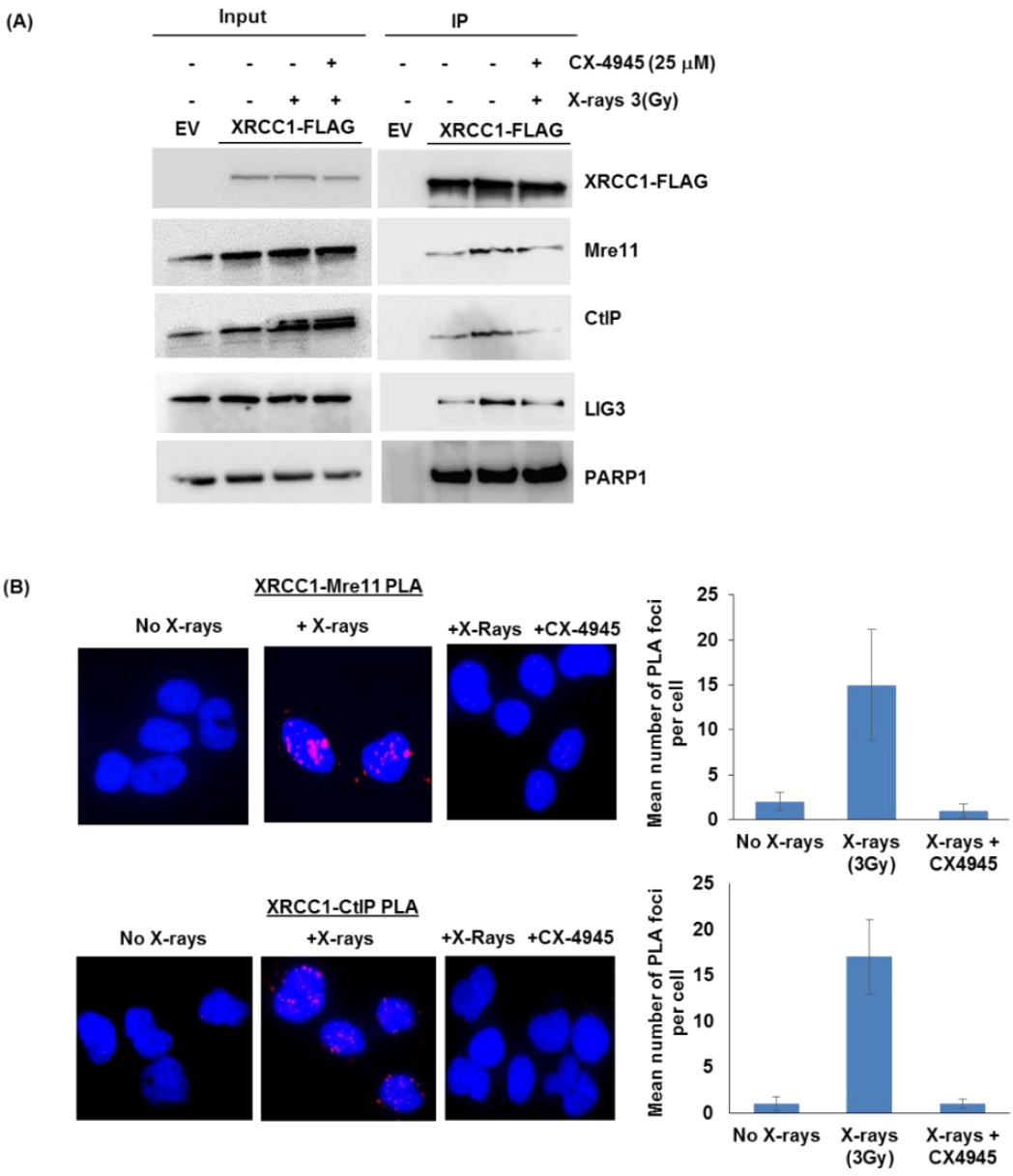

Figure 28. CK2 is required for MMEJ complex formation. (A) Western blot analysis of XRCC1, phospho-XRCC1, MRE11, CtIP, and LIG3 in endogenous XRCC1-IP isolated from nuclear extract of U2OS cells pretreated with X-rays (3 Gy) and/or CX-4945 (50 μM) treatment as indicated. (B) PLA for XRCC1-MRE11 (top panel) and XRCC1-CtIP (bottom panel) interactions in U2OS cells with the same treatments. Reprinted from (156) with permission from Oxford University Press.

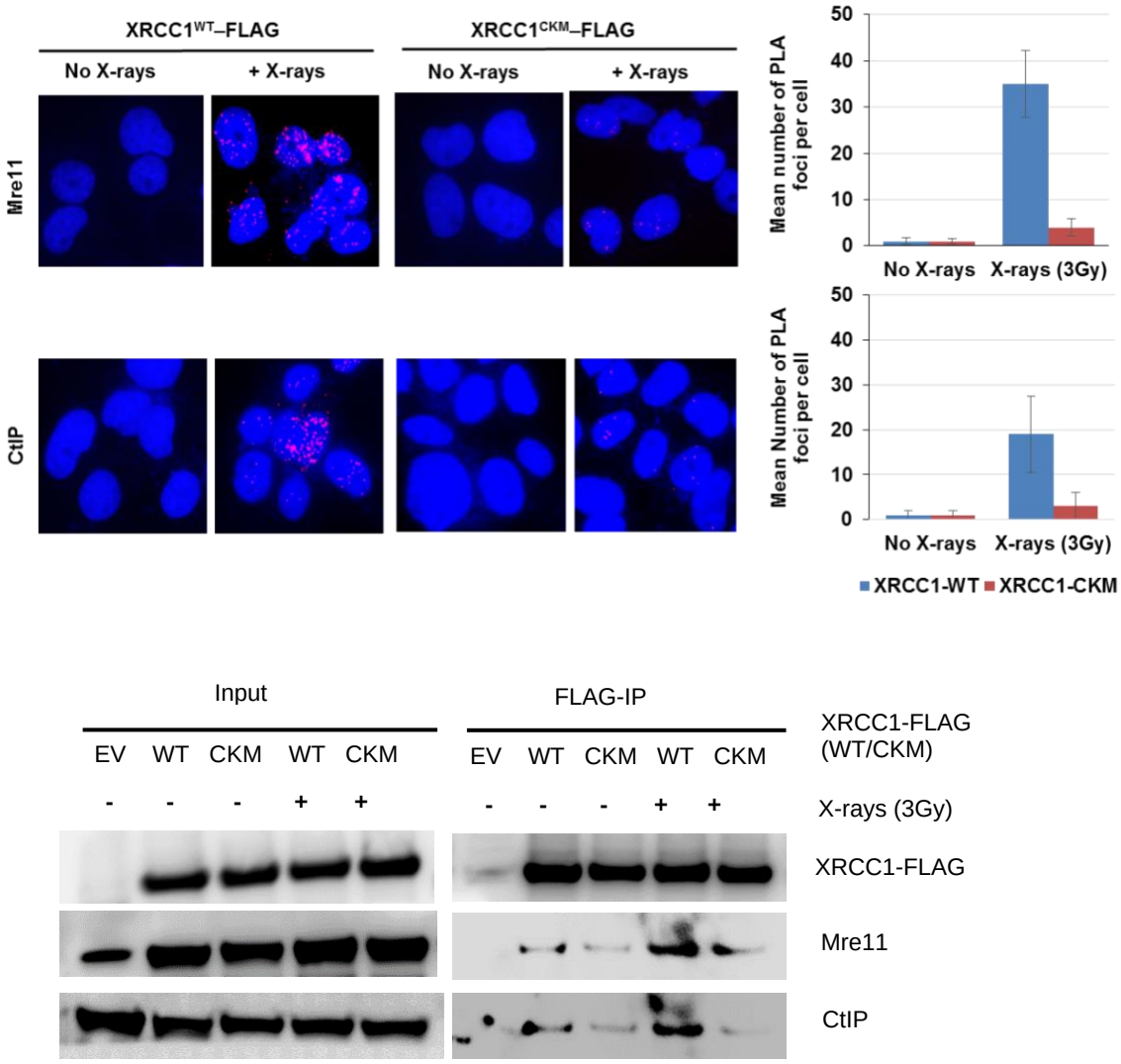

Figure 29. CK2 phosphorylation of XRCC1 is required for MMEJ complex formation. (A) PLA for interaction of MRE11 and CtIP with XRCC1 WT-FLAG (left panels) or XRCC1 CKM-FLAG (right panels) in control or irradiated cells. (B) Western blot analysis of MRE11 and CtIP in XRCC1 WT- or XRCC1 CKM-FLAG IP isolated from nuclear extract of U2OS cells transiently expressing XRCC1 WT- or XRCC1 CKM-FLAG. Reprinted from (156) with permission from Oxford University Press.

3.2.7 XRCC1-MRE11 Interaction is Not Mediated by LIG3/NBS1

The XRCC1/LIG3 complex has been shown to interact with the MRN complex via the BRCT domain of LIG3 and the FHA domain of NBS1 (30). However, we found that the level of MRE11 in XRCC1-FLAG IP was unaffected by siRNA-mediated depletion of LIG3 or NBS1

(Figure 30), strongly suggesting direct interaction between XRCC1 and MRE11 rather than indirect association via LIG3–NBS1 interaction.

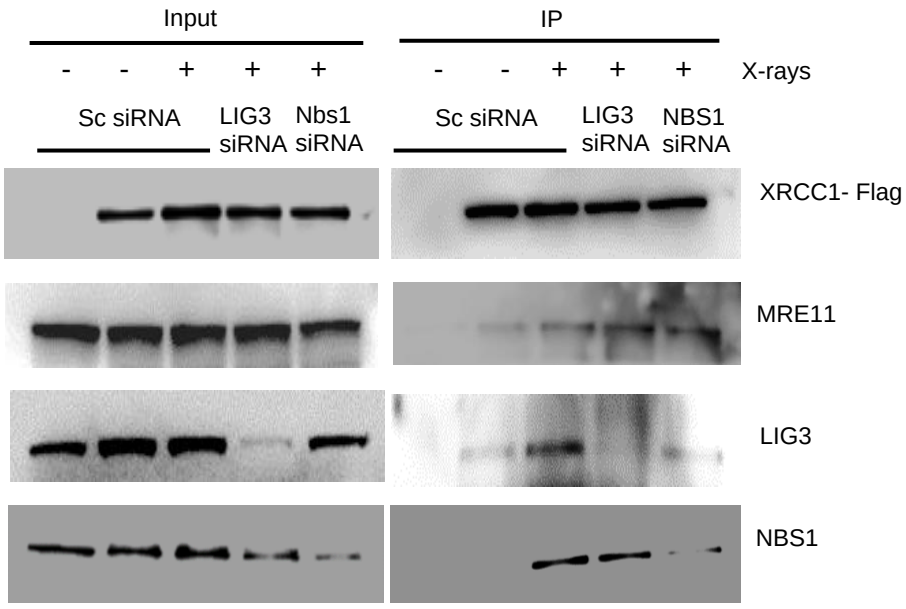

Figure 30. XRCC1 and MRE11 do not interact through Ligase 3/NBS1. Western blot analysis of MRE11, LIG3 and NBS1 in XRCC1-FLAG IP from control or irradiated U2OS cells transfected with XRCC1-WT-FLAG (48 h), and scrambled (Sc), LIG3, or NBS1 siRNA (100 nM, 72 h), as indicated. Reprinted from (156) with permission from Oxford University Press.

3.2.8 CK2 Phosphorylation of XRCC1 Promotes MMEJ

Based on the observation that irradiation enhances the XRCC1-MRE11/CtIP interaction via XRCC1 phosphorylation, we tested if CK2 inhibition or depletion reduces MMEJ activity. Significant reversal of radiation-induced MMEJ in U2OS cells pretreated with CX-4945 or CK2α siRNA suggests a critical role of CK2-mediated XRCC1 phosphorylation in MMEJ (Figure 31). This was further supported by restoration of radiation-induced enhancement of MMEJ by ectopic WT-XRCC1 but not the phosphomutant XRCC1-CKM in cells depleted of endogenous XRCC1, even though the ectopic proteins were similarly localized at the DSB sites (Figure 31).

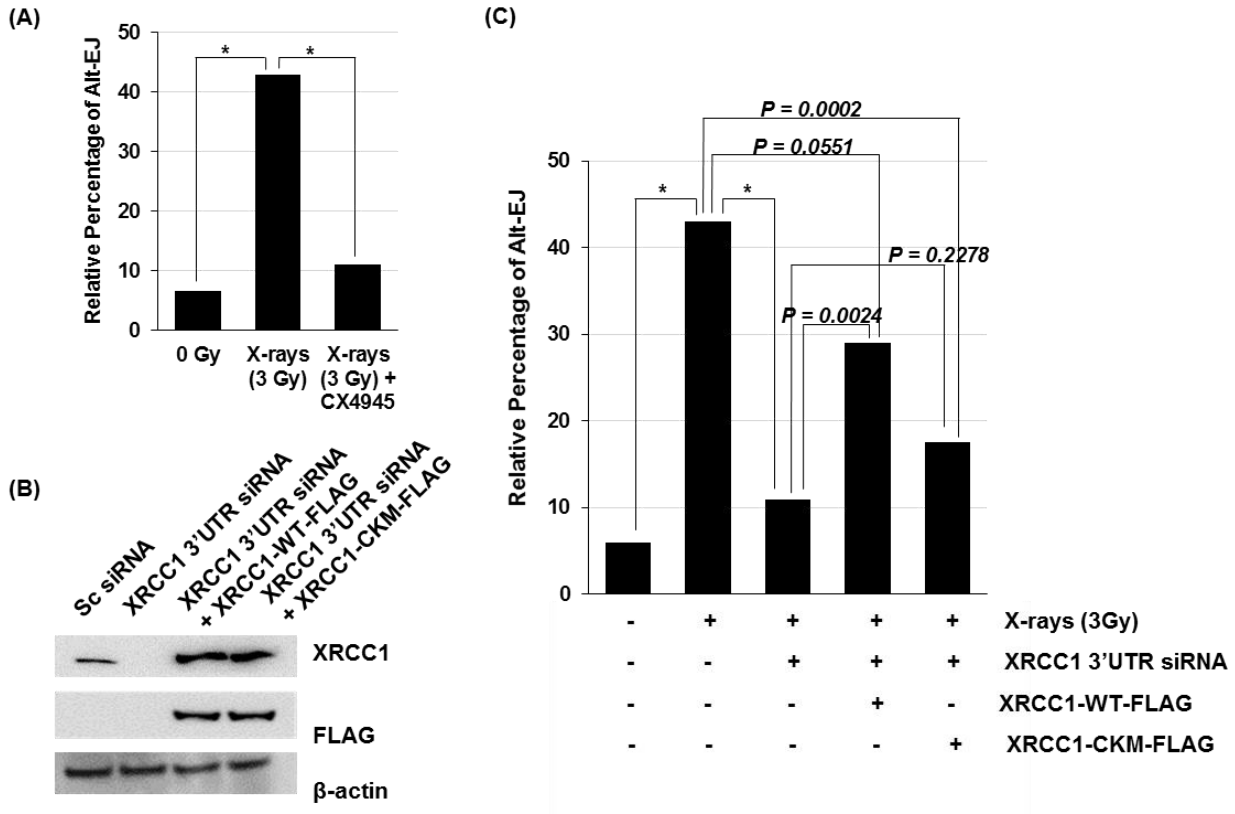

Figure 31. CK2 phosphorylation of XRCC1 promotes MMEJ *in cell.* (A) In cell repair of pNS, in control or preirradiated U2OS cells, pretreated wih CX-4945 (25 μM). (B) Western analysis for endogenous XRCC1 and ectopic XRCC1 WT- or XRCC1 CKM-FLAG after XRCC1 3' UTR siRNA treatment. (C) In cell repair of pNS in U2OS cells transfected with either empty vector, XRCC1 WT-FLAG or XRCC1 CKM-FLAG plasmids, along with either scrambled siRNA or XRCC1 3' UTR siRNA, as indicated, with/without preirradiation. Reprinted from (156) with permission from Oxford University Press.

3.2.9 XRCC1 Performs MMEJ *In Vitro*

Because we detected XRCC1 interaction with the DSB processing nucleases MRE11 and CtIP, we asked if the XRCC1-IP could carry out MMEJ in vitro. The XRCC1-FLAG IP isolated from the nuclear extract of U2OS cells expressing ectopic XRCC1-FLAG was incubated with pNS for 30 minutes at 37°C in a buffer containing ATP and dNTPs, and supplemented with purified recombinant protein complex XRCC1/LIG3α, followed by incubation for 15 h at 16°C (Figure 32).

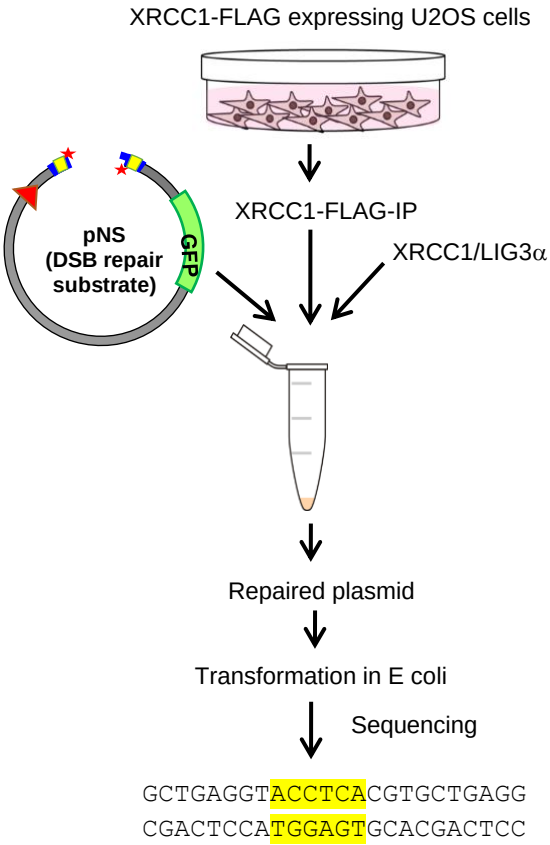

Figure 32. Schematic outline of MMEJ *in vitro* assay using XRCC1-FLAG IP. Reprinted from (156) with permission from Oxford University Press.

After transformation, the plasmids recovered from E. coli showed that XRCC1-FLAG IP was able to carry out MMEJ in vitro with moderate efficiency (Figure 33). However, unlike plasmids recovered after the in cell repair of pNS, which showed both NHEJ and MMEJ products, only MMEJ products were observed for the plasmid substrate repaired in vitro with XRCC1-IP. This was expected because the XRCC1-IP should contain only proteins involved in MMEJ/BER, and not in NHEJ. This novel observation provides the first direct evidence for a specific MMEJ protein complex functioning in cell. Irradiation of U2OS cells before isolation of the XRCC1 IP increased its MMEJ activity (Figure 33), consistent with the in cell data. Importantly, pretreatment of the XRCC1-FLAG IP with the MRE11 inhibitors mirin and PFM03

(129) strongly inhibited MMEJ activity (Figure 33), further validating the in vitro assay and supporting the functional requirement for both MRE11's exonuclease and endonuclease activities in MMEJ. Moreover, pretreatment of cells with CX4945 prior to isolation of XRCC1 IP reduced the ability of the isolated complex to carry out MMEJ in vitro (Figure 33). This supports our in cell results showing the requirement for CK2-mediated XRCC1 phosphorylation for MMEJ. We further confirmed this by comparing MMEJ activity in FLAG-IPs isolated from cells ectopically expressing XRCC1-WT- or XRCC1-CKM-FLAG (Figure 33). Although significantly lower than XRCC1-WT-IP, XRCC1-CKM-IP from irradiated cells showed some activity in plasmid circularization, presumably because it partially mimics phosphorylated XRCC1.

3.2.10 XRCC1 Interacts Directly With MRE11 *In Vitro*

Based on our findings that the LIG3/NBS1 interface does not mediate the XRCC1-MRE11 interaction, we decided to test whether purified XRCC1 and MRE11 interacted *in vitro.* Full-length XRCC1-His tagged and XRCC1-GST tagged, and three truncated forms, one lacking the NTD and first linker region (Δ293-XRCC1-GST), the second consisting of only the BRCT1 domain (BRCT1-XRCC1-GST), and the third consisting of only the BRCT2 domain (BRCT2-XRCC1-GST), were purified from E. coli. Full length MRE11-FLAG was a gift from Tanya Paull. MRE11 regions encompassing aa 1-273 (MRE11-A-GST), aa 223-535 (MRE11-B-GST), and aa 487-708 (MRE11-C-GST) were purified from E. coli. Purified proteins were incubated for 1h at 4°C, followed by addition of either Ni-NTA beads (for His-tag isolation) or FLAG beads (for FLAG isolation). After washing, proteins were eluted with 2X LDS and run on a NuPage gel. We found that the Δ293-XRCC1-GST construct was able to pull down full-length MRE11-FLAG, as was the BRCT1 domain (Figure 34). However, the BRCT2 domain was not,

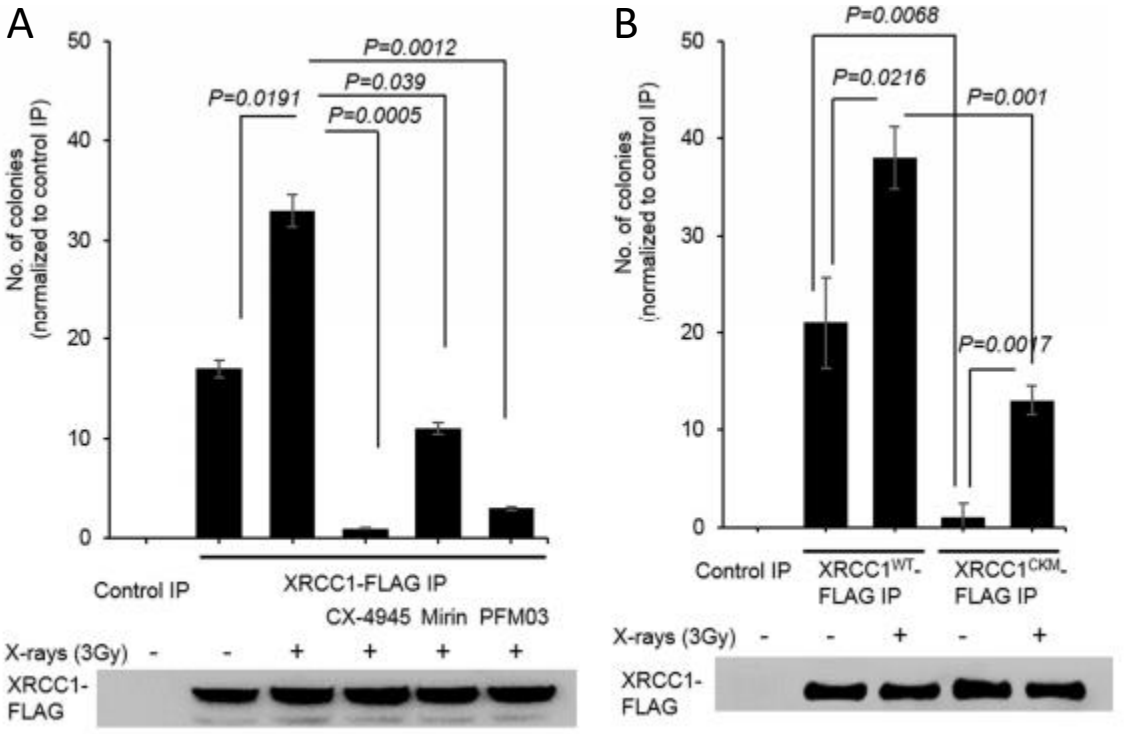

Figure 33. CK2 phosphorylation of XRCC1 promotes MMEJ *in vitro.* (A) Mean number of colonies obtained from the in vitro repair assay with empty vector (EV) or XRCC1-FLAG IP from control, irradiated cells and those treated with CX-4945 before irradiation; XRCC1-FLAG IP from irradiated cells was separately incubated with 100 μM mirin or PFM03 before performing in vitro repair of pNS. The amount of IP used was normalized to the XRCC1 level. (C) In vitro repair of pNS with XRCC1 WT or XRCC1 CKM-FLAG IP from control or irradiated cells. Western blot analysis of XRCC1-FLAG levels in the IPs for each experiment are shown. Reprinted from (156) with permission from Oxford University Press.

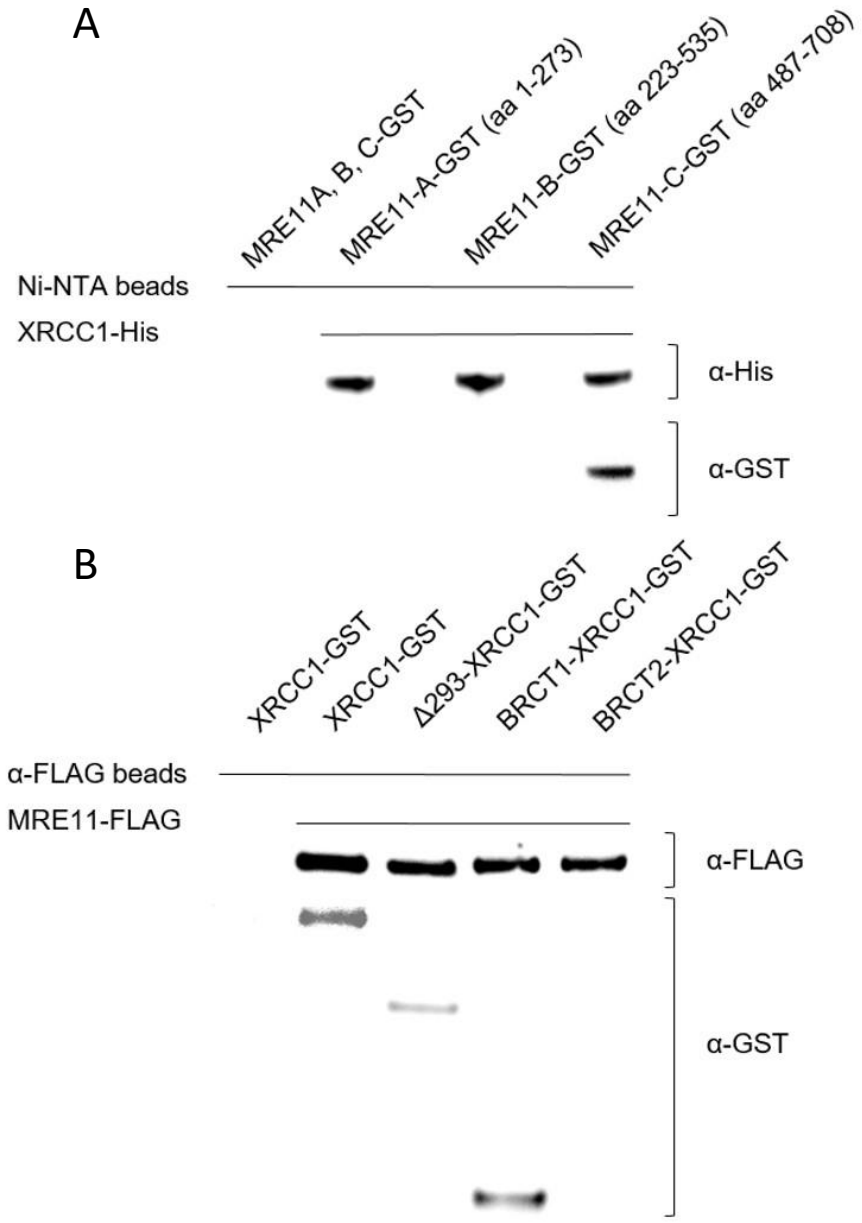

Figure 34. XRCC1 and MRE11 interact *in vitro.* (A) *In vitro* pulldown of XRCC1-His incubated with various MRE11-GST domains with Ni-NTA beads. (B) *In vitro* pulldown of MRE11-FLAG incubated with various XRCC1-GST domains with FLAG beads. Reprinted from (156) with permission from Oxford University Press.

indicating that this interaction was specific to the BRCT1 domain (Figure 34). Pulldown of full-length XRCC1 with domains of MRE11 indicated that XRCC1 interacts specifically with the C-terminal region of MRE11 (Figure 34).

3.3 Discussion

NHEJ, the predominant pathway for DSB repair in the human genome in both growing and quiescent cells, repairs ~75% of DSBs within 30 min (8). However, DNA breaks with complex damage, such as those induced by IR, require additional processing and may therefore not be repaired via NHEJ (130). For such complex breaks, slower repair processes that involve end trimming, such as accurate HR or error-prone MMEJ, may be critical. While HR critically contributes to DSB repair in the replicating cancer cell genome, MMEJ's role in survival of cancer cells is becoming increasingly evident, particularly in cancers with HR defects (24). Furthermore, MMEJ could be particularly pronounced in DSB repair at repetitive sequences, which are abundant in mammalian genomes(131). Thus, the microhomology sequences observed at chromosomal breaks in many cancers implicate MMEJ in DSBR and radioresistance (108,132). In order to unravel the regulation, molecular mechanisms and prevalence of MMEJ, it is important to establish cellular and in vitro assays for this pathway of DSB repair. To explore repair of IR-induced DSBs containing 3'-blocked termini (132), we developed a linear plasmid substrate containing 3'P and DSB-flanking microhomology sequences, and were able to estimate the relative contribution of NHEJ and MMEJ to DSB repair. Although the particular sequence arrangement in this plasmid may not commonly occur in the human genome, it does represent genomic DSBs with microhomology sequences, and thus facilitates identification of the parameters that regulate MMEJ. In spite of the presence of microhomologies, NHEJ was found to be the preferred pathway of repair in two distinct plasmid substrates in untreated cells, which

is in agreement with published reports of the comparatively a minor contribution of MMEJ to DSB repair in normal human cells. At the same time, this provides strong validation for our assay. While our system of repairing naked plasmid DNA does not completely simulate DSB repair at the chromatin level, and cannot exclude possible nonspecific degradation of the DNA substrate during its intracellular transit, it recapitulates the known requirements for NHEJ and MMEJ in mammalian genomes. Thus, this straightforward assay allowed us to identify external factors, such as radiation exposure and kinase signaling, that regulate MMEJ. Moreover, our discovery of the ability of XRCC1-IP to carry out MMEJ in vitro (in which no possibility of intracellular nonspecific substrate degradation exists) provides an opportunity for establishing biochemical requirements for MMEJ.

During elucidation of BER mechanisms, the formation of dynamic repair complexes that enhance repair of diverse DNA lesions in response to genotoxic stress has been documented (133-135). It is evident that the formation of such complexes is facilitated by the nonenzymatic scaffold protein XRCC1. The stability of such repair complexes is likely to be dependent on binary interactions among the components of the complex, which are modulated by their reversible, covalent modifications (136). In delineating the mechanisms of MMEJ, we discovered XRCC1's key role in this repair pathway. Because XRCC1 appears to be limiting in MMEJ, we tested whether radiation-induced covalent modifications of XRCC1 promote its interactions and involvement in MMEJ. XRCC1 is phosphorylated at multiple sites, particularly at the linker regions between the conserved domains (137). Notably, CK2-mediated phosphorylation of XRCC1 at the inter-BRCT domain linker region prevents proteasomal degradation (83), and also reduces its affinity for naked DNA (84). Thus, XRCC1, normally sequestered in chromatin (138), may be mobilized by phosphorylation to form multiprotein

repair complexes, mediated by interactions involving its conserved N-terminal and BRCT domains, as well as the unstructured linker domains. Here, we have shown that XRCC1 depends on CK2-mediated phosphorylation for its interaction with MRE11 in irradiated cells, distinct from the interaction between the XRCC1-LIG3 and MRN complexes occurring via LIG3-BRCT and NBS1-FHA domains (30). Our identification that XRCC1 and MRE11 interact *in vitro* supports the model where MRE11 and XRCC1 interact directly to mediate repair. Our data suggest that phospho-XRCC1 directly interacts with MRE11, which could be further stabilized by LIG3-NBS1 interaction. Hence, it is possible that XRCC1 is recruited at DSBs via MRN rather than PARP1, as is currently believed (104). Future structural studies may illuminate how XRCC1's conformational changes induced by phosphorylation facilitate specific protein-protein interactions. Importantly, we have shown that the induction of XRCC1 repair complexes via IR-induced CK2 phosphorylation could account for the increase in MMEJ-mediated DSBR in irradiated cells. Based on such a scenario, it would be worth investigating how MMEJ is affected by XRCC1 phosphorylation at other sites by CHK2 and DNA-PK (137). MMEJ, which utilizes the SSBR proteins, is distinct from the HDR and NHEJ pathways for DSB repair. However, several variations of MMEJ likely exist depending on the cell type and the nature of DNA strand breaks. For example, XRCC1 is apparently dispensable for Alt-EJ/MMEJ mediated class-switch recombination or IgH/c-myc translocation in XRCC4-deficient B cells (139). This is evidently distinct from the MMEJ of IR-induced DSBs. The clustered damage induced by IR in the genome contains a large number of closely spaced bi-stranded lesions that could lead to secondary DSBs formed as BER intermediates (52). These secondary DSBs, possibly with ssDNA overhangs, have poor affinity for Ku, whose binding to the DSB termini is a prerequisite for NHEJ (140,141). Their repair may thus exploit multiple modes of Alt-EJ, including MMEJ,

whose initiation is dependent on the recruitment of the SSB factors XRCC1 and PARP1, which compete with Ku (20). Additionally, in the absence of microhomology spanning the DSB, MMEJ could utilize microhomology sequences synthesized de novo, for which Pol θ is a likely candidate. Another unanswered question that our assay helps address is how resection at the DSB termini regulates MMEJ. Both MMEJ and HR require generation of 3' overhangs through resection at the 5' end. Nonetheless, a profound difference exists between the extended overhang required in HR versus the short overhang promoting MMEJ. We have shown that MMEJ is dependent on both endo- and 3' →5' exonuclease activities of MRE11, as was also shown in HR (129). Furthermore, the endonuclease inhibitor showed a stronger inhibitory effect on MMEJ, suggesting that an initial endonuclease nick followed by exonuclease excision generates the 3' overhang at blocked DNA breaks in irradiated cells. Overall, the contribution of MRE11, CtIP, EXO1 and DNA2 to excision during DSBR is poorly understood (142). Our results have established a functional role for both nuclease activities of MRE11 in MMEJ. However, extensive end resection by MRE11/CtIP could lead to generation of long ssDNA overhangs where RPA binding would inhibit MMEJ (143). It is therefore important to investigate if XRCC1 regulates end resection at DSBs during MMEJ, similar to the BRCA2 and FANC protein-mediated regulation of MRE11 activity for replication fork protection or inter-strand crosslink repair (47). In summary, we have shown that the contribution of MMEJ to DSB repair in the genome is affected by radiation exposure via enhancement of the formation of MMEJ-proficient XRCC1 complex. Paradoxically, radiation therapy, while killing tumor cells, may induce radioresistance in surviving cells by activating MMEJ to repair radiation-induced genome damage, possibly leading to increased mutations. It is possible that the altered phenotype caused by some of these mutations provides growth advantage to the surviving cells and may promote

tumor regrowth. Our results showing that XRCC1-MRE11 interaction, dependent on XRCC1 phosphorylation by CK2, activates MMEJ, suggests that this interaction could be a potential therapeutic target for inhibiting MMEJ, thereby increasing radiosensitivity of cancer cells.

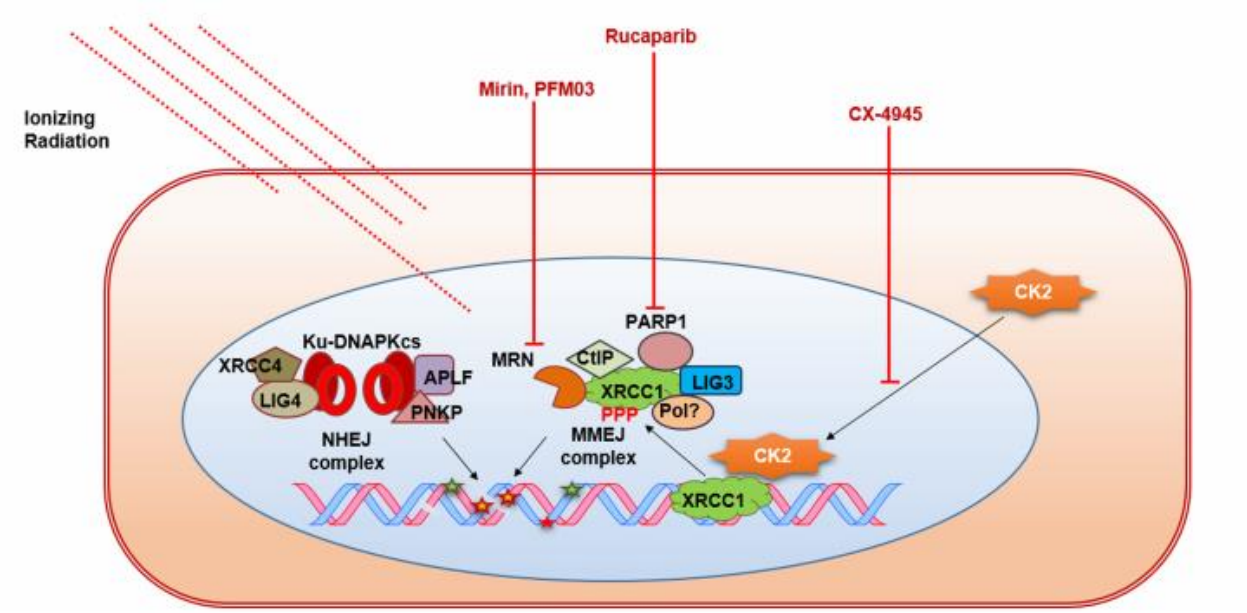

Figure 35. Model for activation of XRCC1-MMEJ repair complex by CK2 after IR. In cancer cells treated with X-rays, CK2 is activated, localizes to the nucleus, phosphorylates XRCC1 bound to chromatin or in the nuclear lamina, and promotes the formation of MMEJ complexes that consist of MRN, CtIP, LIG3 and possibly other MMEJ factors such as DNA polymerases. The active XRCC1 repair complexes then localize to DSB sites (overt or secondarily generated) to carry out MMEJ, possibly competing with or complementing NHEJ. MRE11 endonuclease and exonuclease, PARP1 and CK2 inhibitors prevent activation of MMEJ.

4. XRCC1 PROMOTES MUTAGENIC DNA REPAIR AND REGULATES REPLICATION FORK DYNAMICS IN BRCA2-DEFICIENT CELLS*

4.1 Introduction

Mutations can confer selective growth advantages on cancer cells, which leads to their clonal selection and expansion. DNA damage due to high levels of oxidative stress and replication stress, in combination with aberrant DNA repair mechanisms, drives mutation accumulation and genomic instability in cancer cells. Chemoradiation therapy induces DNA damage in order to kill cancer cells, however, DNA repair processes can lead to post-therapy survival of cancer cells (92).

DNA double-strand breaks (DSBs) are the most lethal DNA damage, which are induced by cancer therapies, replication stress, and oxidative stress (52). DSBs generated during S/G2 phases of the cell cycle are typically repaired accurately via homologous recombination (HR), which utilizes the undamaged sister chromatid as a template (17). Several HR factors, including BRCA1, BRCA2, PALB2, and RAD51, have been identified as cancer susceptibility genes (144). When they are mutated or deleted, HR is impaired, and DSBs that arise during S/G2 phases have to rely on alternative pathways for repair, which are often error-prone (24-26,64,65). These breast cancer susceptibility genes have also been found to have HR-independent roles in replication fork protection (44,46). In their absence, stalled forks are degraded by nucleases, including MRE11. This degradation also depends on a number of other factors, including

*Parts of this chapter are reprinted with permission from "XRCC1 promotes replication restart, nascent fork degradation and mutagenic DNA repair in BRCA2-deficient cells" by Eckelmann B, Bacolla A, Wang H, Ye Z, Guerrero EN, Jiang W, *et al.*, 2020. *Nucleic Acids Research Cancer*, 2, 3, Copyright 2020 by Oxford University Press.

PARP1, and replication restart of degraded forks has been demonstrated to contribute to genome instability of HR-deficient (HRD) tumors (145-147).

Genome instability arising from error-prone DSB repair and restart of degraded forks has been observed in whole-genome sequencing studies of HRD tumors. A specific mutational signature, signature 3, characterized by chromosomal translocations whose breakpoints are flanked by microhomology (MH) sequences, is associated with HRD tumors (60,144,148-151). Whether these rearrangements result from HR failure at DSBs, extensive fork degradation and restart, or both is unknown. Regardless, the observation of MH at breakpoints implicates microhomology-mediated end joining (MMEJ), a backup, error-prone repair pathway, in DSB repair and/or fork restart in these tumors.

MMEJ involves limited resection at DSBs by the MRE11 and CtIP nucleases, gap filling synthesis by DNA polymerase θ (POLQ), scaffolding by XRCC1, and ligation by DNA ligase 1 or 3 (LIG1/LIG3) (19). MMEJ was discovered as a backup end-joining pathway for non-homologous end-joining (NHEJ), which directly joins two double-stranded DNA ends, and has a minor role in NHEJ and HR-proficient cells. Despite its minor role, MMEJ contributes to chromosomal rearrangements and genomic instability in aneuploid cancer cells (108,152), which tolerate MMEJ-mediated mutations. Recent studies showed that MMEJ is also a backup pathway for HR, as it is upregulated in BRCA2-deficient tumors, where POLQ in particular is critical for genome maintenance and tumor survival (24-26,64,65). Several MMEJ factors, including POLQ, PARP1, and XRCC1 were identified as synthetic lethal with BRCA2 in a recent CRISPR screen (67). Previous reports have implicated XRCC1 in genomic stability of HRD breast and ovarian cancers (153-155), however the precise role of XRCC1 in these cancers is not well-studied.

XRCC1 canonically coordinates base excision repair (BER) and single-strand break repair (SSBR), through scaffolding and stimulation of several factors involved in these repair pathways (81). Recent evidence point towards additional roles of XRCC1 in DNA metabolism beyond these functions, specifically in DSB repair (DSBR) and the resolution of DNA replication intermediates (3,30,75,89,90). We recently observed that XRCC1 plays a direct role in MMEJ, an alternative form of DSBR, by scaffolding MRE11 and CtIP in response to radiation to form a MMEJ-competent complex (156). Collectively, these observations led us to hypothesize that XRCC1 has a role in resolving single-ended DSBs (seDSBs) that arise at collapsed replication forks through a MH-based mechanism.

Whether XRCC1 and MMEJ have roles in resolving stalled and collapsed replication forks in HRD tumors is a critical question. The efficacy of PARP inhibitors (PARPi) in HRD tumors may be linked to the role of XRCC1 in these tumors, as XRCC1 is one of the primary targets of PARP1 (157). Additionally, POLQ is a promising chemotherapeutic target in HRD tumors, and discovering how it participates in active repair complexes is an important goal. In this study, we have examined the role of XRCC1 in HRD cancers using several approaches. We show that replication fork collapse stimulates a MH-based repair process that involves formation of a MMEJ-competent XRCC1 complex containing end resection factors and DNA polymerases. This process is suppressed by BRCA2, implicating XRCC1 in MMEJ in HRD cancers. We find that XRCC1 promotes replication fork restart, and discover that XRCC1 promotes stalled fork degradation in BRCA2-deficient cells. Our findings thus provide mechanistic insight into the MMEJ pathway in HRD cells, and add evidence to the growing connection between MH usage in DSBR and replication fork protection and restart, with broad implications in carcinogenesis and genetic disease. Finally, we provide evidence of a novel gene

expression program in HRD cells that may be linked to platinum and PARPi sensitivity of these tumors.

4.2 Results

4.2.1 XRCC1 has a Minor Contribution to Cellular Survival and DSB Repair After Replication Stress in HR-proficient Cells

DSBs arising during S/G2 phases of the cell cycle are typically repaired via HR (17). High levels of replication stress that occur in cancers lead to increased levels of S/G2 DSBs (158), and when HR is defective in cancer cells, alternative methods of DNA repair have to be engaged during S/G2 phases for cell survival (26). However, seDSBs that result from replication stress and replication fork collapse are not preferred substrates for NHEJ (45). Whether these seDSBs are a substrate for MMEJ or related repair pathways is an important question in cancer biology. Previous studies (26,43,103,159) have suggested that replication stress causes DSBs that can be repaired via MMEJ. Whether XRCC1 is involved in MMEJ after replication stress, and in particular in BRCA-deficient cancer cells, is unknown.

Based on our identification of XRCC1 as a critical component of MMEJ (156), in addition to observations that XRCC1-depleted cells are sensitive to ATR inhibition (160), we explored XRCC1's role in the replication stress response. Hydroxyurea (HU), an inhibitor of ribonucleotide reductase (RNR), depletes the cells of deoxyribonucleotides, causing replication fork stalling (161). ATR prevents fork collapse in several ways, and the combination of HU with an ATR inhibitor (ATRi) is known to cause fork collapse (162). Downregulation of XRCC1 by siRNA was confirmed by Western Blotting (Figure 36). Survival assays indicate that XRCC1-depleted cells are mildly sensitive to HU and VE-821, an ATRi (Figure 36). The neutral comet assay indicated that more DSBs accumulated in XRCC1-depleted cells than control cells (Figure

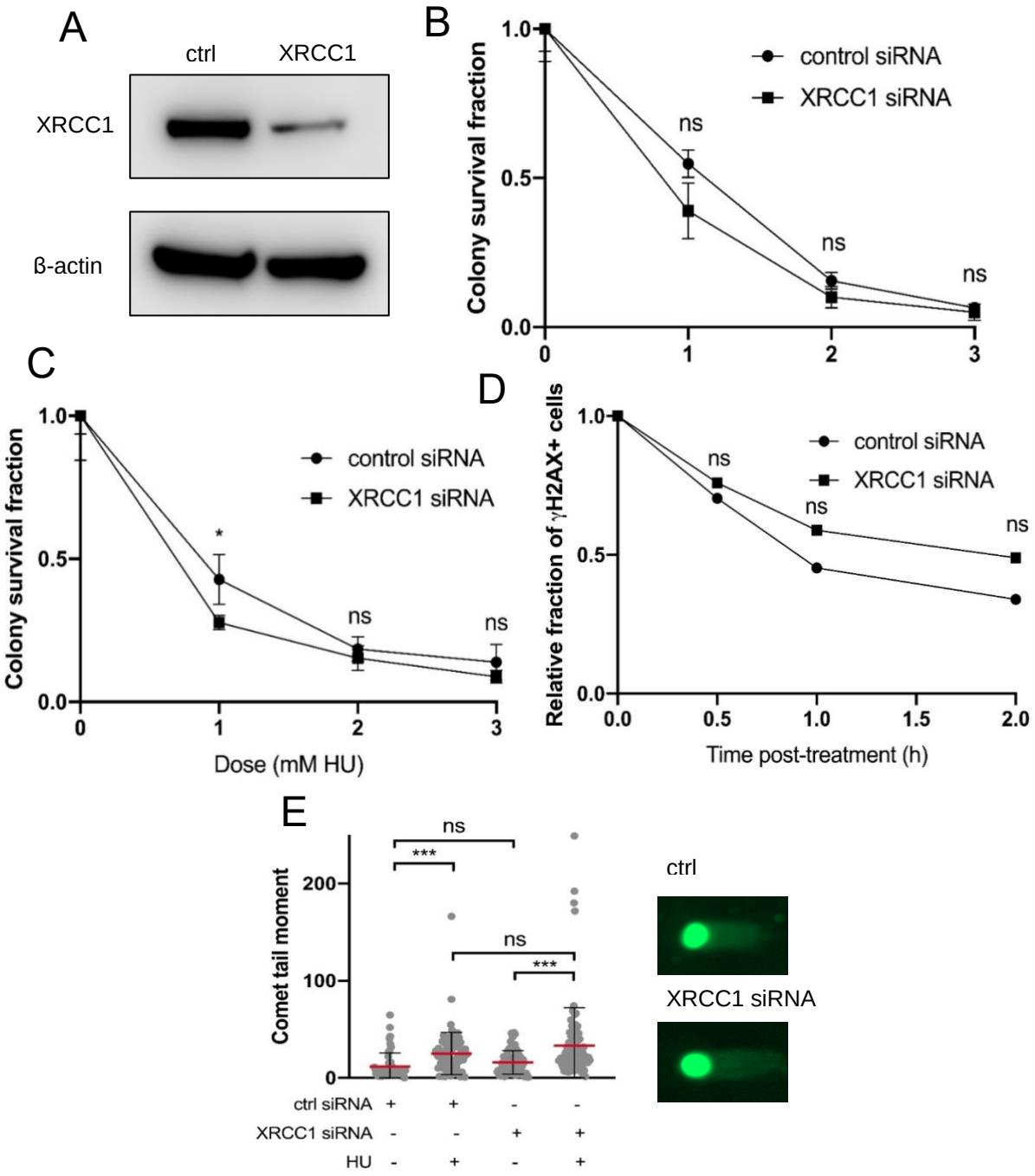

Figure 36. XRCC1 is moderately involved in DSBR in HR-proficient cells. (A) Western Blot of XRCC1 depletion by siRNA. (B) Clonogenic survival assay of XRCC1-depleted cells to ATRi. (C) Clonogenic survival assay of XRCC1-depleted cells to HU. (D) Relative fraction of U2OS cells positive for the DSB marker γH2AX by immunofluorescence. Cells were treated with 3mM HU for 3h and then allowed to recover for the indicated times. Cells were marked positive if they contained more than 10 foci. (E) Neutral comet assay in ctrl and XRCC1 siRNA-treated cells after HU. Cells were treated with 3mM HU for 8h where indicated.

36). We monitored the DSB marker γH2AX after treatment with HU and found that XRCC1-depleted cells had moderately more persistent DSBs than control cells (Figure 36). These results collectively indicate that XRCC1 does not significantly promoting DSBR after replication stress in WT cells, in contrast to its clear role in HR-deficient cells that we describe later, consistent with the established minor role for MMEJ in HR-proficient cells.

4.2.2 XRCC1 is Recruited to Sites of Replication Stress to Complex with Diverse DNA Repair Factors

We identified distinct XRCC1 foci that formed in response to both HU and HU+ATRi (Figure 37), which colocalized with yH2AX (Figure 37). To determine whether XRCC1 is recruited to stalled and collapsed replication forks, we utilized the proximity ligation assay (PLA), which produces a fluorescent focus when two distinct antibodies are in close proximity (~40 nm; Duolink). Briefly, we pulse labeled asynchronous U2OS cells with BrdU, then treated them with HU or ATRi+HU for the indicated times. PLA analysis using BrdU and XRCC1 antibodies detects the presence of XRCC1 at sites of replication fork stalling or collapse. We

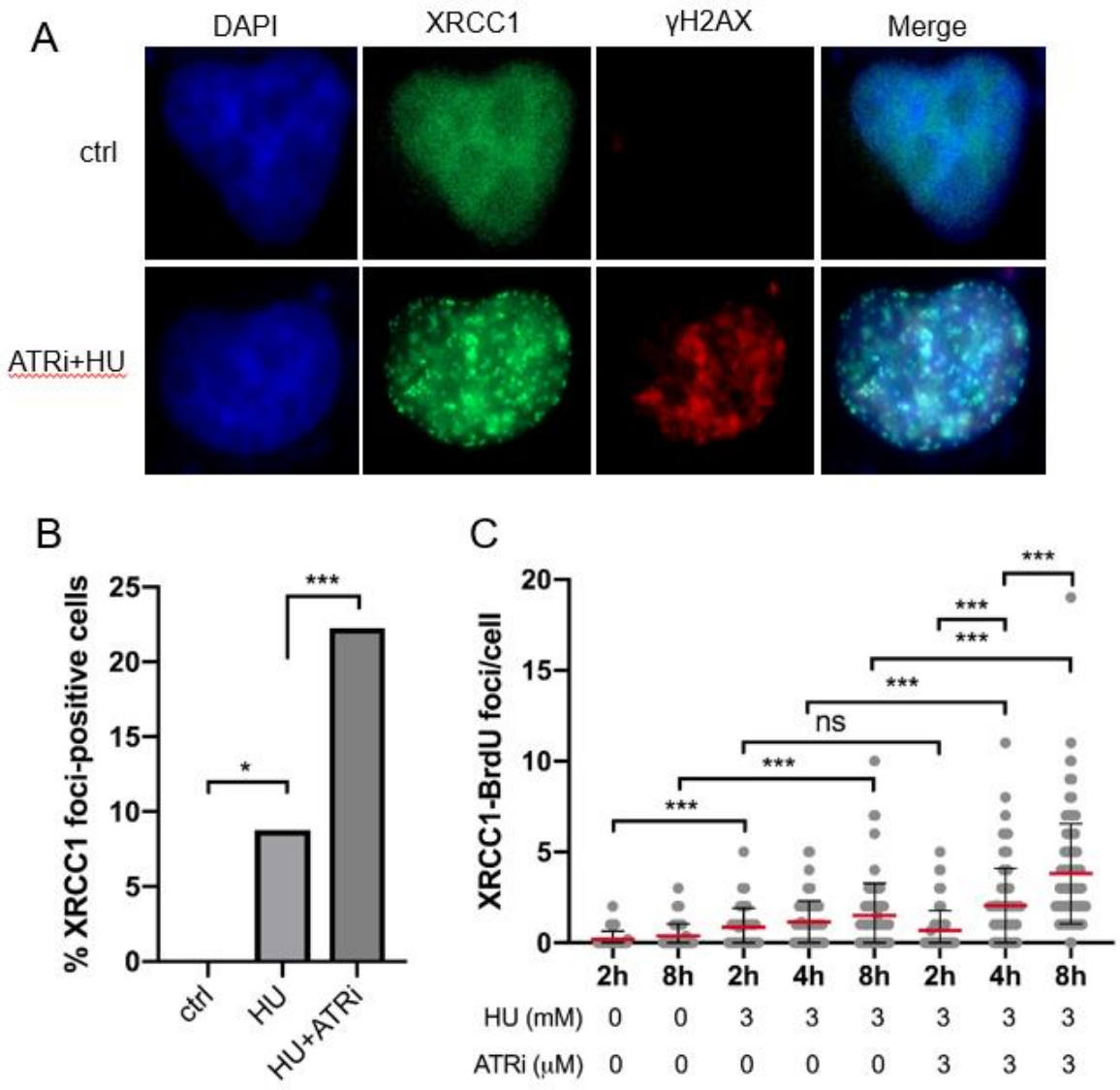

Figure 37. XRCC1 localizes to sites of replication stress. (A) XRCC1 foci formation after treatment of U2OS cells with 3mM HU and/or 3μM ATRi for 8h where indicated. (B) Colocalization of XRCC1 with γH2AX after ATRi+HU. (C) XRCC1 localization to sites of replication stress, as measured by BrdU-XRCC1 PLA Asynchronous cells were pulsed with 10μM BrdU for 15 minutes before treatment with 3mM HU and/or 3μM ATRi for the indicated times.

observed progressive recruitment of XRCC1 to sites of replication stress (Figure 37), consistent with previous studies (162).

We then utilized PLA to quantify changes in interaction between XRCC1 and its partners in various DNA repair pathways. Marked increases in foci number were observed between XRCC1 and several DSBR and SSBR factors (Figure 38). The most prominent increases occurred between XRCC1 and MRE11, POLQ, and γH2AX, implying a role for XRCC1 in DSBR at sites of replication stress (Figure 38). The interaction between XRCC1 and POLβ, the canonical gap-filling polymerase in SSBR, decreased after replication stress, suggesting that SSBR is not stimulated by replication stress (Figure 38).

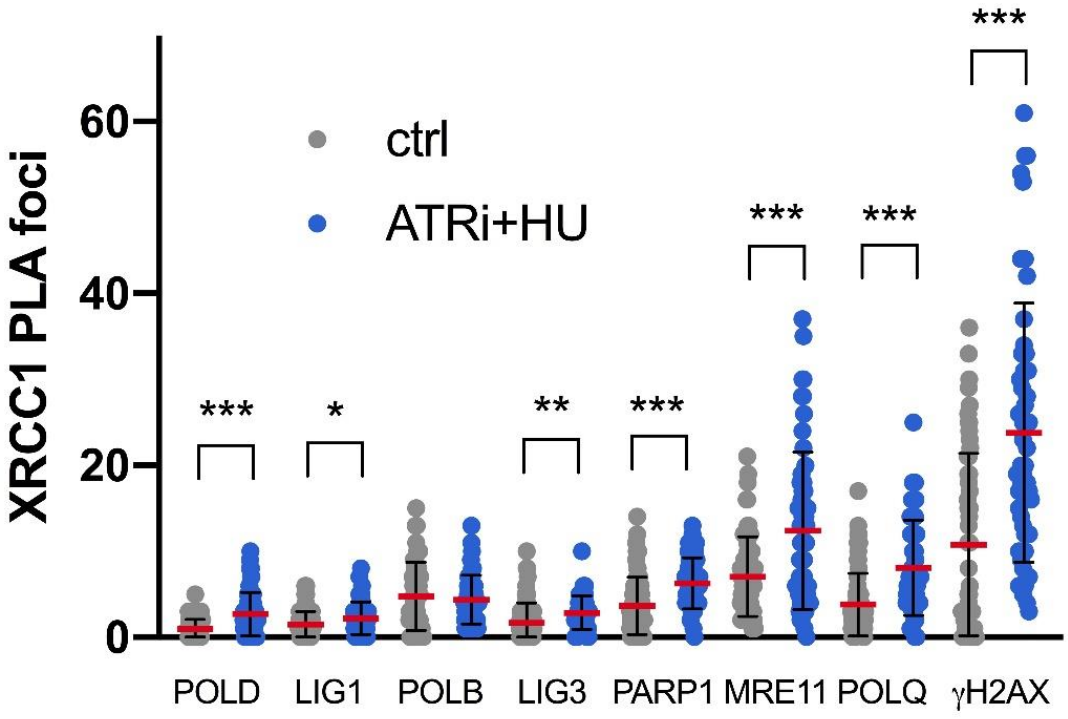

Figure 38. XRCC1-PLA after replication stress. PLA between XRCC1 and the indicated factors in control cells and after treatment for 8h with 3mM HU and 3μM ATRi.

4.2.3 Replication Stress Stimulates MMEJ via XRCC1 Repair Complex Formation

Based on these observations that XRCC1 complexes with DSBR factors after replication stress, we decided to examine the effect of replication stress on MMEJ.

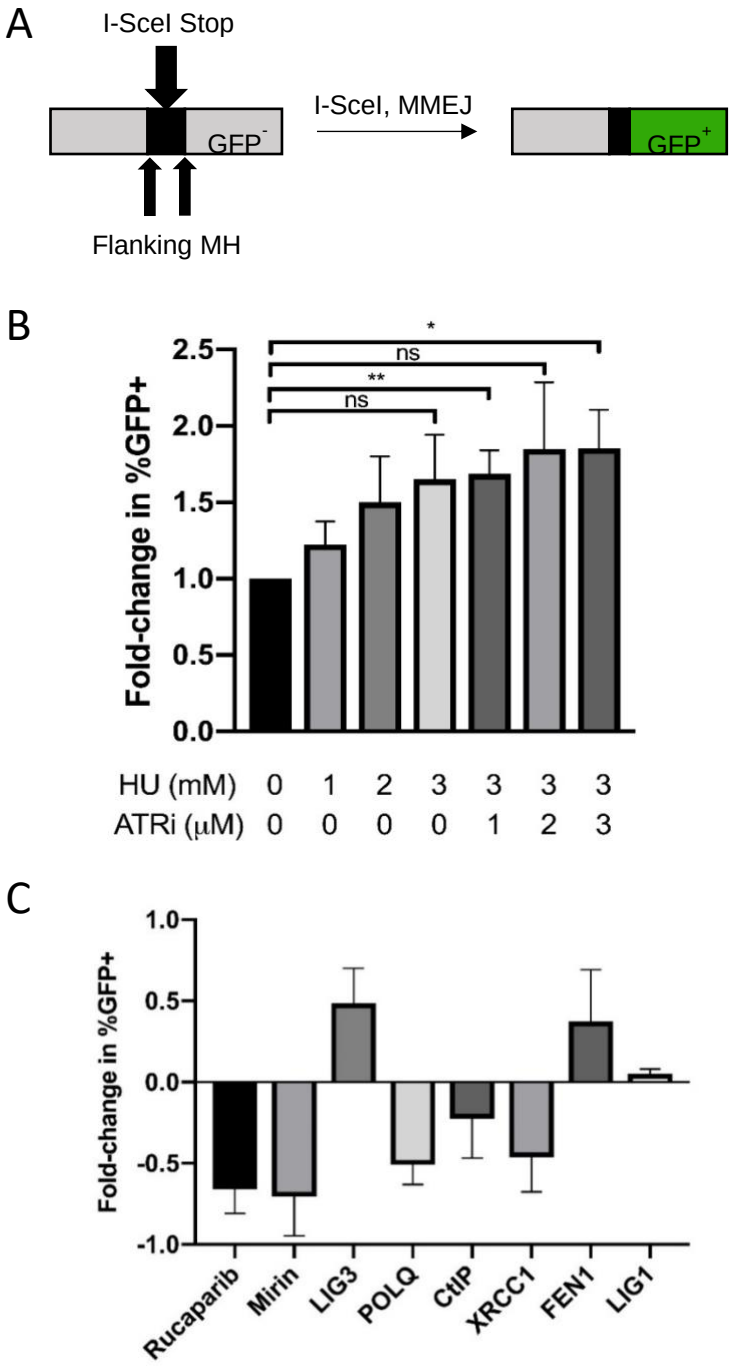

Figure 39. Replication stress stimulates EJ2-MMEJ. (A) Scheme for repair of I-SceI-induced DSBs via MMEJ in the EJ2 U2OS cell line. (B) Repair of ISceI-induced DSBs after replication stress. EJ2 U2OS cells were treated with the indicated doses of HU and VE-821 (ATRi) for 8h before DSB induction. (C) Dependence of EJ2-MMEJ on MMEJ factors.

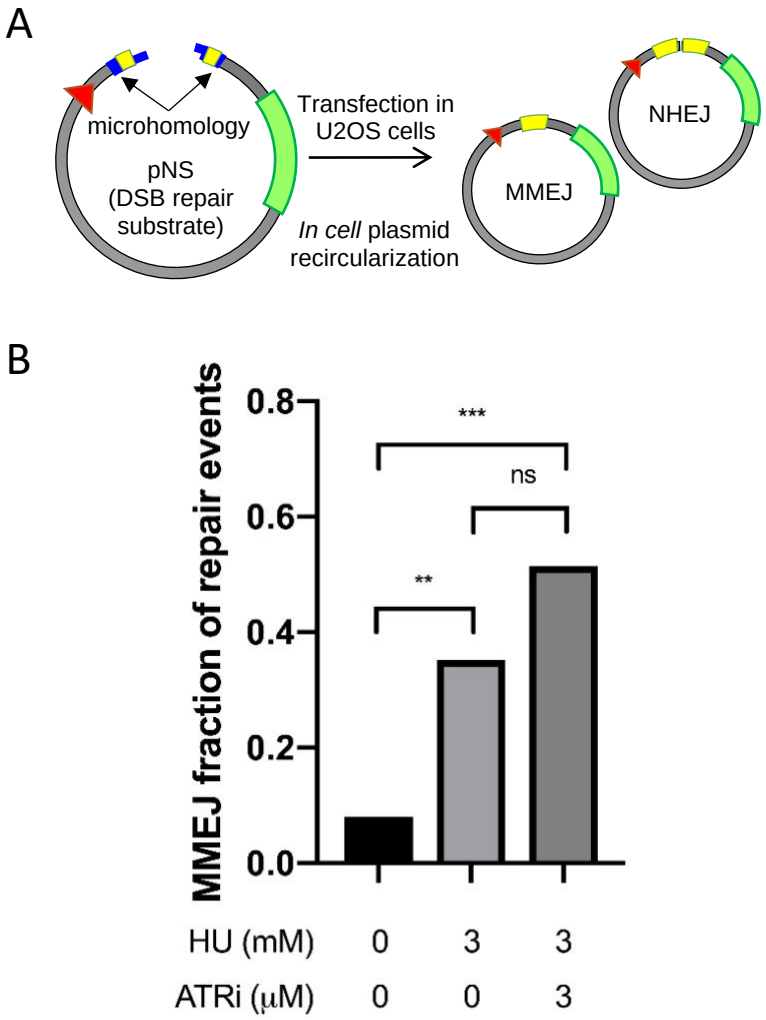

Figure 40. Replication stress stimulates pNS-MMEJ. (A) Scheme for repair of pNS plasmid in mammalian cells after transfection. (B) Repair of linearized plasmid substrate pNS after replication stress.

We utilized two separate MMEJ assay systems, the chromosomally integrated MMEJ reporter system (EJ2) developed by J. Stark (Figure 39) (112), which measures MMEJ by restoration of GFP after cutting by ISceI, and a linearized plasmid substrate system we previously established (Figure 40) (156), where MMEJ and NHEJ are scored separately based on the sequencing of DSB joints in recovered plasmids that are repaired *in cell*. Treating U2OS-EJ2 cells with HU or a combination of HU and ATRi led to an increase in the total number of MMEJ events (Figure 39).

Pre-treating U2OS cells with HU or HU+ATRi led to an increase in MMEJ events relative to the total number of end-joining events sequenced (Figure 40). These results indicate that replication fork collapse stimulates the MMEJ pathway, in agreement with previous observations (103). As expected, this stimulation was dependent on XRCC1, CtIP, and POLQ level, in addition to PARP1 and MRE11 activity (Figure 39).

We have previously shown that MMEJ factors, including XRCC1, form a complex which when isolated via immunoprecipitation is able to carry out MH-based end joining of the linearized pNS plasmid (156). To quantify the ability of the replication stress-induced XRCC1 complex to perform MMEJ and SSBR, we utilized two separate *in vitro* DNA repair assays. Briefly, we expressed FLAG-tagged XRCC1 in WT U2OS cells, then immunoprecipitated XRCC1-FLAG from control cells and cells treated with ATRi+HU. After washing, we incubated XRCC1-FLAG beads with linearized pNS substrate in reaction buffer. After ligation of the reaction mix, we transformed competent E coli cells with the reaction mix, and the number of colonies (reflecting individual repair events that restored expression of antibiotic resistance) were counted (Figure 41). We found that after ATRi+HU, the activity of the XRCC1 complex dramatically increased, indicating that XRCC1 is recruited to sites of replication stress to perform DSBR (Figure 41), as expected from the PLA data. All colonies sequenced were repaired via MMEJ (as expected with an XRCC1-IP). For assaying ligation activity, *in vitro* DNA nick ligation activity assays were performed with annealed nicked duplex oligomers labeled with Cy3 fluorescent dye (Figure 41). The direct ligation activity of the XRCC1 complex did not increase after ATRi+HU, suggesting that XRCC1 recruitment to collapsed replication forks is not to perform the final ligation step of BER/SSBR in association with LIG3 (Figure 41).

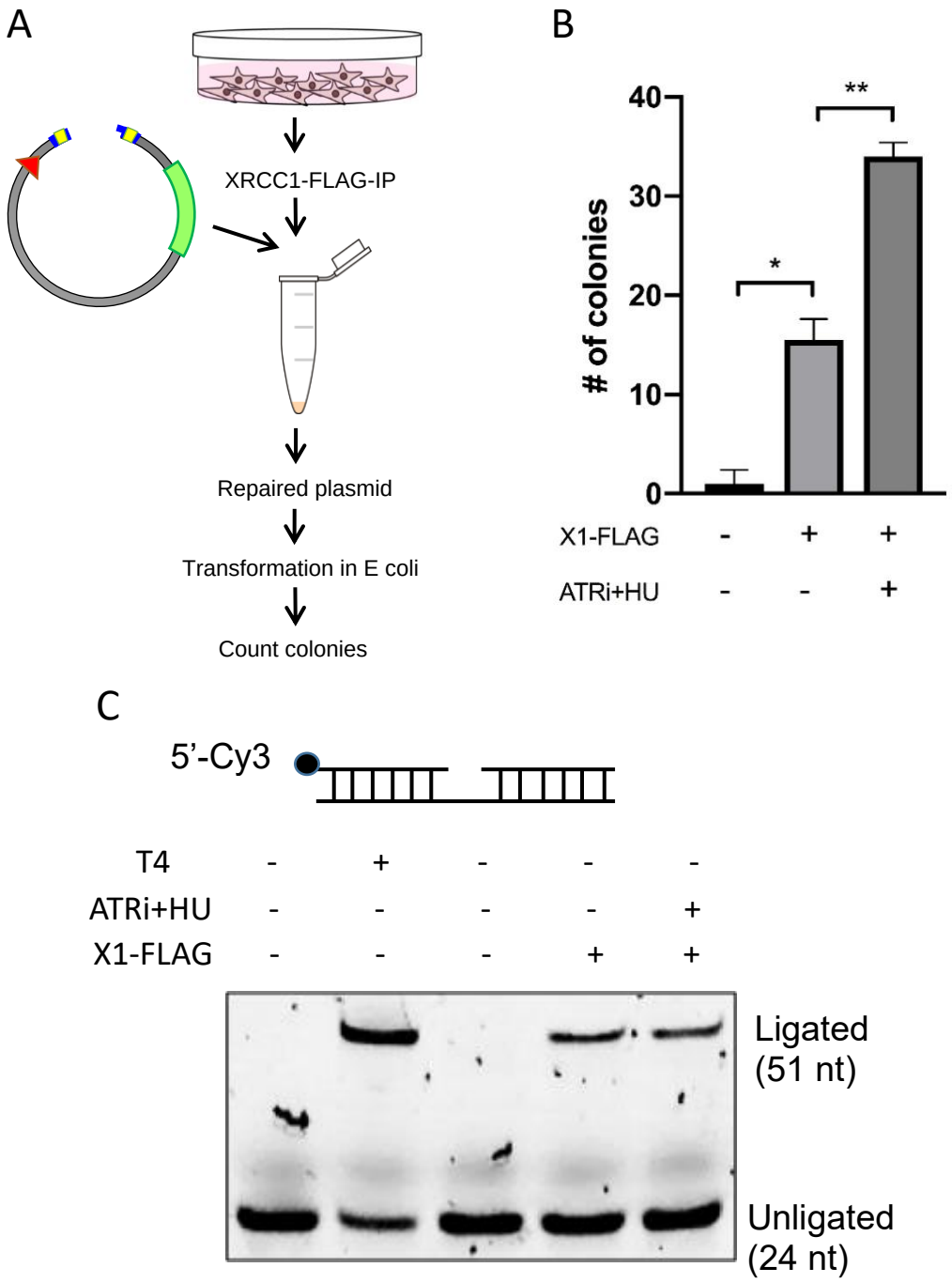

Figure 41. Replication stress stimulate MMEJ *in vitro*. (A) *In vitro* MMEJ repair activity assay scheme. (B) MMEJ repair activity of XRCC1 FLAG-IP with and without ATRi+HU treatment. (C) Nick ligation assay scheme. Nick ligation activity of XRCC1-FLAG IP with and without ATRi+HU treatment.

4.2.4 BRCA2 and XRCC1-depleted Cells are Sensitive to Replication Stress and Repair DSBs Inefficiently

BRCA1/2 deficiency is strongly associated with mutational signatures characterized by microhomology at chromosome breakpoint junctions (60). This, in addition to other evidence (24-26), suggests that HRD tumors utilize MMEJ for DSBR, which promotes chromosomal rearrangements and genomic instability. Whether increased MMEJ usage in HRD tumors is the reason for the synthetic lethal relationship between BRCA2 and XRCC1 (67,153) is unknown.

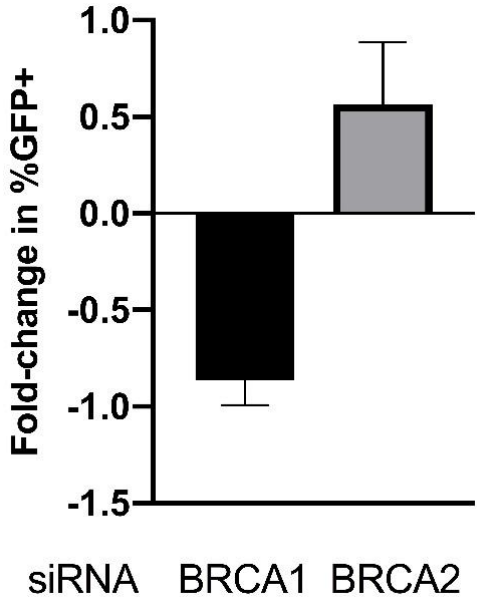

Figure 42. Effect of BRCA1/2 depletion on EJ2-MMEJ.

We decided to explore the relationship between XRCC1 and BRCA2 to understand the mechanistic basis for this synthetic lethality. First, we used BRCA1 and BRCA2-specific siRNAs to assess their role in replication stress-induced MMEJ. BRCA2 depletion led to a marked increase in EJ2-MMEJ events, whereas BRCA1 depletion led to a decrease in EJ2-

MMEJ events (Figure 42), in agreement with previous work (65,163) although there is conflicting evidence as to the effect of BRCA1 on MMEJ (164-167).

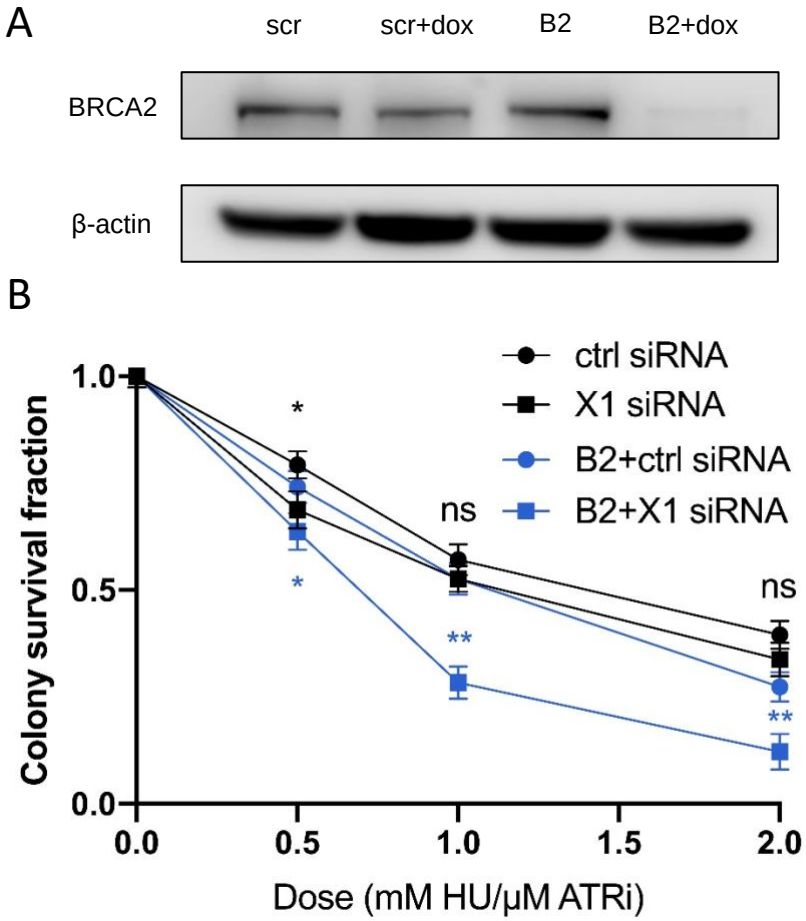

Figure 43. XRCC1 depletion in BRCA2-deficient cells affects sensitivity to replication stress. (A) Western Blot of inducible knockdown of BRCA2 in scr-U2OS and B2-U2OS cells. (B) Clonogenic survival of scr-U2OS and B2-U2OS XRCC1-depleted cells to ATRi+HU.

To examine the relationship between XRCC1 and BRCA2, we utilized a set of isogenic U2OS cells with integrated TRIPZ inducible shRNA for BRCA2, as well as a scrambled control. This tet-on system allows for reversible knockdown of BRCA2 in the presence of doxycycline (Figure 43). BRCA2-deficient cells were depleted of XRCC1 using siRNA, and then subjected to replication stress treatment with ATRi+HU. BRCA2-XRCC1 co-depleted cells were more sensitive to ATRi+HU (Figure 43), accumulated more DSBs (Figure 44), and repaired DSBs less

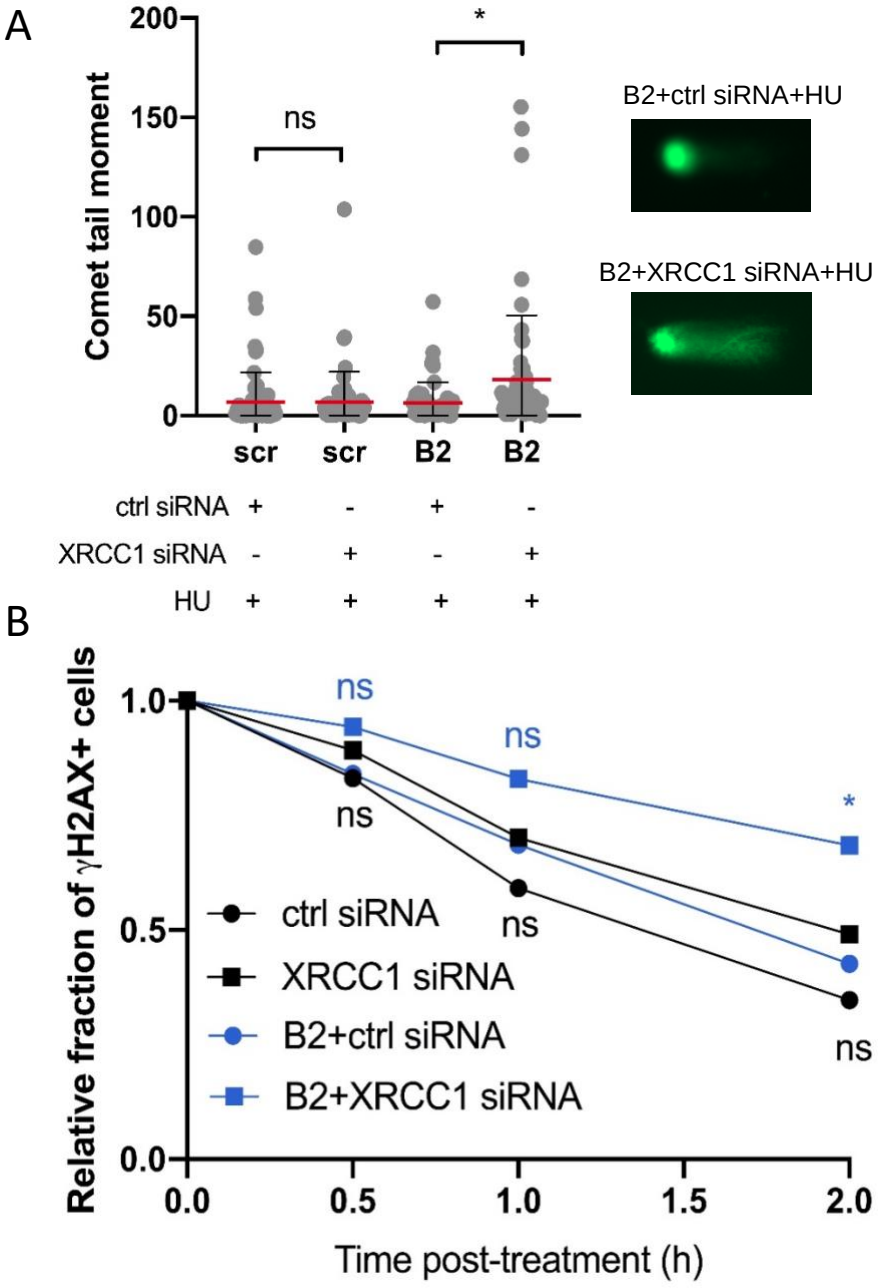

Figure 44. XRCC1 affects DSBR in BRCA2-deficient cells. **(**A) Neutral comet assay in scr-U2OS and B2-U2OS cells treated with ctrl and XRCC1 siRNA and/or HU. (B) Relative fraction of scr-U2OS and B2-U2OS cells positive for the DSB marker γH2AX by immunofluorescence. XRCC1 or ctrl siRNA-treated cells were treated with 3mM HU for 3h and then allowed to recover for the indicated times. Cells were marked positive if they contained more than 10 foci.

efficiently (Figure 44), indicating that XRCC1 has a higher level of engagement in DSBR in BRCA2-deficient cells relative to WT cells.

4.2.5 BRCA2 Suppresses MMEJ by Preventing XRCC1 Recruitment and Repair Complex Formation

We examined XRCC1 localization and complex formation in BRCA2-deficient cells. More XRCC1 foci formed in response to replication stress in BRCA2-deficient cells than control cells (Figure 45).

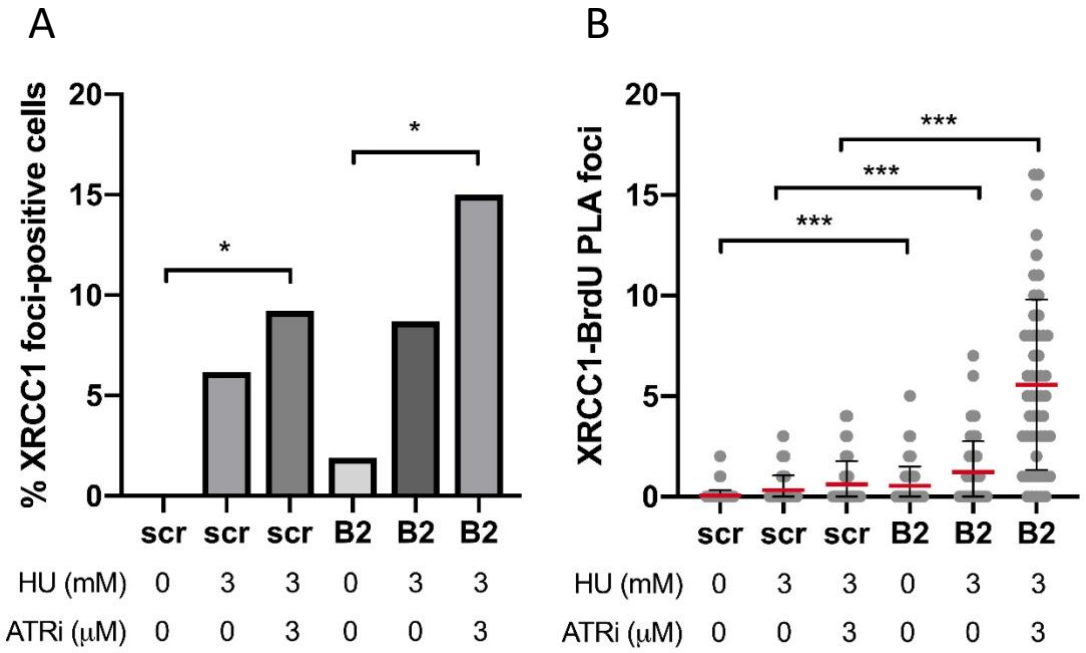

Figure 45. XRCC1 recruitment to sites of replication stress is suppressed by BRCA2. (A) XRCC1 foci formation after treatment of scr-U2OS or B2-U2OS cells with 3mM HU and/or 3μM ATRi for 8h where indicated. (B) XRCC1 localization to sites of replication stress in scr-U2OS or B2-U2OS cells, as measured by BrdU-XRCC1 PLA. Asynchronous cells were pulsed with 10μM BrdU for 15 minutes before treatment with 3mM HU and/or 3μM ATRi for the indicated times.

Using PLA between XRCC1 and BrdU as described previously, we found that knockdown of BRCA2 specifically increased XRCC1 recruitment to sites of replication stress (Figure 45).

Knockdown of BRCA2 also led to a marked increase in XRCC1 interaction with yH2AX, PARP1, and MRE11, as measured by PLA (Figure 46). These data strongly suggest that BRCA2 suppresses MMEJ through suppression of the XRCC1-MMEJ complex.

We expressed human POLQ-FLAG in both BRCA2-proficient and BRCA2-deficient U2OS cell lines. After inducing replication stress, we immunoprecipitated POLQ-FLAG and used Western Blot to detect XRCC1 and MRE11 in complex with POLQ. BRCA2 significantly suppressed interactions between POLQ and both XRCC1 and MRE11 (Figure 46). We then utilized *in vitro* repair assays as before to quantify the relative repair activities of XRCC1-FLAG IP from BRCA2-depleted and control cells. We found that XRCC1-FLAG IP from BRCA2-depleted cells performed MMEJ at a much higher level than control cells (Figure 47). XRCC1-FLAG IP performed SSBR at a moderately higher level in BRCA2-depleted cells relative to control cells (Figure 47). Together these data indicate that BRCA2 suppresses formation of the XRCC1-POLQ-MRE11 complex, thereby inhibiting MMEJ.

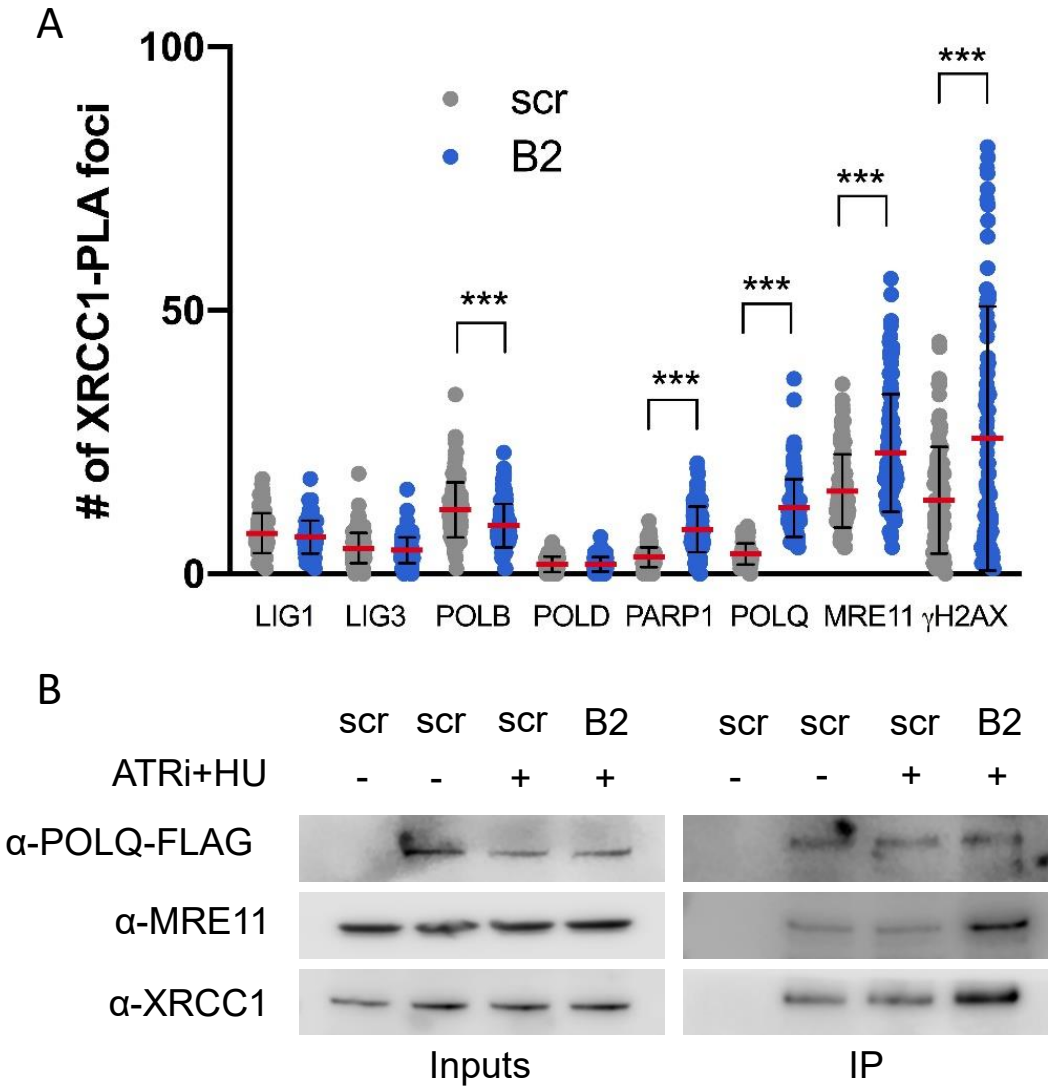

Figure 46. BRCA2 suppresses XRCC1-MMEJ complex formation. **(**A) PLA between XRCC1 and the indicated factors in scr-U2OS and B2-U2OS cells treated for 8h with 3mM HU and 3μM ATRi. (B) Western Blot of POLQ-FLAG IP from scr-U2OS and B2-U2OS cells with and without ATRi+HU treatment.

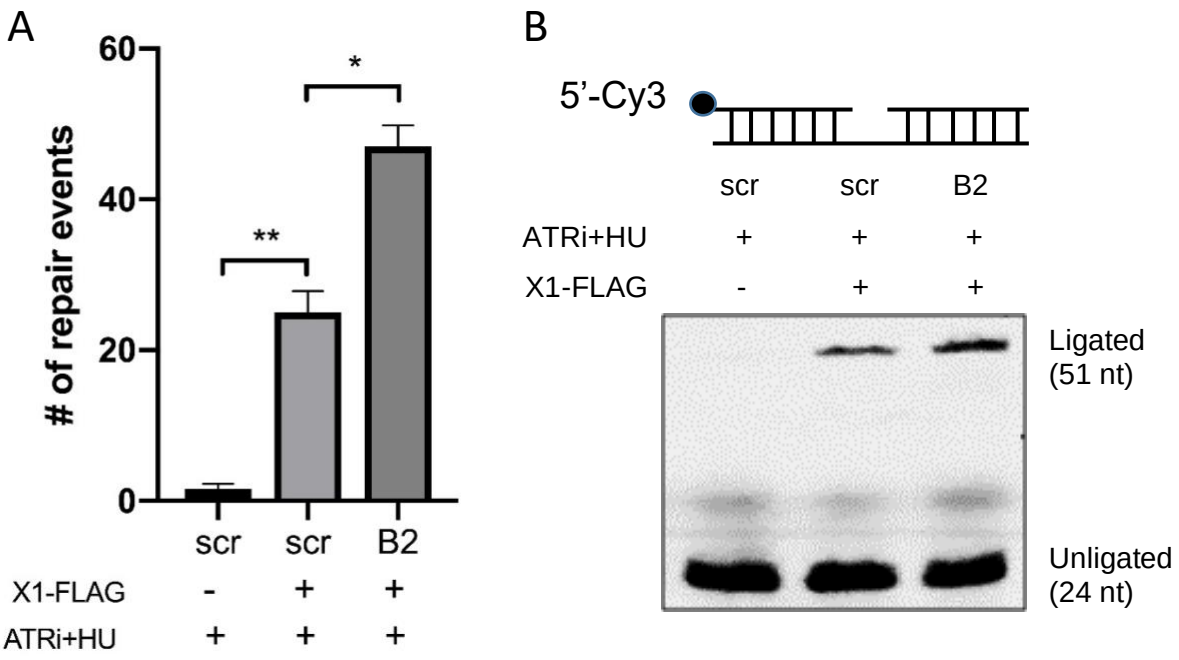

Figure 47. BRCA2 suppresses XRCC1-MMEJ repair activity. (A) MMEJ repair activity of XRCC1 FLAG-IP from scr and B2 cells treated with ATRi+HU. (B) Nick ligation assay scheme. Nick ligation activity of XRCC1-FLAG IP from scr and B2 cells treated with ATRi+HU.

4.2.6 XRCC1 Contributes to Replication Fork Restart

Based on our observations that XRCC1 is recruited to sites of replication stress to perform DSBR via MMEJ, we examined the effect of XRCC1 depletion on replication progression, replication fork protection, and replication restart using DNA fiber analysis (168). Some evidence for involvement of XRCC1 in replication restart exists (90), although its exact role is unclear. We found that XRCC1 depletion did not affect DNA replication progression (Figure 48) or fork protection (Figure 49) in WT U2OS cells. As expected, it did significantly limit the extent of replication fork restart (Figure 50).

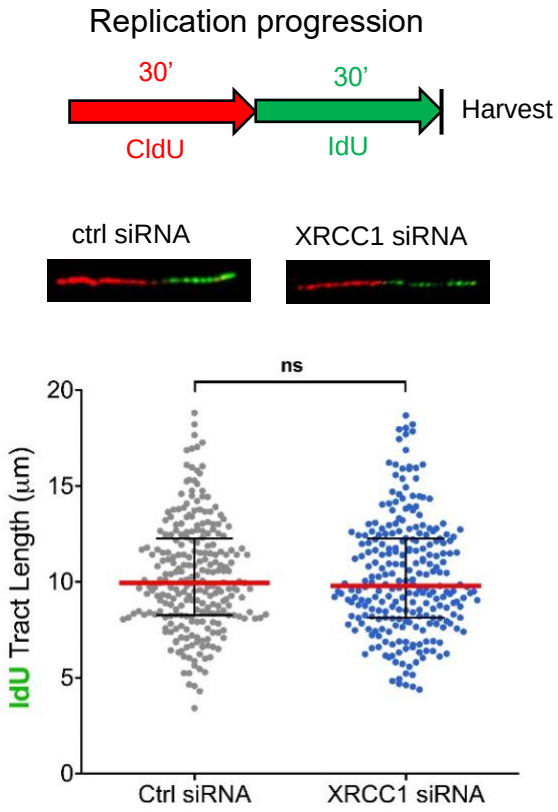

Figure 48. Effect of XRCC1 depletion on replication fork progression in U2OS cells. Schematic of fork progression assay and representative images are shown.

4.2.7 BRCA2 Changes the Effect of XRCC1 Depletion on Replication Fork Dynamics

A major phenotype of BRCA2-deficient cells is the degradation of nascent DNA at stalled forks by nucleases, including MRE11. Degradation of stalled forks leads to chromosomal aberrations and genomic instability (46). Based on our observations that XRCC1 scaffolds MRE11, and on published evidence for a pathway of break-induced replication (BIR) that depends on microhomology (MMBIR) (44,169-172) we depleted XRCC1 in our BRCA2-depleted and control U2OS cell lines and examined replication fork dynamics. We found that XRCC1 depletion limits the extent of degradation of stalled forks in BRCA2-deficient cells,

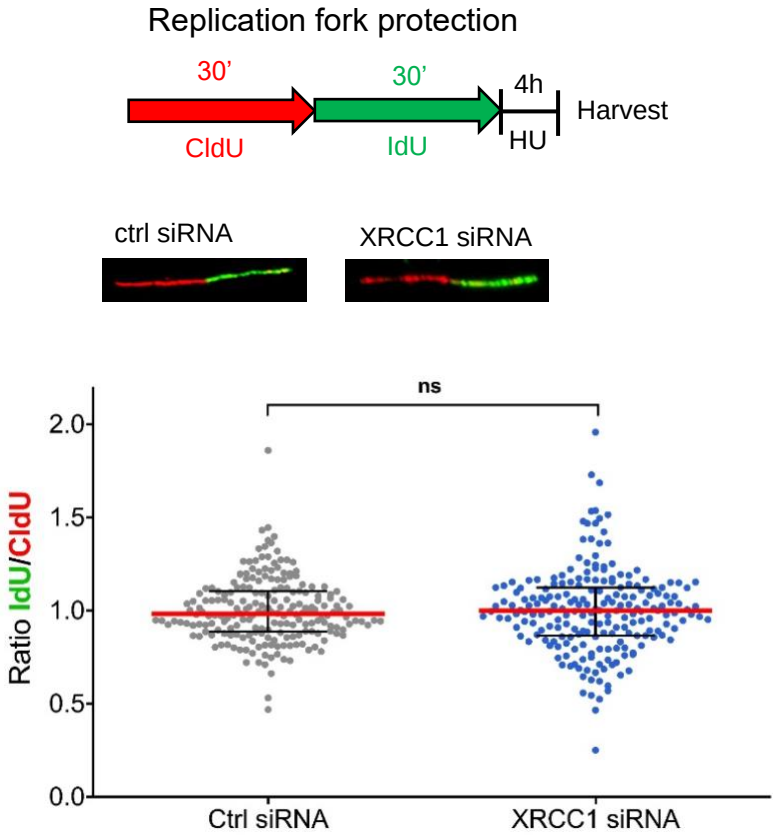

Figure 49. Effect of XRCC1 depletion on replication fork protection in U2OS cells. Schematic of fork protection assay and representative images are shown.

similarly to the effect of inhibition of the MRE11 nuclease by Mirin (Figure 52). This result suggests that XRCC1 cooperates with MRE11 in resection of stalled forks in BRCA2-deficient cells. We also found that the effect of XRCC1 depletion on fork restart is increased when BRCA2 is depleted (Figure 51). Collectively, these results reveal that XRCC1 plays specific roles in BRCA2-deficient cells in balancing the extent of fork degradation and fork restart to promote cell survival.

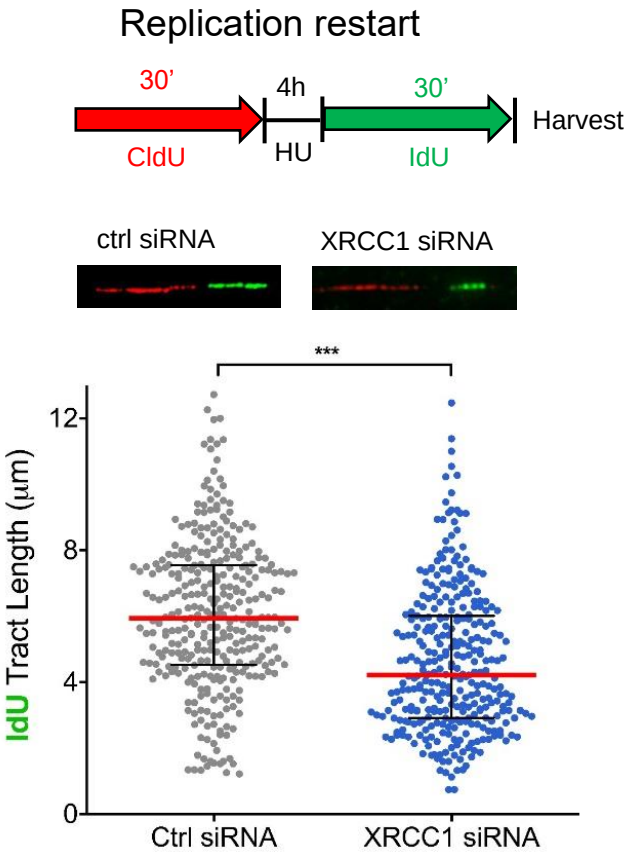

Figure 50. Effect of XRCC1 depletion on replication fork restart in U2OS cells. Schematic of fork restart assay and representative images are shown.

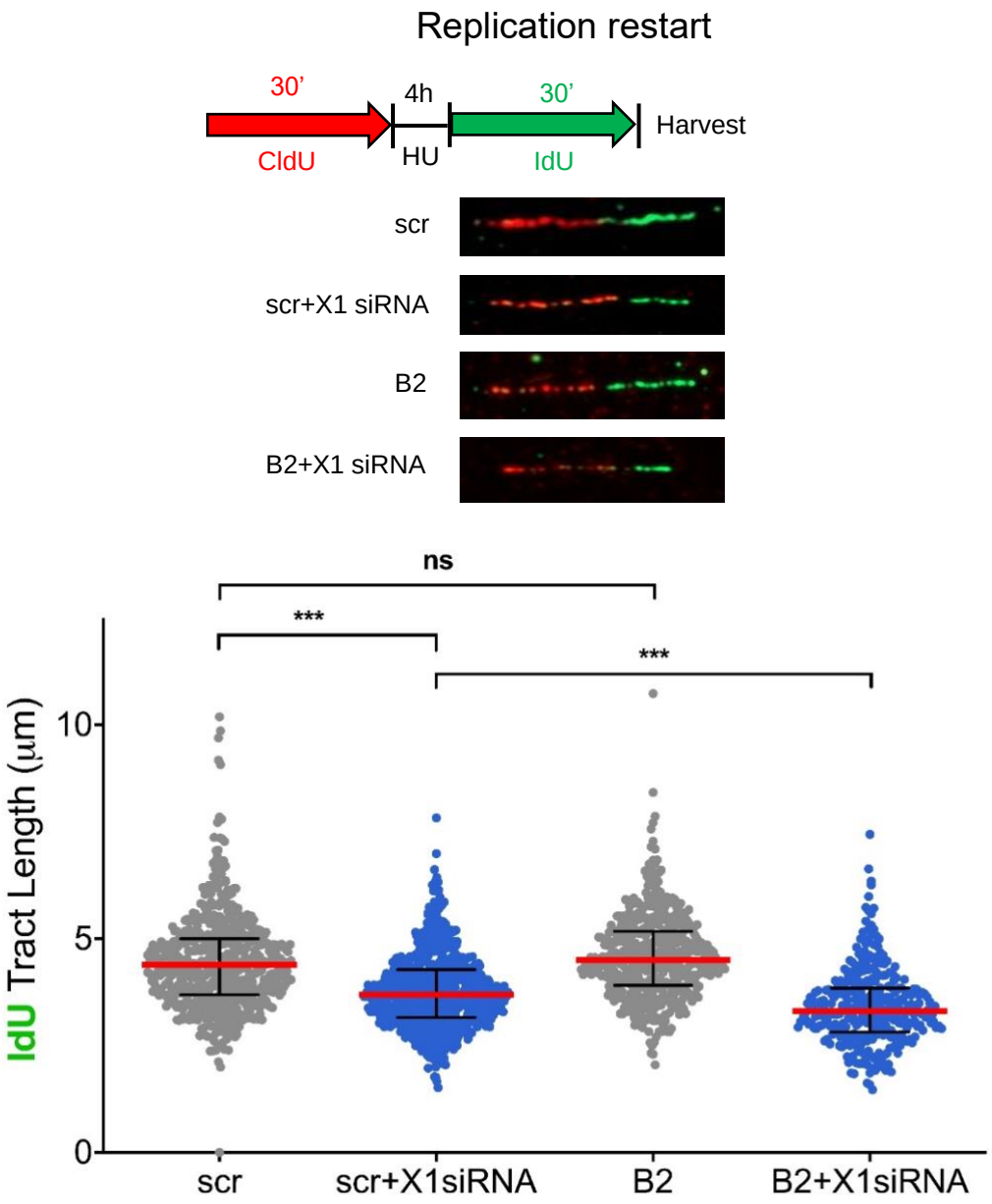

Figure 51. Effect of XRCC1 depletion on fork restart in scr-U2OS and B2-U2OS cells. Schematic of fork restart assay and representative images are shown.

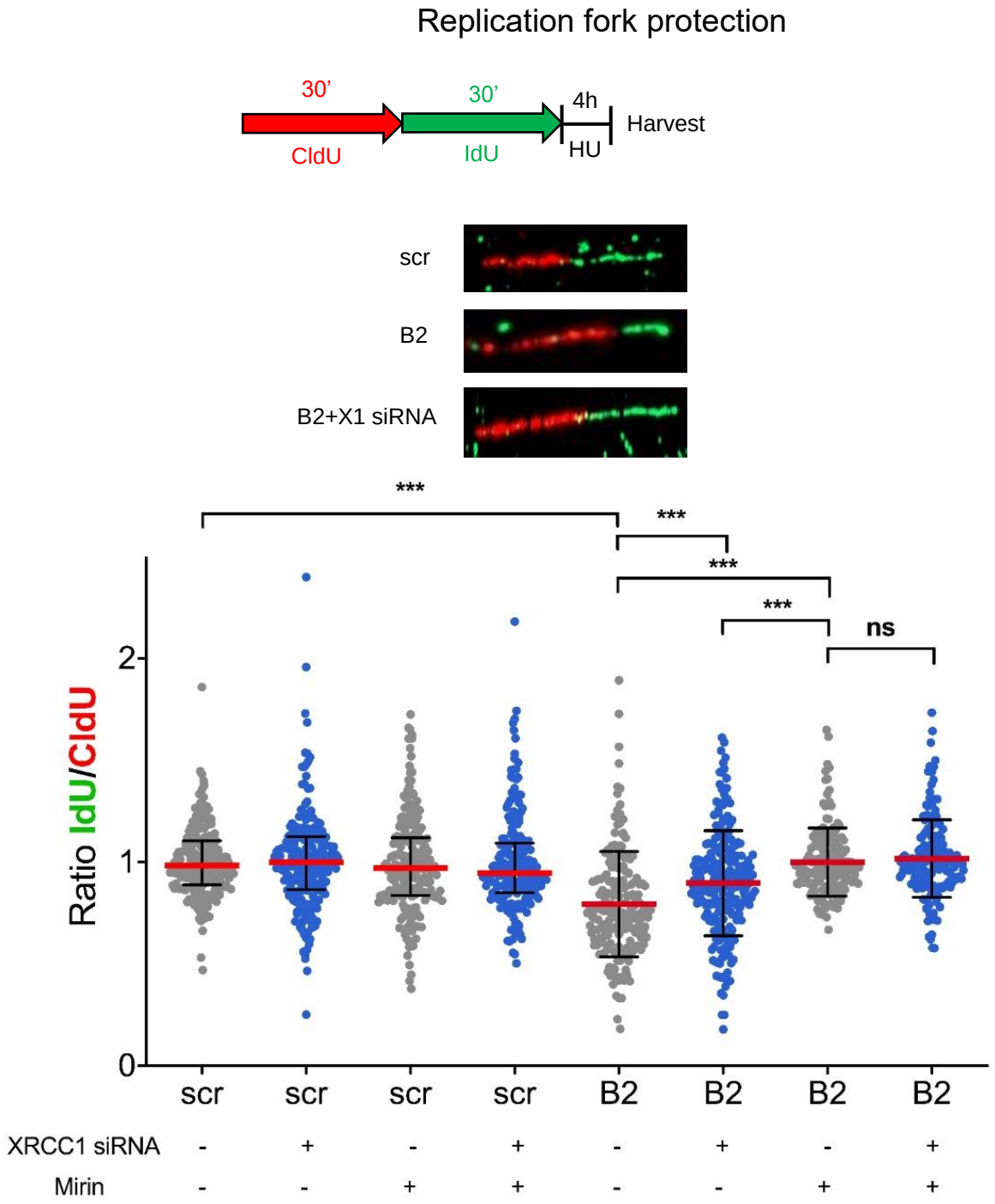

Figure 52. Effect of XRCC1 depletion and MRE11 inhibition on fork protection in scr-U2OS and B2-U2OS cells. Schematic of fork protection assay and representative images are shown.

4.2.8 DNA Repair Gene Expression is Correlated with Survival and HRD Mutational Signatures in Breast Cancer

We examined the effect of XRCC1 expression on survival in breast cancer using available data from The Cancer Genome Atlas (TCGA) (173). We found that low expression of XRCC1 was associated with poor survival (Figure 53). Interestingly, close gene expression

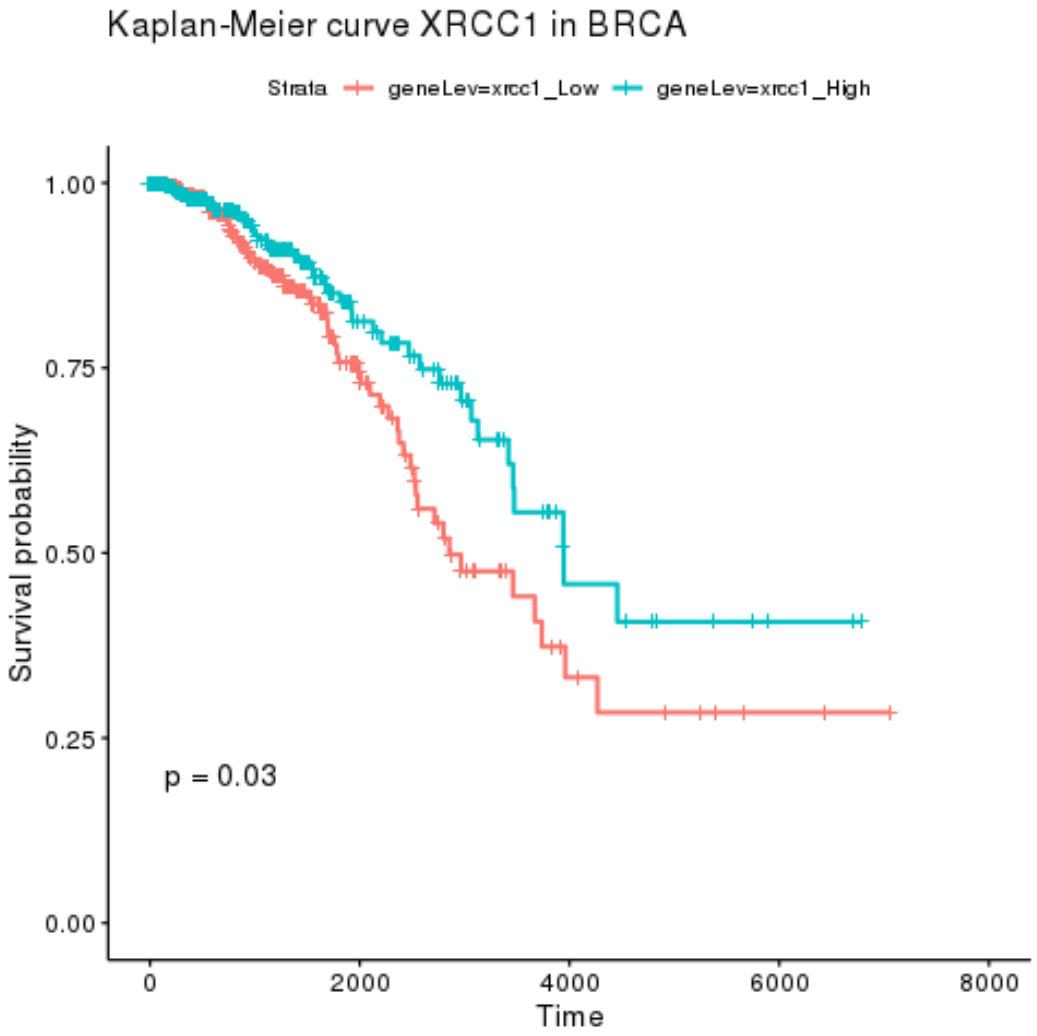

Figure 53. XRCC1 gene expression affects breast cancer survival. Survival curves of the top 50% (xrcc1_High) and bottom 50% (xrcc1_Low) XRCC1 gene expression groups of breast cancer patients in TCGA.

correlates of XRCC1 in breast cancer were all positive, and all were located in the same genomic region (19q13.3), and the DNA repair genes ERCC1 and PNKP were among the top 5 correlates (Table 5, Figure 54). The DNA repair genes ERCC2, POLD1, and LIG1 were also among the top correlates.

Gene Name	XRCC1 correlation	p-value	Genome Location
ERCC1	0.621122	1.02057e-117	19q13.32
PNKP	0.616526	1.57795e-115	19q13.33
LIG1	0.487981	1.59022e-66	19q13.33
ERCC2	0.462252	5.1842e-59	19q13.32
POLD1	0.439	9.41139e-53	19q13.33

Table 5. Gene expression correlates of XRCC1 on 19q13 involved in DNA repair.

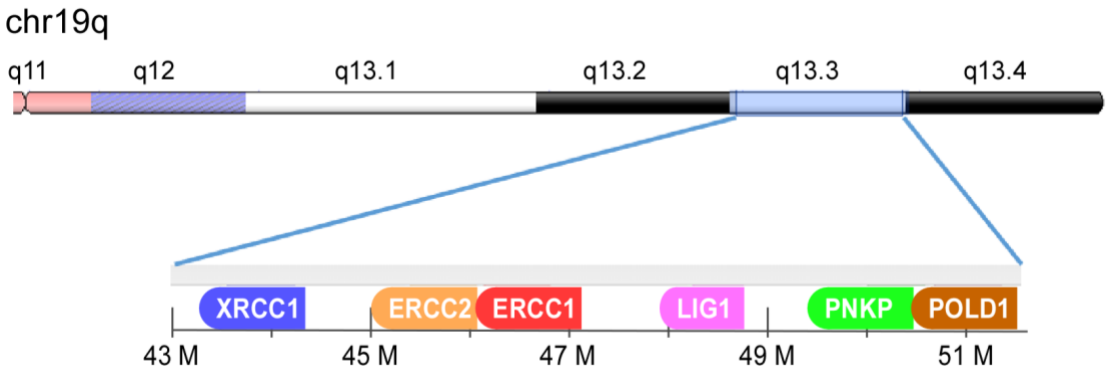

Figure 54. Organization of DNA repair genes in human 19q13.3.

PNKP and ERCC1 expression were also associated with breast cancer survival (Figure 55). We then examined whether XRCC1 expression was correlated with mutational signatures in breast cancer, as defined by Alexandrov et al. (59). There are roughly 30 mutational signatures in all human cancers, and 13 in breast cancer. After partitioning breast cancers into XRCC1_low

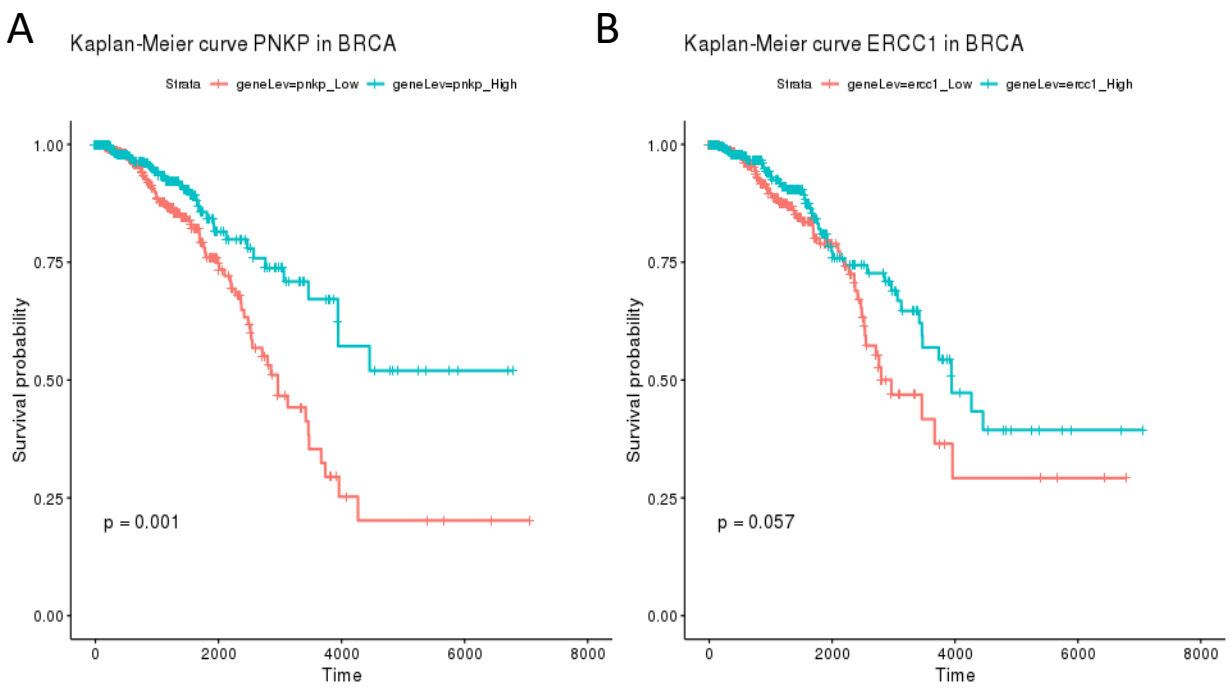

Figure 55. PNKP and ERCC1 gene expression affect breast cancer survival. Survival curves of the top 50% (_High) and bottom 50% (_Low) PNKP and ERCC1 gene expression groups of breast cancer patients in TCGA.

and XRCC1_high expression groups (Figure 56) we analyzed the enrichment of each of the 30 mutational signatures in these groups. Of the 13 signatures occurring frequently in breast cancers, XRCC1 expression was associated with only signature 3 (Figure 56). Signature 3 is primarily associated with HRD and an elevated number of large insertions and deletions with overlapping microhomology at breakpoint junctions, characteristic of MMEJ (59). Surprisingly, the association of XRCC1 expression with Signature 3 enrichment was negative, contrary to our expectation that XRCC1 might be upregulated in BRCA-deficient, Signature 3 cancers to perform MMEJ. ERCC1 and PNKP expression were similarly negatively associated with Signature 3 (Figure 55). Remarkably, XRCC1, ERCC1, PNKP, and ERCC2 have all been independently found to be determinants of PARPi and platinum sensitivity (174-178), effective

therapies for HRD cancers. Thus, these results link the PARPi and platinum sensitivity of HRD tumors to a clustered gene expression program in these tumors.

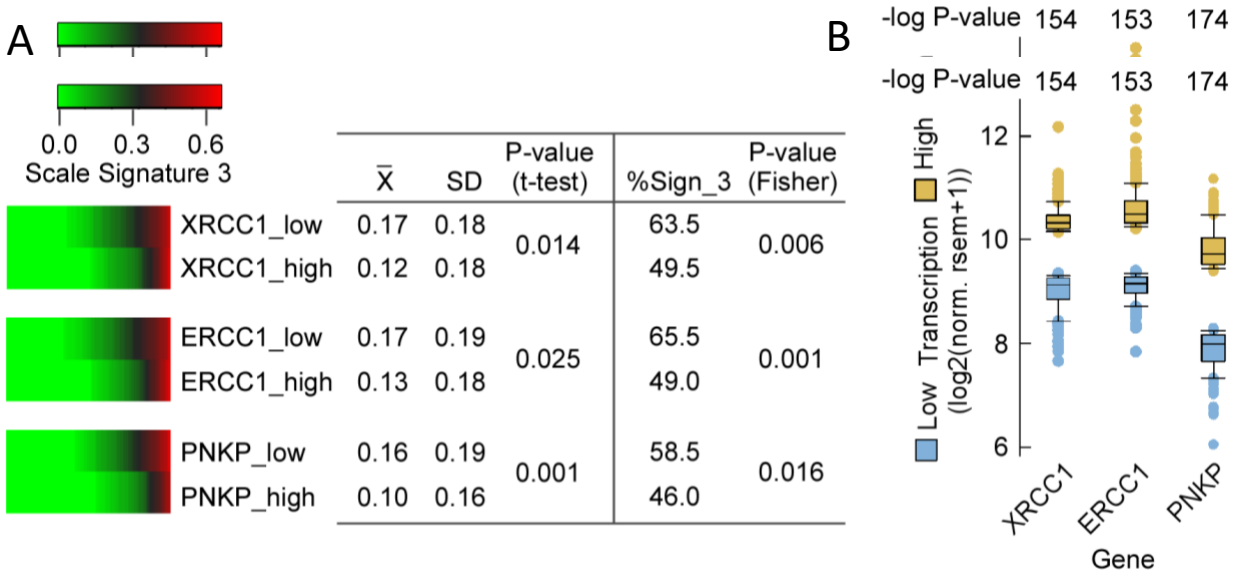

	$\bar{X}$	SD	P-value (t-test)	%Sign_3	P-value (Fisher)
XRCC1_low	0.17	0.18	0.014	63.5	0.006
XRCC1_high	0.12	0.18		49.5	
ERCC1_low	0.17	0.19	0.025	65.5	0.001
ERCC1_high	0.13	0.18		49.0	
PNKP_low	0.16	0.19	0.001	58.5	0.016
PNKP_high	0.10	0.16		46.0	

Figure 56. chr19q13.3 gene expression correlates with mutational signature 3 in breast cancer. (A) Signature 3 association with XRCC1_low, ERCC1_low, and PNKP_low expression groups. Mean Signature 3 score, standard deviation, and t-test P-value. The percentage of tumors within that group that have a nonzero Signature 3 score (%Sign_3) is also given along with Fisher's exact test. (B) Gene expression of _low (blue) and high (gold) groups. Roughly the top 20% and bottom 20% were used for analyses.

4.3 Discussion

4.3.1 MMEJ is Activated by Replication Stress

The origin of microhomology at chromosome breakpoint junctions is an important topic in human genetics and disease. Generally, cellular stress, including replication stress, ionizing radiation, and metabolic stress, increases the usage of error-prone repair pathways to promote cell survival at the cost of genome stability (156,172,179). Increased genomic instability using MH-based pathways leads to copy number variation (CNV) (59), which contributes to genetic disorders and cancers (169,172), chromosome fragile site (CFS) breakage and repair, which can lead to rearrangements and CNV in cancers, and the chromosomal rearrangement phenotype

observed in several different cancers, including HR-deficient breast and ovarian cancers (59). Additionally, increased usage of MH-based pathways of repair may promote survival of cancer cells undergoing chemoradiation therapy (156,180,181).

Chromosome rearrangements can be caused by replication-associated DSBs, which can be generated during replication by several different pathways (34). Critically, these DSBs are single-ended, precluding their repair by direct end-joining mechanisms and necessitating recombination. These structures can be repaired by the process of break-induced replication (BIR), which involves canonical HR factors including RAD51 (182). There is a RAD51-independent method of BIR termed microhomology-mediated BIR (MMBIR), which utilizes MH to facilitate multiple template switching events (39,183). In situations where RAD51 is limiting, as in HDR cancers or hypoxia, replication-associated seDSBs cannot be repaired via BIR and instead use MMBIR (183,184). BIR/MMBIR models suggest that fork stalling and template switching to restart replication may be the cause of chromosomal breakpoint junctions. In this model, MH at chromosomal breakpoints in cancers reflects priming of replication using MH, indicating use of MMBIR for replication restart in these cancers (179). The enrichment of these breakpoints and the biological importance of MMEJ factors in HDR cancers suggest a connection between replication restart, fork protection, and MMBIR/MMEJ that warrants further exploration.

Our finding that replication stress activates MMEJ and specific participation of MMEJ factors in the replication stress response is supported by previous observations (103,159), including the repair of replication stress-induced DSBs at CFS sites using MH (43). While the limitations of the systems used in this study prevent us from making any direct conclusions about the use of an MMBIR-like mechanism at seDSBs, biochemical steps of MMEJ, including

resection and annealing, are still required in our systems. Thus, our observation that XRCC1 forms a complex after replication stress that promotes resection and annealing of MH, and facilitates replication fork protection and restart, strongly suggests a connection between MMEJ and MMBIR mechanisms. Our result that XRCC1 facilitates replication restart fits with previous studies identifying roles for the MMEJ factors POLQ, MRE11, and PARP1 in replication restart (25,185,186). We propose a model where resection of single-ended DSBs at collapsed forks by the MMEJ machinery, scaffolded by XRCC1, exposes MH that is needed for template switching to restart replication.

4.3.2 XRCC1 has Diverse Roles in DNA Metabolism in BRCA2-deficient Cells

Our study also helps to explain the sensitivity of BRCA2-deficient cells to depletion of XRCC1 (67,153). While it has been postulated (90) that XRCC1 is recruited to sites of replication stress to couple excision repair and/or ligation to fork reversal and restart, XRCC1 interactions with LIG3 and POLβ do not increase after replication stress or BRCA2 knockdown. This implies that the scaffolding of fork remodeling/MMEJ factors is the primary role of XRCC1 during replication stress and the underlying reason for the synthetic lethality of BRCA2 and XRCC1. Previous observations that BRCA2 suppresses MMEJ (65) are extended here by showing that in BRCA2-deficient cells, XRCC1 complexes preferentially with MMEJ resection factors and DNA polymerases. Additionally, the XRCC1 repair complex more efficiently repairs DSBs via MMEJ in BRCA2-deficient cells than in WT cells.

Our observations that XRCC1 is intimately linked with fork degradation and restart in BRCA2-deficient cells also support a model where XRCC1 preferentially scaffolds nucleases and polymerases in HRD cancers. Identification of specific interactions between POLQ and other DNA repair factors (XRCC1, MRE11) that are suppressed by BRCA2 has implications for

cancer therapy. Direct interactions between protein factors that are both required for and specific to MMEJ are potential targets for small molecule inhibitors. Additionally, defining the mechanism of POLQ and PARP activity more precisely will inform the applications of these inhibitors to BRCA-deficient cancer therapy (57,58).

4.3.3 A Genomic Cluster of DNA Repair Genes are Underexpressed in BRCA-deficient Breast Tumors

The close connection of XRCC1 to both PARP1 and BRCA2 may be important in PARPi therapy for HRD cancers. PARP inhibition and XRCC1 deficiency have been observed to be synthetic lethal in multiple contexts (67,155,174), perhaps because of PARP1 hyperactivation in the absence of XRCC1 (7). Our observation that low XRCC1 expression is associated with poor survival in breast cancers is supported by previous studies (187). Our finding that XRCC1 expression is closely correlated with other 19q13.3 genes is surprising, and may be indicative of amplifications and/or deletions in that region. Additionally, the cluster of DNA repair genes in 19q13.3-4 implies that large functional changes in DNA repair capacity may occur as a result of regulatory or structural changes to this region of the genome. In fact, copy number variation in this region has been reported in several cancers, including breast and ovarian cancers (188-190). The underexpression of XRCC1, ERCC1, ERCC2, and PNKP in Signature 3 breast cancers, combined with our observation that XRCC1, ERCC1 and PNKP expression impacts breast cancer survival, indicate a functional DNA repair change in HRD cancers that affects treatment response. Additionally, XRCC1, ERCC1, ERCC2, and PNKP deficiencies have been independently implicated in both PARPi and platinum compound sensitivity (174-178), linking the sensitivity of HRD tumors to these agents with this change in DNA repair program.

The underexpression of XRCC1 in specifically Signature 3 (HR-deficient) breast cancers is surprising, based on the abundance of evidence supporting a role for XRCC1 in MMEJ, including our own data that XRCC1 activity is suppressed by BRCA2. This is in contrast to the overexpression of the MMEJ polymerase POLQ in Signature 3 cancers (24). One possible explanation for this observation is that XRCC1 and POLQ act separately in MMEJ variant pathways that compete and are differentially mutagenic, and low XRCC1 expression in HR-deficient cells allows POLQ to repair breaks via a pathway that creates Signature 3 mutations. Another explanation is that XRCC1's role in fork restart and fork stability in conjunction with MRE11 promotes genome stability in BRCA2-deficient cells. XRCC1 promotes both fork restart and fork degradation in BRCA2-deficient cells, as does MRE11. It is possible that when XRCC1 is unable to act at stalled and collapsed forks, POLQ/RAD52 pathways can hijack stalled forks, as was shown recently for p53/MRE11-defective cancers (186). Supporting both these models is evidence that PARP1 is hyperactivated in the absence of XRCC1 and BRCA2 (7,191), which may mediate increased recruitment of POLQ to DSBs (26).

In summary, our identification of an MMEJ-competent protein complex that is suppressed by BRCA2 and is activated by replication stress is a mechanistic step forward for our understanding of MH-based repair that may be important for HRD cancer therapy. Underexpression of a genomic cluster of DNA repair genes is a unique characteristic of HRD cancers, and may contribute to the efficacy of PARPi and platinum compounds in these settings. Further investigation of the relationship between POLQ, MRE11, PARP1, and XRCC1 should be fruitful, especially as PARPi and POLQ inhibitors continue to be developed for clinical applications.

5. SUMMARY AND FUTURE DIRECTIONS

Our evidence that IR induces MMEJ is an important result that has since been validated by independent studies. The Wellcome Trust Sanger Institute published a paper documenting the mutational signatures of second malignancies that arose as a result of IR therapy for a first malignancy (192). The found that, relative to IR-naive tumors, IR-associated tumors had a higher burden of small deletions, which often had microhomology at the junction (192). Cornforth et al. recently found that radiation-induced translocations were mediated by microhomology (193). Irradiation using high-LET titanium ions led to misjoining of Cas9-induced DSBs via microhomology, which was not observed after low-LET irradiation (194). The Cas9-DSBs were induced several days after exposure, indicating a persistent signal that activates MMEJ that is dependent on strand break complexity (194).

Activation of MMEJ by IR has implications for RT, space exploration, and other exposures, as this work rationalizes testing of MMEJ inhibitors, including PARPi, CK2i, and POLQi in these contexts. High-LET radiation in space and proton therapy environments stimulates MMEJ, possibly increasing the efficacy of MMEJ inhibition in these contexts. However, the multiple roles of CK2, PARP1, and POLQ in the cell complicate their targeting with chemicals, as they may have toxic or carcinogenic outcomes due to their roles in normal genome repair and cell signaling. Therefore, a specific MMEJ inhibitor is desired. Our identification of an MMEJ-specific interaction in XRCC1-MRE11 raises the possibility of targeting their interaction using small molecules to inhibit MMEJ.

The discovery that XRCC1 plays multiple roles in DNA metabolism in BRCA2-deficient cells is surprising. While increased MMEJ activity of the XRCC1 complex in BRCA2-deficient cells was anticipated, the strong replication restart and degradation phenotypes of XRCC1 depletion we observed were not, and suggest a close connection with MRE11 in these tumors. The increased interaction between XRCC1 and POLQ after BRCA2 depletion was also

unexpected. Further investigation of how MRE11, POLQ, and XRCC1 cooperate (or compete) in both MMEJ and replication fork dynamics is necessary.

The identification of 19p13.3 XRCC1 gene correlates in breast cancer is an exciting observation with potential therapeutic implications. However, we are currently working to better understand how XRCC1 and these correlates impacts survival. For example, whether sensitivity of BRCA-deficient tumors to platinum agents or PARPi is mitigated by overexpression of any of these 19p13.3 factors is an important question. Furthermore, it is unclear whether XRCC1 expression correlates more strongly with survival specifically in BRCA1, BRCA2, or other germline HR mutants. Similarly, whether 19p13.3 genes correlate more closely in germline mutants is unknown. We are hopeful that the ideas and results of this work will be impactful in the future.

REFERENCES

1. Lindahl T, Barnes DE. Repair of endogenous DNA damage. Cold Spring Harb Symp Quant Biol **2000**;65:127-33

2. Wallace SS. Base excision repair: a critical player in many games. DNA Repair (Amst) **2014**;19:14-26

3. Hanssen-Bauer A, Solvang-Garten K, Sundheim O, Pena-Diaz J, Andersen S, Slupphaug G, *et al.* XRCC1 coordinates disparate responses and multiprotein repair complexes depending on the nature and context of the DNA damage. Environmental and molecular mutagenesis **2011**;52:623-35

4. Kim YJ, Wilson DM, 3rd. Overview of base excision repair biochemistry. Curr Mol Pharmacol **2012**;5:3-13

5. Caldecott KW. Single-strand break repair and genetic disease. Nature reviews Genetics **2008**;9:619-31

6. Ahel I, Rass U, El-Khamisy SF, Katyal S, Clements PM, McKinnon PJ, *et al.* The neurodegenerative disease protein aprataxin resolves abortive DNA ligation intermediates. Nature **2006**;443:713-6

7. Hoch NC, Hanzlikova H, Rulten SL, Tetreault M, Komulainen E, Ju L, *et al.* XRCC1 mutation is associated with PARP1 hyperactivation and cerebellar ataxia. Nature **2017**;541:87-91

8. Davis AJ, Chen DJ. DNA double strand break repair via non-homologous end-joining. Translational cancer research **2013**;2:130-43

9. Bunting SF, Nussenzweig A. End-joining, translocations and cancer. Nat Rev Cancer **2013**;13:443-54

10. Xu Y. DNA damage: a trigger of innate immunity but a requirement for adaptive immune homeostasis. Nat Rev Immunol **2006**;6:261-70

11. Prakash R, Zhang Y, Feng W, Jasin M. Homologous recombination and human health: the roles of BRCA1, BRCA2, and associated proteins. Cold Spring Harb Perspect Biol **2015**;7:a016600

12. Nimonkar AV, Genschel J, Kinoshita E, Polaczek P, Campbell JL, Wyman C, *et al.* BLM-DNA2-RPA-MRN and EXO1-BLM-RPA-MRN constitute two DNA end resection machineries for human DNA break repair. Genes Dev **2011**;25:350-62

13. Langerak P, Mejia-Ramirez E, Limbo O, Russell P. Release of Ku and MRN from DNA ends by Mre11 nuclease activity and Ctp1 is required for homologous recombination repair of double-strand breaks. PLoS Genet **2011**;7:e1002271

14. Daley JM, Sung P. 53BP1, BRCA1, and the choice between recombination and end joining at DNA double-strand breaks. Mol Cell Biol **2014**;34:1380-8

15. Fanning E, Klimovich V, Nager AR. A dynamic model for replication protein A (RPA) function in DNA processing pathways. Nucleic Acids Res **2006**;34:4126-37

16. Taylor MRG, Spirek M, Chaurasiya KR, Ward JD, Carzaniga R, Yu X, *et al.* Rad51 Paralogs Remodel Pre-synaptic Rad51 Filaments to Stimulate Homologous Recombination. Cell **2015**;162:271-86

17. Chen CC, Feng W, Lim PX, Kass EM, Jasin M. Homology-Directed Repair and the Role of BRCA1, BRCA2, and Related Proteins in Genome Integrity and Cancer. Annu Rev Cancer Biol **2018**;2:313-36

18. Boulton SJ, Jackson SP. Saccharomyces cerevisiae Ku70 potentiates illegitimate DNA double-strand break repair and serves as a barrier to error-prone DNA repair pathways. Embo j **1996**;15:5093-103

19. Sallmyr A, Tomkinson AE. Repair of DNA double-strand breaks by mammalian alternative end-joining pathways. J Biol Chem **2018**;293:10536-46

20. Wang M, Wu W, Wu W, Rosidi B, Zhang L, Wang H, *et al.* PARP-1 and Ku compete for repair of DNA double strand breaks by distinct NHEJ pathways. Nucleic Acids Res **2006**;34:6170-82

21. Haince JF, McDonald D, Rodrigue A, Dery U, Masson JY, Hendzel MJ, *et al.* PARP1-dependent kinetics of recruitment of MRE11 and NBS1 proteins to multiple DNA damage sites. J Biol Chem **2008**;283:1197-208

22. Grabarz A, Guirouilh-Barbat J, Barascu A, Pennarun G, Genet D, Rass E, *et al.* A role for BLM in double-strand break repair pathway choice: prevention of CtIP/Mre11-mediated alternative nonhomologous end-joining. Cell Rep **2013**;5:21-8

23. Paull TT, Gellert M. A mechanistic basis for Mre11-directed DNA joining at microhomologies. Proc Natl Acad Sci U S A **2000**;97:6409-14

24. Ceccaldi R, Liu JC, Amunugama R, Hajdu I, Primack B, Petalcorin MI, *et al.* Homologous-recombination-deficient tumours are dependent on Poltheta-mediated repair. Nature **2015**;518:258-62

25. Kent T, Chandramouly G, McDevitt SM, Ozdemir AY, Pomerantz RT. Mechanism of microhomology-mediated end-joining promoted by human DNA polymerase theta. Nat Struct Mol Biol **2015**;22:230-7

26. Mateos-Gomez PA, Gong F, Nair N, Miller KM, Lazzerini-Denchi E, Sfeir A. Mammalian polymerase theta promotes alternative NHEJ and suppresses recombination. Nature **2015**;518:254-7

27. Kent T, Mateos-Gomez PA, Sfeir A, Pomerantz RT. Polymerase theta is a robust terminal transferase that oscillates between three different mechanisms during end-joining. eLife **2016**;5

28. Zahn KE, Averill AM, Aller P, Wood RD, Doublie S. Human DNA polymerase theta grasps the primer terminus to mediate DNA repair. Nat Struct Mol Biol **2015**;22:304-11

29. Caldecott KW, Tucker JD, Stanker LH, Thompson LH. Characterization of the XRCC1-DNA ligase III complex in vitro and its absence from mutant hamster cells. Nucleic Acids Res **1995**;23:4836-43

30. Della-Maria J, Zhou Y, Tsai MS, Kuhnlein J, Carney JP, Paull TT, *et al.* Human Mre11/human Rad50/Nbs1 and DNA ligase IIIalpha/XRCC1 protein complexes act together in an alternative nonhomologous end joining pathway. J Biol Chem **2011**;286:33845-53

31. Liang L, Deng L, Nguyen SC, Zhao X, Maulion CD, Shao C, *et al.* Human DNA ligases I and III, but not ligase IV, are required for microhomology-mediated end joining of DNA double-strand breaks. Nucleic Acids Res **2008**;36:3297-310

32. Paul K, Wang M, Mladenov E, Bencsik-Theilen A, Bednar T, Wu W, *et al.* DNA ligases I and III cooperate in alternative non-homologous end-joining in vertebrates. PLoS One **2013**;8:e59505

33. van Schendel R, van Heteren J, Welten R, Tijsterman M. Genomic Scars Generated by Polymerase Theta Reveal the Versatile Mechanism of Alternative End-Joining. PLoS Genet **2016**;12:e1006368

34. Cortez D. Replication-Coupled DNA Repair. Mol Cell **2019**;74:866-76

35. Quinet A, Lemacon D, Vindigni A. Replication Fork Reversal: Players and Guardians. Mol Cell **2017**;68:830-3

36. Pasero P, Vindigni A. Nucleases Acting at Stalled Forks: How to Reboot the Replication Program with a Few Shortcuts. Annu Rev Genet **2017**;51:477-99

37. Sakofsky CJ, Malkova A. Break induced replication in eukaryotes: mechanisms, functions, and consequences. Crit Rev Biochem Mol Biol **2017**;52:395-413

38. Kramara J, Osia B, Malkova A. Break-Induced Replication: The Where, The Why, and The How. Trends Genet **2018**;34:518-31

39. Carvalho CM, Lupski JR. Mechanisms underlying structural variant formation in genomic disorders. Nature reviews Genetics **2016**;17:224-38

40. Ottaviani D, LeCain M, Sheer D. The role of microhomology in genomic structural variation. Trends Genet **2014**;30:85-94

41. Halazonetis TD, Gorgoulis VG, Bartek J. An oncogene-induced DNA damage model for cancer development. Science **2008**;319:1352-5

42. Alexander JL, Orr-Weaver TL. Replication fork instability and the consequences of fork collisions from rereplication. Genes Dev **2016**;30:2241-52

43. Wei PC, Chang AN, Kao J, Du Z, Meyers RM, Alt FW, *et al.* Long Neural Genes Harbor Recurrent DNA Break Clusters in Neural Stem/Progenitor Cells. Cell **2016**;164:644-55

44. Lemacon D, Jackson J, Quinet A, Brickner JR, Li S, Yazinski S, *et al.* MRE11 and EXO1 nucleases degrade reversed forks and elicit MUS81-dependent fork rescue in BRCA2-deficient cells. Nat Commun **2017**;8:860

45. Balestrini A, Ristic D, Dionne I, Liu XZ, Wyman C, Wellinger RJ, *et al.* The Ku heterodimer and the metabolism of single-ended DNA double-strand breaks. Cell Rep **2013**;3:2033-45

46. Schlacher K, Christ N, Siaud N, Egashira A, Wu H, Jasin M. Double-strand break repair-independent role for BRCA2 in blocking stalled replication fork degradation by MRE11. Cell **2011**;145:529-42

47. Schlacher K, Wu H, Jasin M. A distinct replication fork protection pathway connects Fanconi anemia tumor suppressors to RAD51-BRCA1/2. Cancer Cell **2012**;22:106-16

48. Kolinjivadi AM, Sannino V, De Antoni A, Zadorozhny K, Kilkenny M, Techer H, *et al.* Smarcal1-Mediated Fork Reversal Triggers Mre11-Dependent Degradation of Nascent DNA in the Absence of Brca2 and Stable Rad51 Nucleofilaments. Mol Cell **2017**;67:867-81 e7

49. Daza-Martin M, Starowicz K, Jamshad M, Tye S, Ronson GE, MacKay HL, *et al.* Isomerization of BRCA1-BARD1 promotes replication fork protection. Nature **2019**;571:521-7

50. Begg AC, Stewart FA, Vens C. Strategies to improve radiotherapy with targeted drugs. Nat Rev Cancer **2011**;11:239-53

51. Baskar R, Lee KA, Yeo R, Yeoh KW. Cancer and radiation therapy: current advances and future directions. Int J Med Sci **2012**;9:193-9

52. Lomax ME, Folkes LK, O'Neill P. Biological consequences of radiation-induced DNA damage: relevance to radiotherapy. Clinical oncology (Royal College of Radiologists (Great Britain)) **2013**;25:578-85

53. Hall EJ, Hei TK. Genomic instability and bystander effects induced by high-LET radiation. Oncogene **2003**;22:7034-42

54. Cantor SB, Calvo JA. Fork Protection and Therapy Resistance in Hereditary Breast Cancer. Cold Spring Harb Symp Quant Biol **2017**;82:339-48

55. Bryant HE, Schultz N, Thomas HD, Parker KM, Flower D, Lopez E, *et al.* Specific killing of BRCA2-deficient tumours with inhibitors of poly(ADP-ribose) polymerase. Nature **2005**;434:913-7

56. Farmer H, McCabe N, Lord CJ, Tutt AN, Johnson DA, Richardson TB, *et al.* Targeting the DNA repair defect in BRCA mutant cells as a therapeutic strategy. Nature **2005**;434:917-21

57. Lord CJ, Ashworth A. PARP inhibitors: Synthetic lethality in the clinic. Science **2017**;355:1152-8

58. Pilie PG, Tang C, Mills GB, Yap TA. State-of-the-art strategies for targeting the DNA damage response in cancer. Nat Rev Clin Oncol **2019**;16:81-104

59. Alexandrov LB, Nik-Zainal S, Wedge DC, Aparicio SA, Behjati S, Biankin AV, *et al.* Signatures of mutational processes in human cancer. Nature **2013**;500:415-21

60. Nik-Zainal S, Davies H, Staaf J, Ramakrishna M, Glodzik D, Zou X, *et al.* Landscape of somatic mutations in 560 breast cancer whole-genome sequences. Nature **2016**;534:47-54

61. Davies H, Glodzik D, Morganella S, Yates LR, Staaf J, Zou X, *et al.* HRDetect is a predictor of BRCA1 and BRCA2 deficiency based on mutational signatures. Nat Med **2017**;23:517-25

62. Ma J, Setton J, Lee NY, Riaz N, Powell SN. The therapeutic significance of mutational signatures from DNA repair deficiency in cancer. Nat Commun **2018**;9:3292

63. Alexandrov LB, Nik-Zainal S, Siu HC, Leung SY, Stratton MR. A mutational signature in gastric cancer suggests therapeutic strategies. Nat Commun **2015**;6:8683

64. Mateos-Gomez PA, Kent T, Deng SK, McDevitt S, Kashkina E, Hoang TM, *et al.* The helicase domain of Poltheta counteracts RPA to promote alt-NHEJ. Nat Struct Mol Biol **2017**

65. Han J, Ruan C, Huen MSY, Wang J, Xie A, Fu C, *et al.* BRCA2 antagonizes classical and alternative nonhomologous end-joining to prevent gross genomic instability. Nat Commun **2017**;8:1470

66. Willis NA, Frock RL, Menghi F, Duffey EE, Panday A, Camacho V, *et al.* Mechanism of tandem duplication formation in BRCA1-mutant cells. Nature **2017**;551:590-5

67. Mengwasser KE, Adeyemi RO, Leng Y, Choi MY, Clairmont C, D'Andrea AD, *et al.* Genetic Screens Reveal FEN1 and APEX2 as BRCA2 Synthetic Lethal Targets. Mol Cell **2019**;73:885-99 e6

68. Caldecott KW, McKeown CK, Tucker JD, Ljungquist S, Thompson LH. An interaction between the mammalian DNA repair protein XRCC1 and DNA ligase III. Mol Cell Biol **1994**;14:68-76

69. Caldecott KW, Aoufouchi S, Johnson P, Shall S. XRCC1 polypeptide interacts with DNA polymerase beta and possibly poly (ADP-ribose) polymerase, and DNA ligase III is a novel molecular 'nick-sensor' in vitro. Nucleic Acids Res **1996**;24:4387-94

70. Thompson LH, Brookman KW, Jones NJ, Allen SA, Carrano AV. Molecular cloning of the human XRCC1 gene, which corrects defective DNA strand break repair and sister chromatid exchange. Mol Cell Biol **1990**;10:6160-71

71. Cuneo MJ, London RE. Oxidation state of the XRCC1 N-terminal domain regulates DNA polymerase beta binding affinity. Proc Natl Acad Sci U S A **2010**;107:6805-10

72. Fan J, Otterlei M, Wong HK, Tomkinson AE, Wilson DM, 3rd. XRCC1 co-localizes and physically interacts with PCNA. Nucleic Acids Res **2004**;32:2193-201

73. Vidal AE, Boiteux S, Hickson ID, Radicella JP. XRCC1 coordinates the initial and late stages of DNA abasic site repair through protein-protein interactions. EMBO J **2001**;20:6530-9

74. Campalans A, Marsin S, Nakabeppu Y, O'Connor T R, Boiteux S, Radicella JP. XRCC1 interactions with multiple DNA glycosylases: a model for its recruitment to base excision repair. DNA Repair (Amst) **2005**;4:826-35

75. Levy N, Oehlmann M, Delalande F, Nasheuer HP, Van Dorsselaer A, Schreiber V, *et al.* XRCC1 interacts with the p58 subunit of DNA Pol alpha-primase and may coordinate DNA repair and replication during S phase. Nucleic Acids Res **2009**;37:3177-88

76. Date H, Igarashi S, Sano Y, Takahashi T, Takahashi T, Takano H, *et al.* The FHA domain of aprataxin interacts with the C-terminal region of XRCC1. Biochem Biophys Res Commun **2004**;325:1279-85

77. Ali AA, Jukes RM, Pearl LH, Oliver AW. Specific recognition of a multiply phosphorylated motif in the DNA repair scaffold XRCC1 by the FHA domain of human PNK. Nucleic Acids Res **2009**;37:1701-12

78. Taylor RM, Wickstead B, Cronin S, Caldecott KW. Role of a BRCT domain in the interaction of DNA ligase III-alpha with the DNA repair protein XRCC1. Current biology : CB **1998**;8:877-80

79. Dulic A, Bates PA, Zhang X, Martin SR, Freemont PS, Lindahl T, *et al.* BRCT domain interactions in the heterodimeric DNA repair protein XRCC1-DNA ligase III. Biochemistry **2001**;40:5906-13

80. Almeida KH, Sobol RW. A unified view of base excision repair: lesion-dependent protein complexes regulated by post-translational modification. DNA Repair (Amst) **2007**;6:695-711

81. Hanssen-Bauer A, Solvang-Garten K, Akbari M, Otterlei M. X-ray repair cross complementing protein 1 in base excision repair. International journal of molecular sciences **2012**;13:17210-29

82. Levy N, Martz A, Bresson A, Spenlehauer C, de Murcia G, Menissier-de Murcia J. XRCC1 is phosphorylated by DNA-dependent protein kinase in response to DNA damage. Nucleic Acids Res **2006**;34:32-41

83. Parsons JL, Dianova, II, Finch D, Tait PS, Strom CE, Helleday T, *et al.* XRCC1 phosphorylation by CK2 is required for its stability and efficient DNA repair. DNA Repair (Amst) **2010**;9:835-41

84. Strom CE, Mortusewicz O, Finch D, Parsons JL, Lagerqvist A, Johansson F, *et al.* CK2 phosphorylation of XRCC1 facilitates dissociation from DNA and single-strand break formation during base excision repair. DNA Repair (Amst) **2011**;10:961-9

85. Cherry AL, Nott TJ, Kelly G, Rulten SL, Caldecott KW, Smerdon SJ. Versatility in phospho-dependent molecular recognition of the XRCC1 and XRCC4 DNA-damage scaffolds by aprataxin-family FHA domains. DNA Repair (Amst) **2015**;35:116-25

86. Taylor RM, Moore DJ, Whitehouse J, Johnson P, Caldecott KW. A cell cycle-specific requirement for the XRCC1 BRCT II domain during mammalian DNA strand break repair. Mol Cell Biol **2000**;20:735-40

87. Kubota Y, Horiuchi S. Independent roles of XRCC1's two BRCT motifs in recovery from methylation damage. DNA Repair (Amst) **2003**;2:407-15

88. Simsek D, Furda A, Gao Y, Artus J, Brunet E, Hadjantonakis AK, *et al.* Crucial role for DNA ligase III in mitochondria but not in Xrcc1-dependent repair. Nature **2011**;471:245-8

89. Hanzlikova H, Kalasova I, Demin AA, Pennicott LE, Cihlarova Z, Caldecott KW. The Importance of Poly(ADP-Ribose) Polymerase as a Sensor of Unligated Okazaki Fragments during DNA Replication. Mol Cell **2018**;71:319-31 e3

90. Ying S, Chen Z, Medhurst AL, Neal JA, Bao Z, Mortusewicz O, *et al.* DNA-PKcs and PARP1 Bind to Unresected Stalled DNA Replication Forks Where They Recruit XRCC1 to Mediate Repair. Cancer Res **2016**;76:1078-88

91. Hanahan D, Weinberg RA. Hallmarks of cancer: the next generation. Cell **2011**;144:646-74

92. Willers H, Azzoli CG, Santivasi WL, Xia F. Basic mechanisms of therapeutic resistance to radiation and chemotherapy in lung cancer. Cancer J **2013**;19:200-7

93. Sutherland BM, Bennett PV, Sidorkina O, Laval J. Clustered DNA damages induced in isolated DNA and in human cells by low doses of ionizing radiation. Proc Natl Acad Sci U S A **2000**;97:103-8

94. Jeggo PA, Geuting V, Lobrich M. The role of homologous recombination in radiation-induced double-strand break repair. Radiotherapy and oncology : journal of the European Society for Therapeutic Radiology and Oncology **2011**;101:7-12

95. Schipler A, Iliakis G. DNA double-strand-break complexity levels and their possible contributions to the probability for error-prone processing and repair pathway choice. Nucleic Acids Res **2013**;41:7589-605

96. Betermier M, Bertrand P, Lopez BS. Is non-homologous end-joining really an inherently error-prone process? PLoS Genet **2014**;10:e1004086

97. Mimitou EP, Symington LS. Ku prevents Exo1 and Sgs1-dependent resection of DNA ends in the absence of a functional MRX complex or Sae2. Embo j **2010**;29:3358-69

98. Sharma S, Javadekar SM, Pandey M, Srivastava M, Kumari R, Raghavan SC. Homology and enzymatic requirements of microhomology-dependent alternative end joining. Cell Death Dis **2015**;6:e1697

99. Lu G, Duan J, Shu S, Wang X, Gao L, Guo J, *et al.* Ligase I and ligase III mediate the DNA double-strand break ligation in alternative end-joining. Proc Natl Acad Sci U S A **2016**;113:1256-60

100. McVey M, Lee SE. MMEJ repair of double-strand breaks (director's cut): deleted sequences and alternative endings. Trends Genet **2008**;24:529-38

101. Audebert M, Salles B, Weinfeld M, Calsou P. Involvement of polynucleotide kinase in a poly(ADP-ribose) polymerase-1-dependent DNA double-strand breaks rejoining pathway. J Mol Biol **2006**;356:257-65

102. Mansour WY, Rhein T, Dahm-Daphi J. The alternative end-joining pathway for repair of DNA double-strand breaks requires PARP1 but is not dependent upon microhomologies. Nucleic Acids Res **2010**;38:6065-77

103. Truong LN, Li Y, Shi LZ, Hwang PY, He J, Wang H, *et al.* Microhomology-mediated End Joining and Homologous Recombination share the initial end resection step to repair DNA double-strand breaks in mammalian cells. Proc Natl Acad Sci U S A **2013**;110:7720-5

104. Frit P, Barboule N, Yuan Y, Gomez D, Calsou P. Alternative end-joining pathway(s): bricolage at DNA breaks. DNA Repair (Amst) **2014**;17:81-97

105. Wu W, Wang M, Wu W, Singh SK, Mussfeldt T, Iliakis G. Repair of radiation induced DNA double strand breaks by backup NHEJ is enhanced in G2. DNA Repair (Amst) **2008**;7:329-38

106. Sfeir A, Symington LS. Microhomology-Mediated End Joining: A Back-up Survival Mechanism or Dedicated Pathway? Trends Biochem Sci **2015**;40:701-14

107. Yang L, Luquette LJ, Gehlenborg N, Xi R, Haseley PS, Hsieh CH, *et al.* Diverse mechanisms of somatic structural variations in human cancer genomes. Cell **2013**;153:919-29

108. Mattarucchi E, Guerini V, Rambaldi A, Campiotti L, Venco A, Pasquali F, *et al.* Microhomologies and interspersed repeat elements at genomic breakpoints in chronic myeloid leukemia. Genes, chromosomes & cancer **2008**;47:625-32

109. Povirk LF. Processing of damaged DNA ends for double-strand break repair in mammalian cells. ISRN Mol Biol **2012**;2012

110. Buchko GW, Weinfeld M. Influence of nitrogen, oxygen, and nitroimidazole radiosensitizers on DNA damage induced by ionizing radiation. Biochemistry **1993**;32:2186-93

111. Hegde ML, Hegde PM, Bellot LJ, Mandal SM, Hazra TK, Li GM, *et al.* Prereplicative repair of oxidized bases in the human genome is mediated by NEIL1 DNA glycosylase together with replication proteins. Proc Natl Acad Sci U S A **2013**;110:E3090-9

112. Gunn A, Stark JM. I-SceI-based assays to examine distinct repair outcomes of mammalian chromosomal double strand breaks. Methods Mol Biol **2012**;920:379-91

113. Decottignies A. Microhomology-mediated end joining in fission yeast is repressed by pku70 and relies on genes involved in homologous recombination. Genetics **2007**;176:1403-15

114. Yu AM, McVey M. Synthesis-dependent microhomology-mediated end joining accounts for multiple types of repair junctions. Nucleic Acids Res **2010**;38:5706-17

115. Chappell C, Hanakahi LA, Karimi-Busheri F, Weinfeld M, West SC. Involvement of human polynucleotide kinase in double-strand break repair by non-homologous end joining. EMBO J **2002**;21:2827-32

116. Weinfeld M, Mani RS, Abdou I, Aceytuno RD, Glover JN. Tidying up loose ends: the role of polynucleotide kinase/phosphatase in DNA strand break repair. Trends Biochem Sci **2011**;36:262-71

117. Rasouli-Nia A, Karimi-Busheri F, Weinfeld M. Stable down-regulation of human polynucleotide kinase enhances spontaneous mutation frequency and sensitizes cells to genotoxic agents. Proc Natl Acad Sci U S A **2004**;101:6905-10

118. Scuric Z, Chan CY, Hafer K, Schiestl RH. Ionizing radiation induces microhomology-mediated end joining in trans in yeast and mammalian cells. Radiat Res **2009**;171:454-63

119. Saribasak H, Maul RW, Cao Z, McClure RL, Yang W, McNeill DR, *et al.* XRCC1 suppresses somatic hypermutation and promotes alternative nonhomologous end joining in Igh genes. The Journal of experimental medicine **2011**;208:2209-16

120. Audebert M, Salles B, Calsou P. Involvement of poly(ADP-ribose) polymerase-1 and XRCC1/DNA ligase III in an alternative route for DNA double-strand breaks rejoining. J Biol Chem **2004**;279:55117-26

121. Wei L, Nakajima S, Hsieh CL, Kanno S, Masutani M, Levine AS, *et al.* Damage response of XRCC1 at sites of DNA single strand breaks is regulated by phosphorylation and ubiquitylation after degradation of poly(ADP-ribose). Journal of cell science **2013**;126:4414-23

122. Abdou I, Poirier GG, Hendzel MJ, Weinfeld M. DNA ligase III acts as a DNA strand break sensor in the cellular orchestration of DNA strand break repair. Nucleic Acids Res **2015**;43:875-92

123. Charbonnel C, Gallego ME, White CI. Xrcc1-dependent and Ku-dependent DNA double-strand break repair kinetics in Arabidopsis plants. The Plant journal : for cell and molecular biology **2010**;64:280-90

124. Loizou JI, El-Khamisy SF, Zlatanou A, Moore DJ, Chan DW, Qin J, *et al.* The protein kinase CK2 facilitates repair of chromosomal DNA single-strand breaks. Cell **2004**;117:17-28

125. Yamane K, Kinsella TJ. CK2 inhibits apoptosis and changes its cellular localization following ionizing radiation. Cancer Res **2005**;65:4362-7

126. Olsen BB, Wang SY, Svenstrup TH, Chen BP, Guerra B. Protein kinase CK2 localizes to sites of DNA double-strand break regulating the cellular response to DNA damage. BMC Mol Biol **2012**;13:7

127. Xie A, Kwok A, Scully R. Role of mammalian Mre11 in classical and alternative nonhomologous end joining. Nat Struct Mol Biol **2009**;16:814-8

128. Lee-Theilen M, Matthews AJ, Kelly D, Zheng S, Chaudhuri J. CtIP promotes microhomology-mediated alternative end joining during class-switch recombination. Nat Struct Mol Biol **2011**;18:75-9

129. Shibata A, Moiani D, Arvai AS, Perry J, Harding SM, Genois MM, *et al.* DNA double-strand break repair pathway choice is directed by distinct MRE11 nuclease activities. Mol Cell **2014**;53:7-18

130. Averbeck NB, Ringel O, Herrlitz M, Jakob B, Durante M, Taucher-Scholz G. DNA end resection is needed for the repair of complex lesions in G1-phase human cells. Cell Cycle **2014**;13:2509-16

131. Villarreal DD, Lee K, Deem A, Shim EY, Malkova A, Lee SE. Microhomology directs diverse DNA break repair pathways and chromosomal translocations. PLoS Genet **2012**;8:e1003026

132. Singleton BK, Griffin CS, Thacker J. Clustered DNA damage leads to complex genetic changes in irradiated human cells. Cancer Res **2002**;62:6263-9

133. Hegde PM, Dutta A, Sengupta S, Mitra J, Adhikari S, Tomkinson AE, *et al.* The C-terminal Domain (CTD) of Human DNA Glycosylase NEIL1 Is Required for Forming BERosome Repair Complex with DNA Replication Proteins at the Replicating Genome: DOMINANT NEGATIVE FUNCTION OF THE CTD. J Biol Chem **2015**;290:20919-33

134. Luijsterburg MS, von Bornstaedt G, Gourdin AM, Politi AZ, Mone MJ, Warmerdam DO, *et al.* Stochastic and reversible assembly of a multiprotein DNA repair complex ensures accurate target site recognition and efficient repair. J Cell Biol **2010**;189:445-63

135. Raschle M, Smeenk G, Hansen RK, Temu T, Oka Y, Hein MY, *et al.* DNA repair. Proteomics reveals dynamic assembly of repair complexes during bypass of DNA cross-links. Science **2015**;348:1253671

136. Polo SE, Jackson SP. Dynamics of DNA damage response proteins at DNA breaks: a focus on protein modifications. Genes Dev **2011**;25:409-33

137. London RE. The structural basis of XRCC1-mediated DNA repair. DNA Repair (Amst) **2015**;30:90-103

138. Kubota Y, Takanami T, Higashitani A, Horiuchi S. Localization of X-ray cross complementing gene 1 protein in the nuclear matrix is controlled by casein kinase II-dependent phosphorylation in response to oxidative damage. DNA Repair (Amst) **2009**;8:953-60

139. Boboila C, Oksenych V, Gostissa M, Wang JH, Zha S, Zhang Y, *et al.* Robust chromosomal DNA repair via alternative end-joining in the absence of X-ray repair cross-complementing protein 1 (XRCC1). Proc Natl Acad Sci U S A **2012**;109:2473-8

140. Ristic D, Modesti M, Kanaar R, Wyman C. Rad52 and Ku bind to different DNA structures produced early in double-strand break repair. Nucleic Acids Res **2003**;31:5229-37

141. Daley JM, Wilson TE. Rejoining of DNA double-strand breaks as a function of overhang length. Mol Cell Biol **2005**;25:896-906

142. Hoa NN, Akagawa R, Yamasaki T, Hirota K, Sasa K, Natsume T, *et al.* Relative contribution of four nucleases, CtIP, Dna2, Exo1 and Mre11, to the initial step of DNA double-strand break repair by homologous recombination in both the chicken DT40 and human TK6 cell lines. Genes Cells **2015**;20:1059-76

143. Deng SK, Gibb B, de Almeida MJ, Greene EC, Symington LS. RPA antagonizes microhomology-mediated repair of DNA double-strand breaks. Nat Struct Mol Biol **2014**;21:405-12

144. Cancer Genome Atlas N. Comprehensive molecular portraits of human breast tumours. Nature **2012**;490:61-70

145. Ray Chaudhuri A, Callen E, Ding X, Gogola E, Duarte AA, Lee JE, *et al.* Replication fork stability confers chemoresistance in BRCA-deficient cells. Nature **2016**;535:382-7

146. Ding X, Ray Chaudhuri A, Callen E, Pang Y, Biswas K, Klarmann KD, *et al.* Synthetic viability by BRCA2 and PARP1/ARTD1 deficiencies. Nat Commun **2016**;7:12425

147. Mijic S, Zellweger R, Chappidi N, Berti M, Jacobs K, Mutreja K, *et al.* Replication fork reversal triggers fork degradation in BRCA2-defective cells. Nat Commun **2017**;8:859

148. Banerji S, Cibulskis K, Rangel-Escareno C, Brown KK, Carter SL, Frederick AM, *et al.* Sequence analysis of mutations and translocations across breast cancer subtypes. Nature **2012**;486:405-9

149. Nik-Zainal S, Alexandrov LB, Wedge DC, Van Loo P, Greenman CD, Raine K, *et al.* Mutational processes molding the genomes of 21 breast cancers. Cell **2012**;149:979-93

150. Stephens PJ, Tarpey PS, Davies H, Van Loo P, Greenman C, Wedge DC, *et al.* The landscape of cancer genes and mutational processes in breast cancer. Nature **2012**;486:400-4

151. Yang SYC, Lheureux S, Karakasis K, Burnier JV, Bruce JP, Clouthier DL, *et al.* Landscape of genomic alterations in high-grade serous ovarian cancer from exceptional long- and short-term survivors. Genome Med **2018**;10:81

152. Nussenzweig A, Nussenzweig MC. Origin of chromosomal translocations in lymphoid cancer. Cell **2010**;141:27-38

153. Fan J, Wilson PF, Wong HK, Urbin SS, Thompson LH, Wilson DM, 3rd. XRCC1 down-regulation in human cells leads to DNA-damaging agent hypersensitivity, elevated sister chromatid exchange, and reduced survival of BRCA2 mutant cells. Environmental and molecular mutagenesis **2007**;48:491-500

154. Abdel-Fatah T, Sultana R, Abbotts R, Hawkes C, Seedhouse C, Chan S, *et al.* Clinicopathological and functional significance of XRCC1 expression in ovarian cancer. Int J Cancer **2013**;132:2778-86

155. Ali R, Al-Kawaz A, Toss MS, Green AR, Miligy IM, Mesquita KA, *et al.* Targeting PARP1 in XRCC1-Deficient Sporadic Invasive Breast Cancer or Preinvasive Ductal Carcinoma In Situ Induces Synthetic Lethality and Chemoprevention. Cancer Res **2018**;78:6818-27

156. Dutta A, Eckelmann B, Adhikari S, Ahmed KM, Sengupta S, Pandey A, *et al.* Microhomology-mediated end joining is activated in irradiated human cells due to phosphorylation-dependent formation of the XRCC1 repair complex. Nucleic Acids Res **2017**;45:2585-99

157. Jungmichel S, Rosenthal F, Altmeyer M, Lukas J, Hottiger MO, Nielsen ML. Proteome-wide identification of poly(ADP-Ribosyl)ation targets in different genotoxic stress responses. Mol Cell **2013**;52:272-85

158. Macheret M, Halazonetis TD. Intragenic origins due to short G1 phases underlie oncogene-induced DNA replication stress. Nature **2018**;555:112-6

159. Wang Z, Song Y, Li S, Kurian S, Xiang R, Chiba T, *et al.* DNA polymerase theta (POLQ) is important for repair of DNA double-strand breaks caused by fork collapse. J Biol Chem **2019**;294:3909-19

160. Sultana R, Abdel-Fatah T, Perry C, Moseley P, Albarakti N, Mohan V, *et al.* Ataxia telangiectasia mutated and Rad3 related (ATR) protein kinase inhibition is synthetically lethal in XRCC1 deficient ovarian cancer cells. PLoS One **2013**;8:e57098

161. Vesela E, Chroma K, Turi Z, Mistrik M. Common Chemical Inductors of Replication Stress: Focus on Cell-Based Studies. Biomolecules **2017**;7

162. Dungrawala H, Rose KL, Bhat KP, Mohni KN, Glick GG, Couch FB, *et al.* The Replication Checkpoint Prevents Two Types of Fork Collapse without Regulating Replisome Stability. Mol Cell **2015**;59:998-1010

163. Tutt A, Bertwistle D, Valentine J, Gabriel A, Swift S, Ross G, *et al.* Mutation in Brca2 stimulates error-prone homology-directed repair of DNA double-strand breaks occurring between repeated sequences. EMBO J **2001**;20:4704-16

164. Burdak-Rothkamm S, Short SC, Folkard M, Rothkamm K, Prise KM. ATR-dependent radiation-induced gamma H2AX foci in bystander primary human astrocytes and glioma cells. Oncogene **2007**;26:993-1002

165. Badie S, Carlos AR, Folio C, Okamoto K, Bouwman P, Jonkers J, *et al.* BRCA1 and CtIP promote alternative non-homologous end-joining at uncapped telomeres. EMBO J **2015**;34:410-24

166. Rothkamm K, Lobrich M. Evidence for a lack of DNA double-strand break repair in human cells exposed to very low x-ray doses. Proc Natl Acad Sci U S A **2003**;100:5057-62

167. Rothkamm K, Balroop S, Shekhdar J, Fernie P, Goh V. Leukocyte DNA damage after multi-detector row CT: a quantitative biomarker of low-level radiation exposure. Radiology **2007**;242:244-51

168. Jackson DA, Pombo A. Replicon clusters are stable units of chromosome structure: evidence that nuclear organization contributes to the efficient activation and propagation of S phase in human cells. J Cell Biol **1998**;140:1285-95

169. Hastings PJ, Ira G, Lupski JR. A microhomology-mediated break-induced replication model for the origin of human copy number variation. PLoS Genet **2009**;5:e1000327

170. Hartlerode AJ, Willis NA, Rajendran A, Manis JP, Scully R. Complex Breakpoints and Template Switching Associated with Non-canonical Termination of Homologous Recombination in Mammalian Cells. PLoS Genet **2016**;12:e1006410

171. Kwon MS, Lee JJ, Min J, Hwang K, Park SG, Kim EH, *et al.* Brca2 abrogation engages with the alternative lengthening of telomeres via break-induced replication. FEBS J **2019**;286:1841-58

172. Zhang F, Khajavi M, Connolly AM, Towne CF, Batish SD, Lupski JR. The DNA replication FoSTeS/MMBIR mechanism can generate genomic, genic and exonic complex rearrangements in humans. Nat Genet **2009**;41:849-53

173. Cancer Genome Atlas Research N, Weinstein JN, Collisson EA, Mills GB, Shaw KR, Ozenberger BA, *et al.* The Cancer Genome Atlas Pan-Cancer analysis project. Nat Genet **2013**;45:1113-20

174. Lord CJ, McDonald S, Swift S, Turner NC, Ashworth A. A high-throughput RNA interference screen for DNA repair determinants of PARP inhibitor sensitivity. DNA Repair (Amst) **2008**;7:2010-9

175. Turner NC, Lord CJ, Iorns E, Brough R, Swift S, Elliott R, *et al.* A synthetic lethal siRNA screen identifying genes mediating sensitivity to a PARP inhibitor. EMBO J **2008**;27:1368-77

176. Postel-Vinay S, Bajrami I, Friboulet L, Elliott R, Fontebasso Y, Dorvault N, *et al.* A high-throughput screen identifies PARP1/2 inhibitors as a potential therapy for ERCC1-deficient non-small cell lung cancer. Oncogene **2013**;32:5377-87

177. Cheng H, Zhang Z, Borczuk A, Powell CA, Balajee AS, Lieberman HB, *et al.* PARP inhibition selectively increases sensitivity to cisplatin in ERCC1-low non-small cell lung cancer cells. Carcinogenesis **2013**;34:739-49

178. Ceccaldi R, O'Connor KW, Mouw KW, Li AY, Matulonis UA, D'Andrea AD, *et al.* A unique subset of epithelial ovarian cancers with platinum sensitivity and PARP inhibitor resistance. Cancer Res **2015**;75:628-34

179. Glover TW, Wilson TE, Arlt MF. Fragile sites in cancer: more than meets the eye. Nat Rev Cancer **2017**;17:489-501

180. Sallmyr A, Tomkinson AE, Rassool FV. Up-regulation of WRN and DNA ligase IIIalpha in chronic myeloid leukemia: consequences for the repair of DNA double-strand breaks. Blood **2008**;112:1413-23

181. Tobin LA, Robert C, Nagaria P, Chumsri S, Twaddell W, Ioffe OB, *et al.* Targeting abnormal DNA repair in therapy-resistant breast cancers. Mol Cancer Res **2012**;10:96-107

182. Anand RP, Lovett ST, Haber JE. Break-induced DNA replication. Cold Spring Harb Perspect Biol **2013**;5:a010397

183. Sakofsky CJ, Ayyar S, Deem AK, Chung WH, Ira G, Malkova A. Translesion Polymerases Drive Microhomology-Mediated Break-Induced Replication Leading to Complex Chromosomal Rearrangements. Mol Cell **2015**;60:860-72

184. Bindra RS, Schaffer PJ, Meng A, Woo J, Maseide K, Roth ME, *et al.* Down-regulation of Rad51 and decreased homologous recombination in hypoxic cancer cells. Mol Cell Biol **2004**;24:8504-18

185. Bryant HE, Petermann E, Schultz N, Jemth AS, Loseva O, Issaeva N, *et al.* PARP is activated at stalled forks to mediate Mre11-dependent replication restart and recombination. EMBO J **2009**;28:2601-15

186. Roy S, Tomaszowski KH, Luzwick JW, Park S, Li J, Murphy M, *et al.* p53 orchestrates DNA replication restart homeostasis by suppressing mutagenic RAD52 and POLtheta pathways. eLife **2018**;7

187. Sultana R, Abdel-Fatah T, Abbotts R, Hawkes C, Albarakati N, Seedhouse C, *et al.* Targeting XRCC1 deficiency in breast cancer for personalized therapy. Cancer Res **2013**;73:1621-34

188. Yu W, Kanaan Y, Bae YK, Gabrielson E. Chromosomal changes in aggressive breast cancers with basal-like features. Cancer Genet Cytogenet **2009**;193:29-37

189. Thompson FH, Nelson MA, Trent JM, Guan XY, Liu Y, Yang JM, *et al.* Amplification of 19q13.1-q13.2 sequences in ovarian cancer. G-band, FISH, and molecular studies. Cancer Genet Cytogenet **1996**;87:55-62

190. Kuuselo R, Simon R, Karhu R, Tennstedt P, Marx AH, Izbicki JR, *et al.* 19q13 amplification is associated with high grade and stage in pancreatic cancer. Genes, chromosomes & cancer **2010**;49:569-75

191. Gottipati P, Vischioni B, Schultz N, Solomons J, Bryant HE, Djureinovic T, *et al.* Poly(ADP-ribose) polymerase is hyperactivated in homologous recombination-defective cells. Cancer Res **2010**;70:5389-98

192. Behjati S, Gundem G, Wedge DC, Roberts ND, Tarpey PS, Cooke SL, *et al.* Mutational signatures of ionizing radiation in second malignancies. Nat Commun **2016**;7:12605

193. Cornforth MN, Anur P, Wang N, Robinson E, Ray FA, Bedford JS, *et al.* Molecular Cytogenetics Guides Massively Parallel Sequencing of a Radiation-Induced Chromosome Translocation in Human Cells. Radiat Res **2018**;190:88-97

194. Li Z, Jella KK, Jaafar L, Li S, Park S, Story MD, *et al.* Exposure to galactic cosmic radiation compromises DNA repair and increases the potential for oncogenic chromosomal rearrangement in bronchial epithelial cells. Scientific reports **2018**;8:11038